GEORGIA INSTITUTE OF TECHNOLOGY — OFFICE OF CONTRACT ADMINISTRATION

PROJECT ADMINISTRATION DATA SHEET

[X] ORIGINAL
[ ] REVISION NO. ____

Project No. A-2951 DATE: 5/26/81

Project Director: ~~Dr. D. W. Covington~~ N.W Cox xxxxxx/Lab EML/PSD

Sponsor: Naval Research Laboratory; Washington, D. C. 20375

Type Agreement: Short Form Research Contract (SFRC) No. N00014-81-K-2007

Award Period: From 5/1/81 To ~~4/30/82~~ 8/31/82 (Performance) ~~5/31/82~~ 9/30/82 (Reports)

Sponsor Amount: $99,982 Contracted through:

Cost Sharing: None GTRI ~~GIT~~

Title: Binary, Ternary, Quaternary Hetrojunctions of III-V Semiconductors Grown By Molecular Beam Epitaxy

ADMINISTRATIVE DATA OCA CONTACT Duane Hutchison x 4820

1) Sponsor Technical Contact: Dr. John Davey, Code 6810; Navel Research Laboratory; 4555 Overlook Avenue, S. W., Washington, D. C. 20375 (202) 767-2524.

2) Sponsor Admin./Contractual Contact: Mr. Thomas A. Bryant; ONR Resident Representative; Georgia Institute of Technology; 206 O'Keefe Building; Atlanta, GA 30332

Reports: See Deliverable Schedule Security Classification: None

Defense Priority Rating: None

RESTRICTIONS

See Attached DOD Supplemental Information Sheet for Additional Requirements.

Travel: Foreign travel must have prior approval - Contact OCA in each case. Domestic travel requires sponsor approval where total will exceed greater of $500 or 125% of approved proposal budget category.

Equipment: Title vests with GIT if specified in the proposal and not otherwise indicated in the Short Form Research Contract.

COMMENTS:

COPIES TO:

Administrative Coordinator
Research Property Management
Accounting Office
Procurement/EES Supply Services
Research Security Services
Reports Coordinator (OCA)
Legal Services (OCA)
Library, Technical Reports
EES Research Public Relations (2
Project File (OCA)
Other:

IA INSTITUTE OF TECHNOLOGY OFFICE OF CONTRACT ADMINISTRATION

SPONSORED PROJECT TERMINATION SHEET

Date 1/31/83

Project Title: Binary, Ternary, ~~Quatenary~~ Quaternary ~~Hetrojunctions~~ Heterojunctions of III-V Semiconductors Grown By Molecular Beam Epitaxy

Project No: A-2951

Project Director: N. W. Cox, Jr.

Sponsor: Naval Research Laboratory, Washington, DC

Effective Termination Date: 8/31/82

Clearance of Accounting Charges: 9/30/82

Grant/Contract Closeout Actions Remaining:

- [x] Final Invoice ~~and Closing Documents~~
- [ ] Final Fiscal Report
- [x] Final Report of Inventions
- [x] Govt. Property Inventory & Related Certificate
- [ ] Classified Material Certificate
- [x] Other Certification of Excess Contract/Grant Funds

Assigned to: EML (~~School~~/Laboratory)

COPIES TO:

Administrative Coordinator	Research Security Services	EES Public Relations (2)
Research Property Management	Reports Coordinator (OCA)	Computer Input
Accounting	Legal Services (OCA)	Project File
Procurement/EES Supply Services	Library	Other Pray Der

FORM OCA 10:781

DISCLAIMER:

This document has been proofed and
its original formatting has been retained.

A-2951

BINARY, TERNARY AND QUATERNARY HETEROJUNCTIONS OF III-V SEMICONDUCTORS GROWN BY MOLECULAR BEAM EPITAXY

(A001)

Quarterly Progress Report No. 1

N. W. Cox

Engineering Experiment Station
Georgia Institute of Technology
Atlanta, Georgia 30332

A-2951

August 1981

Report for Period 1 May 1981 - 31 July 1981

Contract No. N00014-81-K-2007

Prepared for

Naval Research Laboratory
Washington, D.C. 20375

OBJECTIVE

This report describes the technical work performed during the first quarter of Contract No. N00014-81-K-2007 by the Engineering Experiment Station at the Georgia Institute of Technology. The objective of this basic research program is to utilize the advantages of molecular beam epitaxy in preparing and characterizing multilayer heterojunctions of III-V semiconductors which extend the range of energy bandgaps, dielectric constants, transport phenomena and surface properties that are currently available with conventional InP, GaAs, and $Al_xGa_{1-x}A_s$.

SUMMARY OF PRINCIPAL ACTIVITIES

Due to the resignation of the project director, Dr. D. W. Covington, during the first month of the program, the technical effort has been delayed until a replacement can be hired. In the interim period, permission was requested and received from NRL to designate Dr. N. W. Cox as temporary project director. Several new staff members with excellent semiconductor materials experinece are currently being considered. Dr. Geoffrey Holah joined our staff on 1 August and will be proposed as project director for the program subject to approval by the NRL Scientific Program Officer. Dr. Holah's research experience includes III-V and II-VI semiconductor materials with emphasis on characterization of the lattice and electronic properties of materials using optical techniques. A formal request will be submitted in September for approval of Dr. Holah as project director. The addition of a second new staff member, who would also participate in the program, is anticipated in October.

Due to the delay in initiation of the technical effort, a no-cost extension will be officially requested later in the program. A four month extension will likely be required.

QUARTERLY PERFORMANCE AND STATUS OF FUNDS

Level of Effort

Categories	1 May 1981 - 31 July 1981	Cumulative Total (man months)
Principal Research Engineer/Scientist	0	0
Senior Research Engineer/Scientist	0	0
Research Engineer/Scientist II	0	0
Research Technologist I	0	0
Graduate Research Assistant	0	0
Co-op, Student	0	0
TOTAL	0	0

Financial Status

1 May 1981 - 31 July 1981	Cumulative Total Expended
0	0

Total Contract Funding	$99,982

A-2951

BINARY, TERNARY AND QUATERNARY HETEROJUNCTIONS OF III-V SEMICONDUCTORS GROWN BY MOLECULAR BEAM EPITAXY

(A002)

Quarterly Report No. 2

G. D. Holah, E. L. Meeks and F. L. Eisele

Engineering Experiment Station
Georgia Institute of Technology
Atlanta, Georgia 30332

Report for Period 1 August 1981 - 31 October 1981

Contract No. N00014-81-K-2007

Prepared for:

Naval Research Laboratory
Washington, D.C. 20375

TABLE OF CONTENTS

LIST OF TABLES

LIST OF ILLUSTRATIONS

1.0 INTRODUCTION

1.1 Background

This report summarizes recent progress in the growth and analysis of $In_{1-x}Ga_xAs_yP_{1-y}$ layers grown using molecular beam epitaxy (MBE).

It is well-known[1] that the quaternary III-V alloys sytem $In_{1-x}Ga_xAs_yP_{1-y}$ can be grown lattice matched to InP and GaAs over a wide range of bandgaps by a suitable choice of x and y. Of particular importance is the fact that, when InP is used as the substrate, material can be grown with bandgaps between 1.3 and 1.55 μm. This covers the technologically important wavelengths used in optical fiber communication[2], and $In_{1-x}Ga_xAs_yP_{1-y}$ has already found application as laser sources[3] and detectors[4] in this region. The material used thus far for lasers and detectors has been grown mainly by liquid-phase epitaxy[5] (LPE), although some success has been achieved using vapor-phase epitaxy[6] (VPE).

In addition to the very important application in optical fiber communications, there was some initial hope that the quaternaries may also offer some advantages over GaAs and InP in application to millimeter and microwave devices, such as FETs and TEOs. This interest was based on some calculations[7] of peak velocities and low-field mobilities which would have increased the cut-off frequency of the aforementioned devices relative to Ga As and InP devices. However, it now appears that the effect of inter-valley scattering was underestimated[8] and such high velocities and high mobilities may not be achievable, at least under steady state conditions. However, as efforts to increase the operating frequency of devices lead to smaller and smaller structures, one enters the submicron size and the situation of transient or ballistic phenomena. Under these con-

litions, the advantage of the quaternary may be realized since the velocity-
vershoot mechanism pertains and here the velocities of the quaternary
re indeed higher than those of GaAs and InP.[7]

.2 Status of MBE Growth

The most extensive effort towards growing these quaternary alloys
sing MBE has been that undertaken at Georgia Tech and is summarized in
he final report submitted to NRL under contract N00173-79-C-0033. Under
his contract, growth conditions were established for a range of composition
arameters and layers were grown on both GaAs and InP substrates. Addition-
lly, dopant studies were carried out, and Mn and Sn were shown to produce
-type and y-type layers, respectively, of quality comparable to that of
PE and VPE grown material. Mobilities of up to 4000 $cm^2V^{-1}s^{-1}$ were reported.
o far, however, no diode lasers have been grown using MBE $In_{1-x}Ga_xAs_yP_{1-y}$.

There are still a number of problems existing with MBE growth of the
uaternary. These include composition control, lattice match, homogeneity,
producibility and lower mobility than predicted. A further difficulty
ises in composition analysis since the usual techniques, such as bandgap
termination, do not determine x and y uniquely except under lattice
tched conditions. A range of characterization techniques are therefore
quired to make meaningful analyses.

Objectives of Second Quarter

The objectives of the second quarter were two-fold:

a) Verify reproducibility of MBE growth system by growing a number of identical layers of $In_{1-x}Ga_xAs_yP_{1-y}$ on semi-insulating Fe-doped (001) InP.

b) Establish characterization techniques which will enable meaningful composition determination to be made. The techniques which have been

used include infrared absorption, electroreflectance and x-ray rocking curves for composition measurements and reflection electron diffraction for surface qualtiy.

1.4 Results

Three films of $In_{1-x}Ga_xAs_yP_{1-y}$ have been grown on InP substrates under similar growth conditions. In an effort to determine long term reproducibility, these conditions were also similar to a layer grown seven months previously. Deposition parameters for all the films are given in Table 1. Since it was believed that thin layers, < 0.5 μm, may have their mobilities reduced due to a significant contribution from interfacial states, it was felt important to grow reasonably thick layers, ~ 1.0 μm. Analysis of all the films by electroreflectance showed that the higher bandgaps were coincident. X-ray rocking curves on one sample were analyzed together with bandgap data to estimate both fundamental bandgap and lattice constant, and hence to determine the composition parameters. Evidence of inhomogeneity was present in the rocking curves. A limit on the accuracy of this technique to measure lattice constant was evaluated; this suggested that the techniques may not be useful for a mismatch $\Delta a/a_o \leq 0.001$, as far as the apparatus here is concerned.

An Auger spectrometer has been incorporated into the MBE system which enables the quality of the substrate surface to be evaluated prior to growth and whilst within the MBE system vacuum. The MBE layer can be evaluated after growth and while still under vacuum conditions.

1.5 Plans for Next Quarter

- Incorporate and test new flux monitoring system
- Grow MBE GaAs on specially prepared substrates supplied by NRL.

Layer	Thickness μm	Mobility $cm^2V^{-1}s^{-1}$	Concentration cm^{-3}	E_1 eV	$E_1 + \Delta_1$ eV
D0206-II	0.8	2126	1.6×10^{17}	2.613	2.883
D0922-II	1.25	4000	1.9×10^{17}	2.615	2.885
D0925	0.39	3635	2.4×10^{17}	2.611	2.876
D1026	0.52			-	-

Table 1. Do

2.0 MBE SYSTEMS

Two MBE systems will be used during the time of the contract. The main system will be used to grow quaternaries, ternaries and binaries involving phosphorous. The other system is used solely for GaAs and any growth concerning GaAs will take place in this system. The GaAs MBE system will be used during the next quarter and will be discussed in detail then.

A schematic of the MBE growth system is shown in Figure 1. The system is pumped by two separate pumping systems, a cryopump working directly into the growth chamber, and an ion pump coupled via the interlock. Initial roughing of the entire system is accomplished using a rotary pump, followed by sorption pumping. All parts of the system, including the pumps, can be baked out at temperatures up to 200 °C. The interlock allows substrates to be loaded without the need to open the main growth chamber to atmosphere, thus reducing the possibility of contamination. The only time the growth chamber is opened is for source replenishment. Six ovens are available and are mounted inside a water cooled cryoshroud. A further cryogenic panel surrounds the region between the sources and substrate to prevent contamination from materials desorbing from the chamber walls.

At the bottom of the growth chamber is an optical viewing port which enables the layer to be visually evaluated during growth. If the layer does not appear to be smooth, growth can be terminated which reduces waste of oven loads. This port can also be used to access a laser, either for surface evaluation or for possible laser annealing during growth.

An ion gauge immediately behind the substrate position is used to determine the flux rates from each oven in turn. Typical base pressures for the complete system, after bakeout and prior to growth, with the

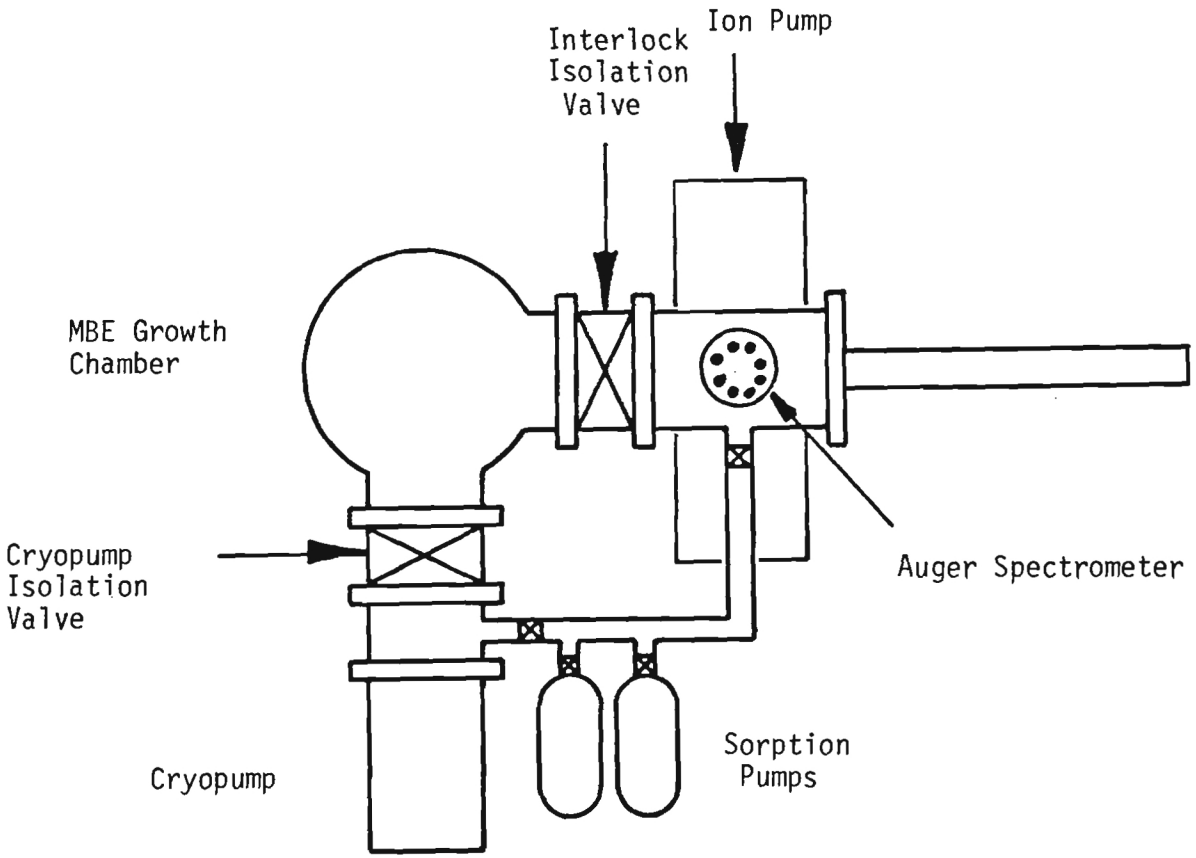

Figure 1. Schematic of MBE Quaternary Growth System.

substrate in position and with ovens at low temperatures, are about 4×10^{-10} Torr.

A major modification during this part of the program has been the incorporation of an Auger spectrometer into the interlock chamber. This allows the surface of the substrate to be evaluated prior to growth. Previously, the substrate had been thermally cleaned at 530 °C for 45 sec. in an arsenic flux in order to remove the oxide layer. This temperature was deduced after an independent study using a separate Auger system. It soon became clear that some discrepancy between that system and the substrate temperature monitor in the growth chamber must exist since an Auger spectrum, after thermal cleaning, clearly detected the presence of oxygen. Thermal cleaning is now performed by heating in the InP substrate at 560 °C for 45 sec. in an arsenic flux.

Various oven loads can be used for quaternary growth, including either elemental or compound loads. For the present case, InP was used as a phosphorous source, GaAs for arsenic, Ga for gallium and In for indium. These were chosen so as to duplicate a previous run and should not necessarily be taken as being the optimum conditions. The only major problem with this combination arises from the InP phosphorous source. The phosphorous depletes very rapidly and only about 5 - 6 hours growth time (3 - 4 μms layer thickness) can be achieved. An effort to increase this by using a larger load in a longer oven (the diameter being fixed by the hole in the cryoshroud) resulted in an increase in the amount of P_4 being emitted, as measured by a quadrupole mass spectrometer.

As mentioned previously, various oven loads may be used. In addition to the compound sources mentioned above (GaAs for As and InP for P), the elemental loads may also be used. The main problem with these is that

flux control is difficult due to the high vapor pressure, and hence low oven temperature of these elemental loads. Compound sources are presently used since the oven temperatures are much higher and flux control is much easier.

It is proposed that a new ion gauge monitoring system be incorporated into the MBE system which will monitor the flux rates of each oven separately and which can be used to control the oven temperatures and therefore enable elemental arsenic to be used with adequate flux control.

3.0 ANALYSIS OF LAYERS

3.1 Purpose of Growth Runs

In an attempt to determine the reproducibility of the quaternary MBE system, three layers of $In_{1-x}Ga_xAs_yP_{1-y}$ have been grown on Fe-dop InP substrates under almost identical conditions which were also sim to a layer grown almost seven months previously. The layers were gr using In, Ga, GaAs and InP ovens. Deposition parameters are given i Table 1. In this table, layer D0206-II has been characterized using Auger spectroscopy to obtain the composition parameters. From this measurement y was estimated to be 0.6 and x as 0.32. From Figure 2, shows the bandgap as a function of x and y when lattice match is not assumed, these values would give $E_g \approx 0.68$ eV. Bandgap measurements however, suggest a value closer to 0.8 eV. As will be shown later, better composition determination can be made using a combination of optical and x-ray techniques. The Auger measurement is, at best, accurate only to within 20%.

3.2 Composition Analysis

3.2.1 X-ray Rocking Curves

X-ray diffraction is a very useful method to determine the lat constant directly. Using diffraction profiles of the substrate as internal calibration, it is only necessary to determine the differe the diffraction angles of the substrate and layer. Thus, it is not necessary to be able to measure the angle of diffraction absolutely The lattice paremeter of the layer can be calculated, using (400) reflection, from the equation

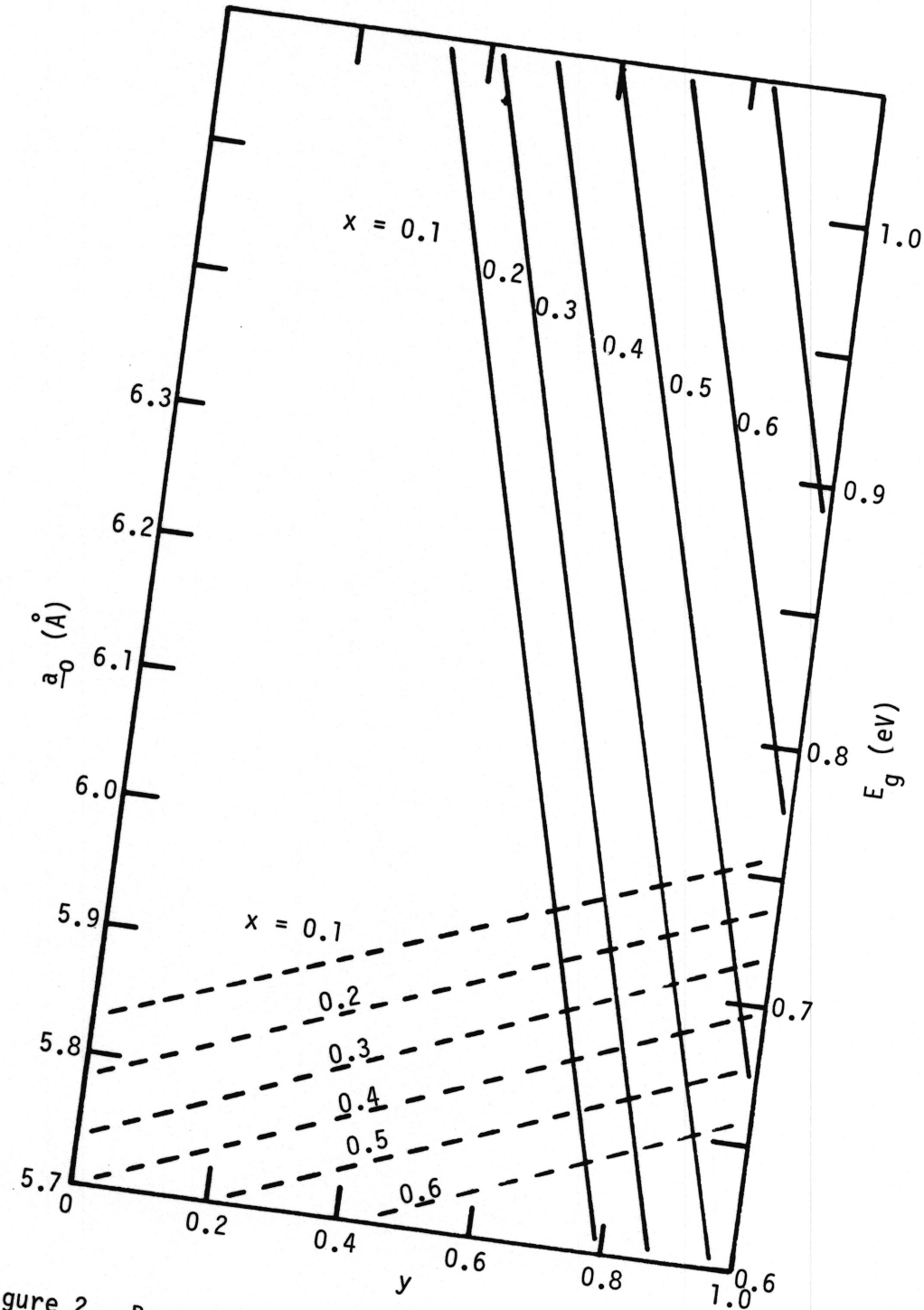

Figure 2. Bandgap (——) and lattice constant (---) of $In_{1-x}Ga_xAs_yP_{1-y}$ as functions of x and y.

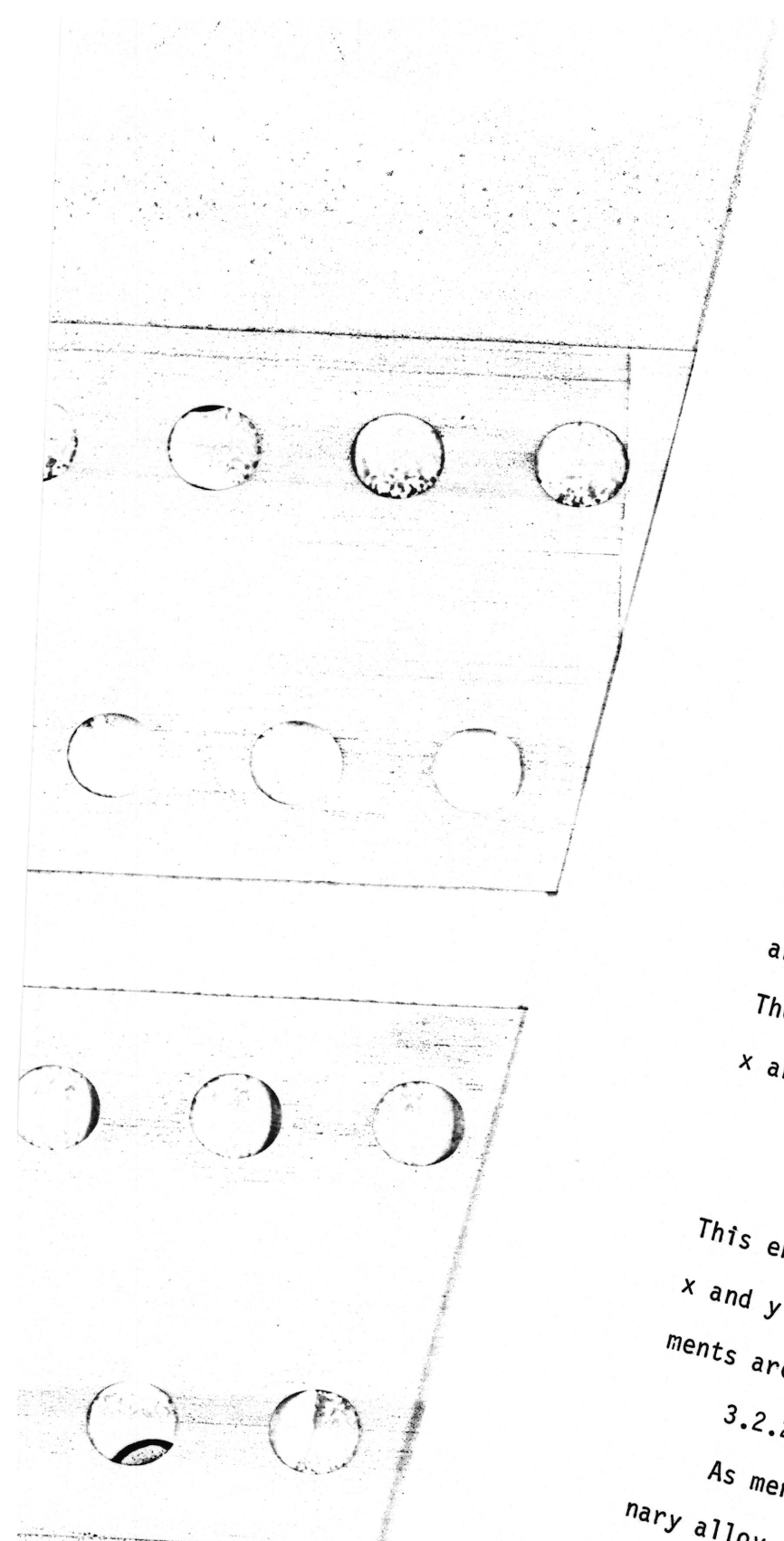

$$\underline{a}_o = \frac{2\lambda}{\sin\{\Delta\theta + \sin}$$

where λ is the x-ray wav

$\Delta\theta$ is the angle betw

the layer peak and

$\underline{a}_s$ is the substrate l

A rocking curve, as this technique is c

D0926-II. The $CuK\alpha_1$ and $K\alpha_2$ lines due

seen. The diffraction profile due to th

intense. This is clearly a limit on dete

When such a broad peak coalesces with the

considerable range of lattice constants whi

This is especially true as better lattice ma

analysis of this profile, a lattice constant

The lattice constant can be expressed in term

x and y, and are given by:

$$\underline{a}_o = 0.1894y - 0.418x + 0.0330xy$$

This enables a relationship between x and y to b

x and y uniquely requires further information. T

ments are based on optical techniques.

3.2.2 Infrared Transmission

As mentioned earlier, one of the most useful a

nary alloy system is to be able to adjust the bandga

parameters x and y. This relationship is given by:[9]

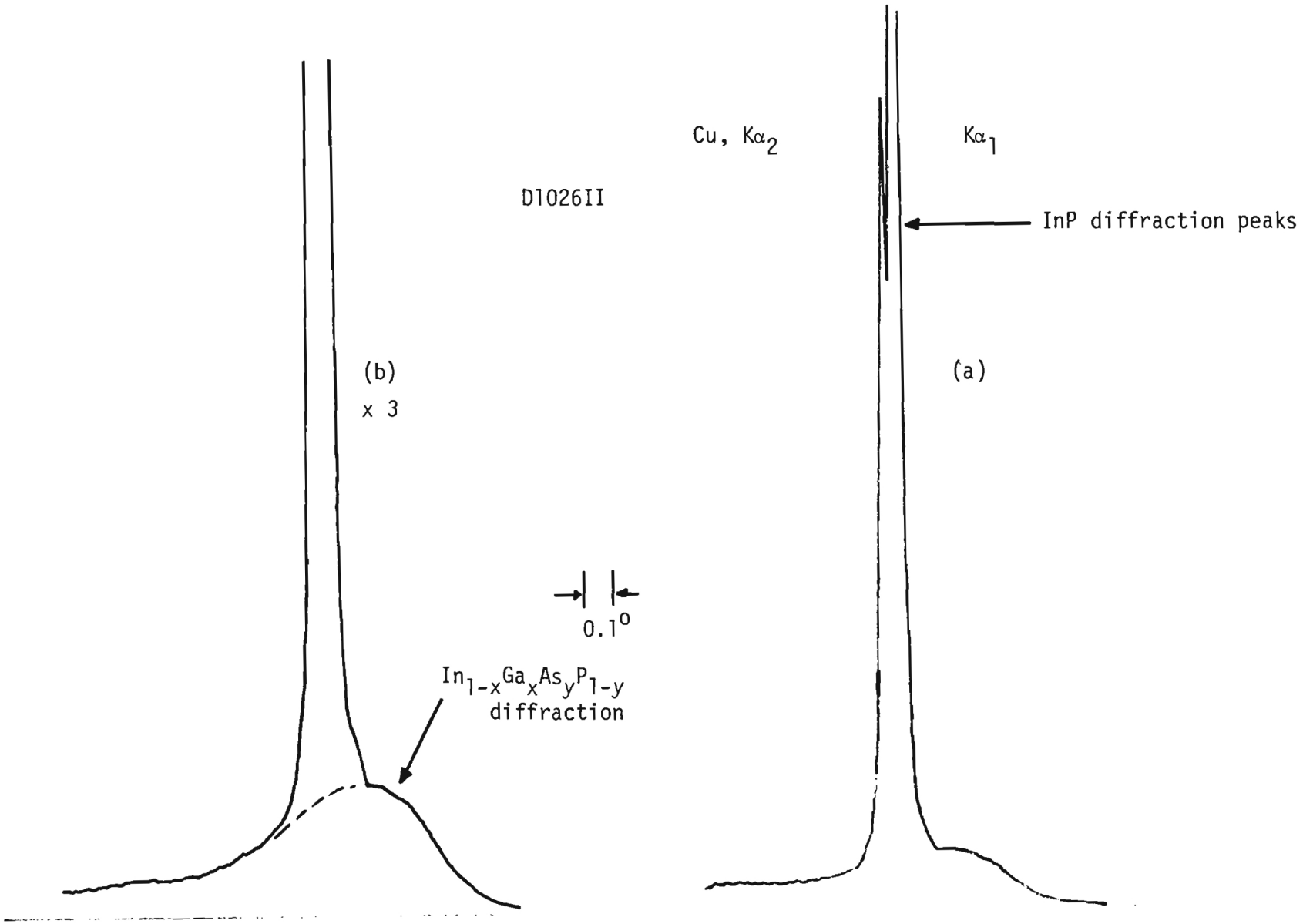

Figure 3. X-ray rocking curve for MBE $In_{1-x}Ga_xAs_yP_{1-y}$ layer on InP substrates. {400} Cu Kα reflection.

$$E_g(x,Y) = 1.35 - y + 1.4x - 0.33y - (0.857 - 0.28y)x\,(1-x) - (0.101 + 0.109x)y\,(1-y)$$

Hence, by measuring E_g, a further relationship between x and y can be obtained. Together with the different functional relation obained from a determination of the lattice constant,[10] this enables, therefore, a precise determination of x and y to be made.

The simplest way to determine E_g is to measure the infrared transmission of the sample. Such a spectrum is shown in Figure 4. This represents the transmission of the combined substrate layer system. Usually the absorption coefficient is used to determine E_g. For the case of a thin film on a substrate, this difficult to calculate, however the general profile does allow a reasonable determination of E_g to be made. In this case a value of $E_g = 0.77 \pm 0.3$ eV would seem to be reasonable.

Before solving this value simultaneously with that derived from the lattice measurement, a more precise measurement teqhnique should be discussed, namely that of electroreflectance.

3.2.3 Electroreflectance

Electroreflectance is one form of modulation spectroscopy. In modulation spectroscopy the optical spectra of a solid is modulated in some way by a periodic variation of the measurement condition. This modulated perturbation gives rise to sharp, differential-like optical features in the region of photon energies where optical excitation processes occur. Changes in reflectance as small as 10^{-6} can be observed using phase sensitive detection. One common technique used to modulate the reflectance is the application of an electric field across the solid. Electroreflectance enables not only the fundamental bandgap to be determined more precisely,

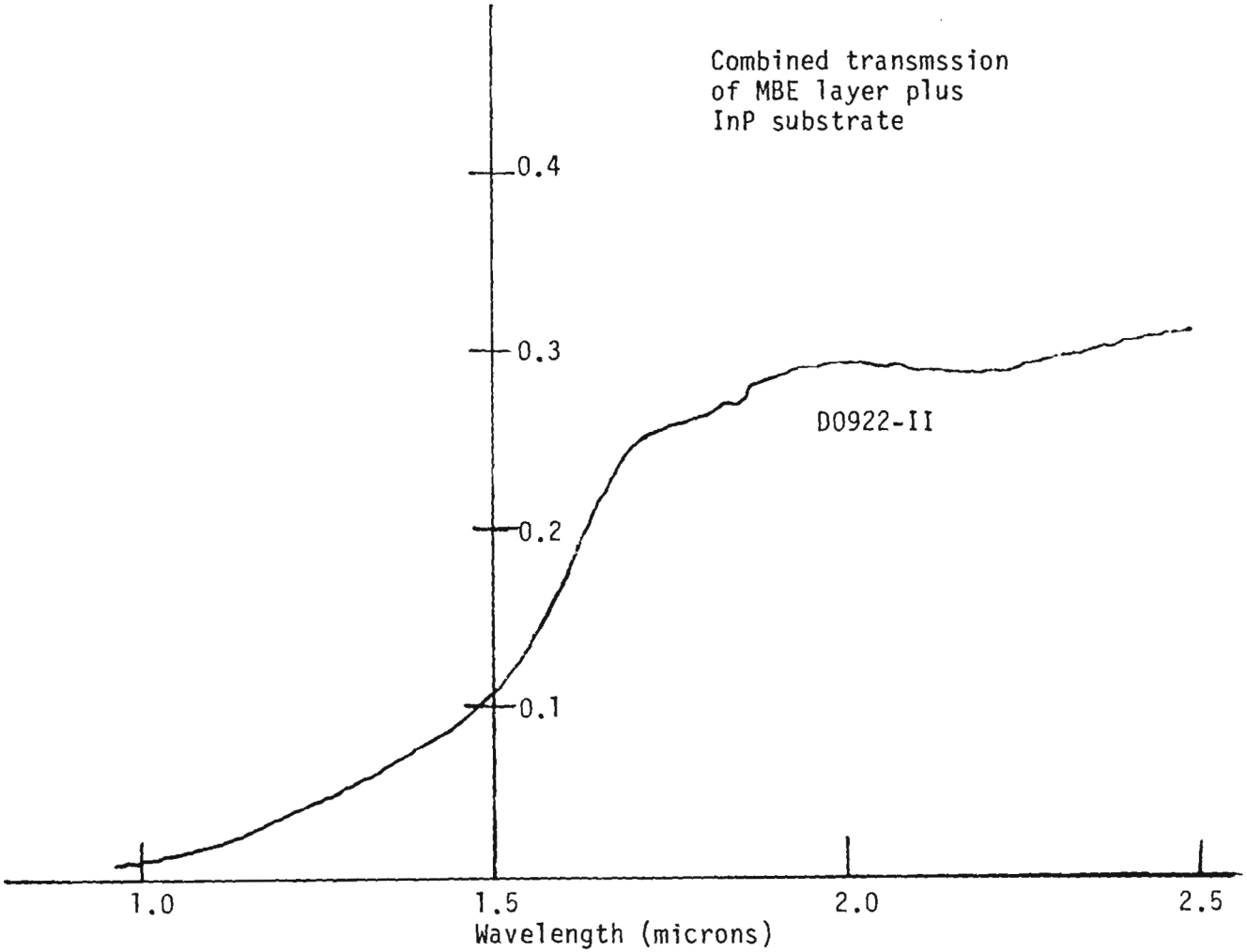
Combined transmssion
of MBE layer plus
InP substrate
0.4
0.3
0.2
0.1
D0922-II
1.0
1.5
2.0
2.5
Wavelength (microns)

due to its derivative property, but also the higher bandgaps, E_1 and E_2 for example, together with spin-orbit spittings. Since the energies E_0, E_1 and E_2 correspond to different wavelengths and hence different absorption coefficients, it is possible to use this technique for depth profiling. Carrier concentrations can also be determined since the strength of the electroreflectance signal is linearly proportional to the carrier concentration.

The technique is essentially quite simple; an audio-frequency modulated-voltage (typically $\sim$ 1V) is placed across the sample. The incident white light is modulated slowly, $\sim$ 100 Hz, the reflected radiation is detected and the output fed into two lock-in amplifiers tuned to both frequencies. The outputs of the lock-ins are fed into a ratiometer to give $\Delta R/R$. ΔR is the signal at the audio frequency and R is the signal at the 100 Hz frequency.

Electroreflectance measurements have been made on a number of samples, in the vicinity of the E_1 and $E_1 + \Delta_1$ peaks. This higher transition ensures that the penetration of the radiation is small and thus only the film is investigated. The results shown in Figure 5 show clearly that although the signal levels vary, the peaks lie at the same energies from sample to sample. This confirms quite clearly the reproducibility of the MBE system.

Following the work by Pollack and co-workers,[11,12] the lattice-matched composition-dependence of the various energy transitions for $Ga_xIn_{1-x}As_yP_{1-y}$ can be determined, and this is shown in Figure 6. Values of E_1 of 2.62 eV and $E_1 + \Delta_1$ of 2.88 eV are consistent with an E_0 of $\sim$ 0.82 eV, which is close to that deduced from the transmission measurement. This has assumed that a slight lattice mismatch, $< 0.5\%$, will not effect these values significantly.

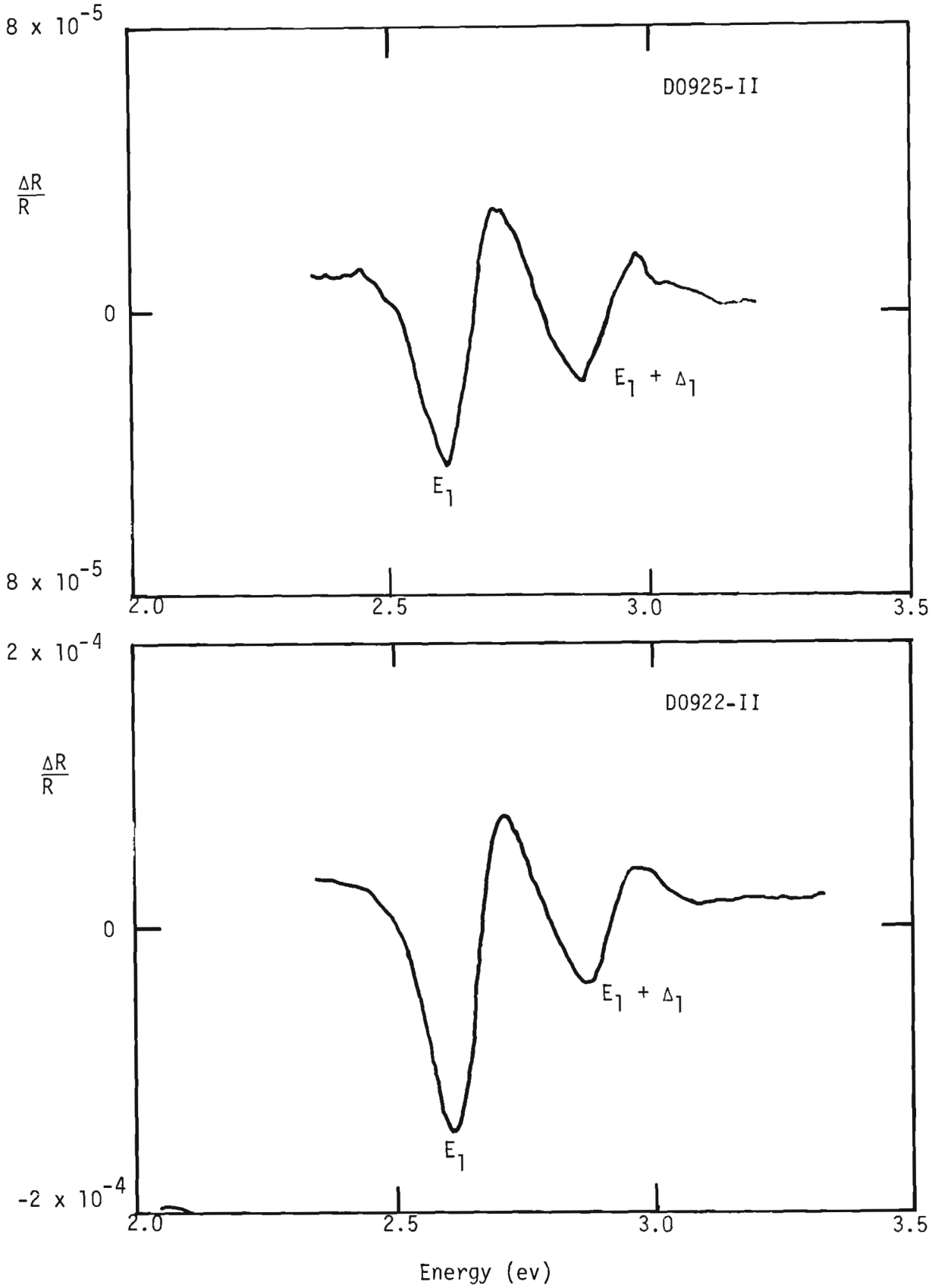

Figure 5(a). Electroreflectance spectra of two $In_{1-x}Ga_xAs_yP_{1-y}$ MBE layers on InP substrates.

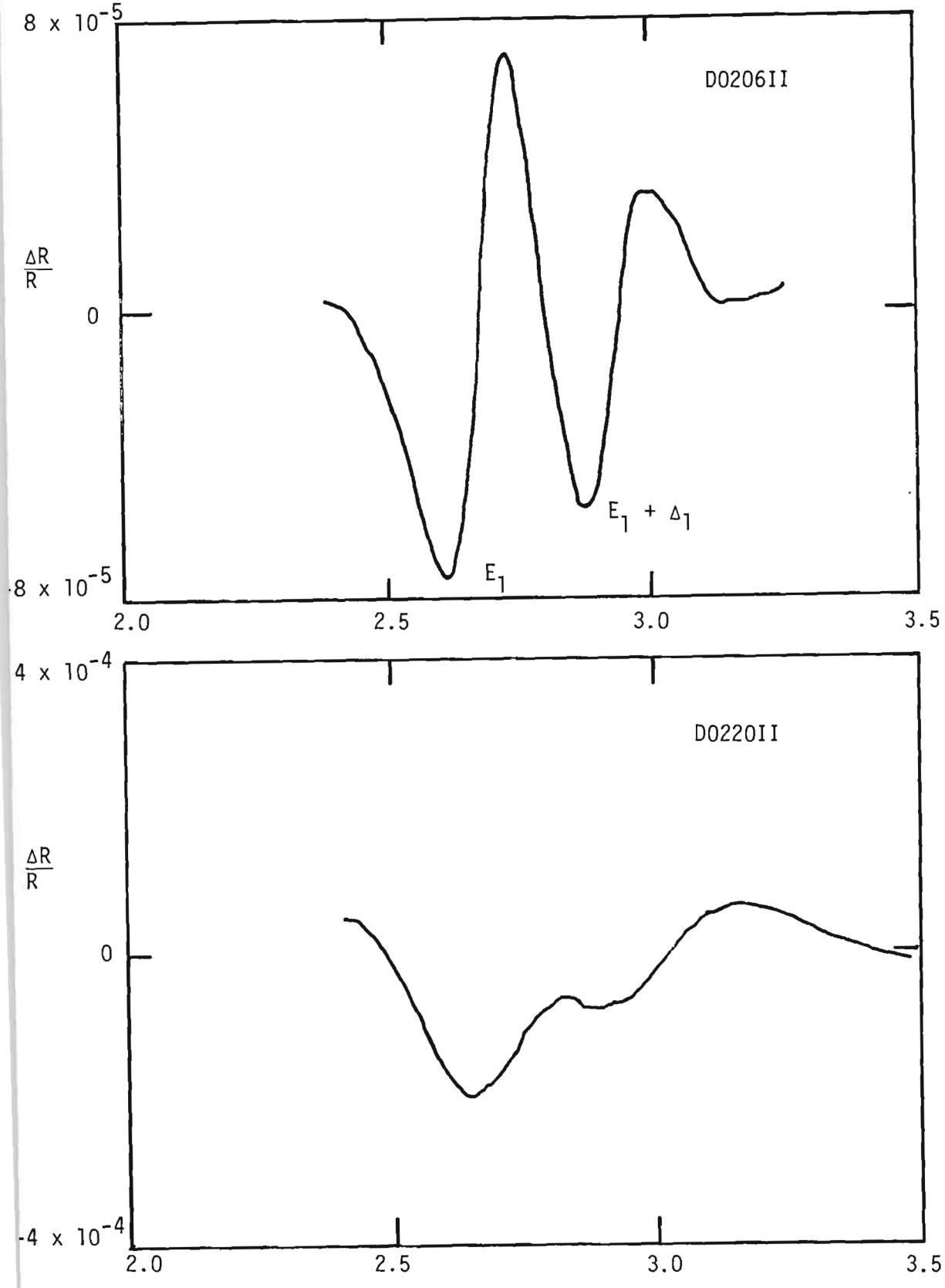

Figure 5(b). Electroreflectance spectra of two $In_{1-x}Ga_xAs_yP_{1-y}$ MBE layers on InP Substrates.

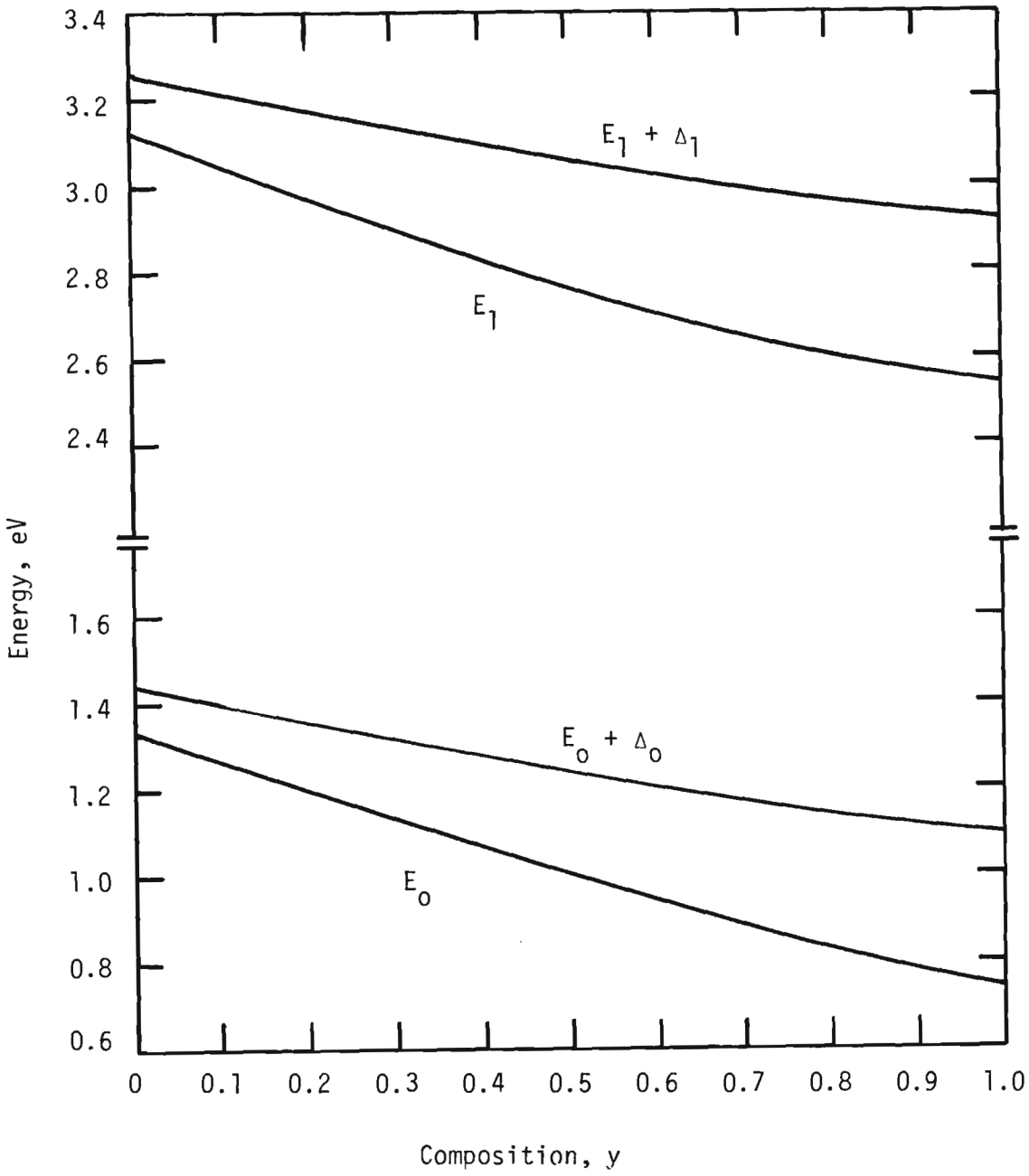

Figure 6. Composition dependence of electroreflectance peaks, after Laufer et.al.

A unique composition can now be determined using a lattice constant of 5.897 Å and a fundamental bandgap of 0.82 eV. The composition parameters are calculated to be, $y = 0.70 \pm 0.01$ and $x = 0.26 \pm 0.01$. The electroreflectance data would suggest this composition for D0206-II also, this must be compared with that deduced from the Auger measurement, of $y = 0.60$ and $x = 0.32$. These lie almost within the 25% expected error and are therefore consistent with the optical measurement.

3.2.4 Reflection Electron Diffraction

Although the aforementioned measurements are adequate to determine composition information on the overall quality of the growth is also of interest.

Reflection electron diffraction (RED) measurements have been made on layer D0922-II. Since the penetration depth of the electron beam is low due to the high probability for inelastic scattering of the incident electrons, with the consequence that only those electrons which are inelastically scattered very near the surface are able to escape, RED only probes the first few atomic layers. The RED pattern of D0922-II is shown in Figure 7. The distinctive streaking confirms the epitaxial single crystal growth and the smooth surface.

3.2.5 Optical Micrograph

Further evidence as to the surface quality of the layers is furnished by the optical micrograph of layer D1026-II shown in Figure 8. The magnification is 500x. All films had a mirror-like appearance. It is clear from the figure that the surface is smooth and free from cross-hatching. The phenomenon of cross-hatching is usually associated with gross lattice mismatch. This correlation has been studied in some detail by Oe[13] et.al. who found that, for LPE grown $In_{1-x}Ga_xAs_yP_{1-y}$ layers grown on InP, cross-

Figure 7. Reflection Electron Diffraction of MBE $In_{1-x}Ga_xAs_yP_{1-y}$ on InP substrate, layer D0922II.

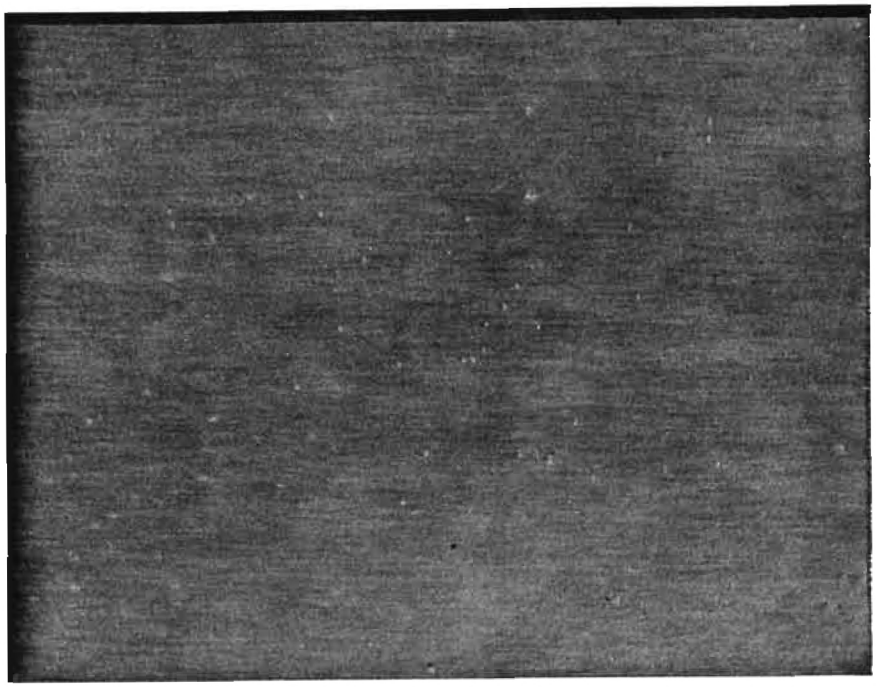

Figure 8. Optical Micrograph, magnification X500, of MBE $In_{1-x}Ga_xAs_yP_{1-y}$ on InP, layer D1026II.

hatching only occurred for lattice mismatch greater than 0.005. Since Figure 8 shows no evidence of such cross-hatching, this would imply an upper limit of mismatch, for the samples grown here, of < 0.005. This figure is consistent with the lattice match as calculated from the composition parameters given by the electroreflectance and x-ray rocking curves.

3.2.6 Summary

The limiting measurement in determining the composition is the x-ray diffraction measurement. The measurement performed here probably represent an upper limit on mismatch. If good lattice match had been achievable, the electroreflectance could have been used to determine composition directly. Under these conditions, the values would be; $y = 0.79$ and $x = 0.38$. It is clear that further improvement in the x-ray technique is needed to determine the composition more precisely. It is probably not feasible to improve the existing apparatus significantly, although there is a possibility of a slight improvement. However, an alternative method which could be used to help in composition analysis is to measure the lattice vibrational frequencies. Using Raman scattering and infrared reflectivity[14] it has been extablished that, for the GaAs-like mode, the longitudinal optical phonon frequency in cm^{-1} can be expressed as

$$W_{LO} = 223 + 48y$$

This assumes approximate lattice match and therefore, further and more complete data are needed before the equation can be confirmed for the complete region. However a similar expression will eventually be obtained. Since it should be possible to measure the phonon frequency to within 2 cm^{-1}, this implies that y can be determined to within $\pm$ 0.02. Although little work has been performed on calculating the phonon frequencies as functions

of x and y, this would be a very useful study. Simple model calculations could be performed without too much effort, based upon existing model calculations.

Experimentally, the reflectivity measurements would be performed using a Fourier Transform Spectrometer. The design and construction of the FTS specifically for semiconductor characterization is presently underway at Georgia Tech.

3.3 Electrical Measurements

As far as device operation is concerned, it is important that the highest mobility is achieved. Presently, the only way of measuring this parameter is to use the Hall effect. Before discussing Hall data on the samples grown here, an alternative technique which will be used in the future to complement the Hall techniques will be discussed.

3.3.1 Optical Technique to Measure Carrier Concentration and Mobility

Free-carrier plasmas in semiconductors dramatically effect the optical properties. Of particular relevance here, is the reflection due to the free-carrier plasma. To demonstrate how this can be used, a simple analysis for GaAs will be discussed. The infrared reflectivity is due to lattice vibration and free-carrier contributions. The dielectric constant can be written, for a binary, as

$$\varepsilon(\omega) = E_\infty + \frac{S_{\omega_0}^2}{(\omega_0^2 - \omega^2 - i\Gamma\omega)} - \frac{\omega_\rho^2 \varepsilon_\infty}{\omega(\omega + i\gamma)}$$

where ε_∞ is the high-frequency dielectric constant

ω_0 is the lattice vibrational frequency

Γ lattice damping

ω_ρ is the free-carrier plasma frequency

γ is the free-carrier damping (inverse of scattering time).

$$\omega_\rho^2 = \frac{4\pi N e^2}{m^* \varepsilon_\infty}$$, N = carrier concentration

e = electronic charge

m^* = electron effective mass

$$\frac{1}{\gamma} = \frac{\mu m^*}{e}$$

Without going into the mathematical detail, it suffices to say that the reflection can be analyzed to yield ω_ρ (and hence N) and γ (hence μ), if the effective mass is known.

The advantage of this technique is that it is contactless and hence problems associated with producing good ohmic contacts do not arise. A full discussion of this technique can be found elsewhere. Figure 9 shows calculated reflection curves for GaAs for various carrier concentrations and mobilities. It can be seen that, depending upon the conditions, it should be possible to measure mobilities down to 1000 $cm^2V^{-1}s^{-1}$ and carrier concentrations between $10^{18}cm^{-3}$ and $10^{-5}cm^{-3}$.

These measurements, together with Hall data, should enable high-confidence values of mobility and carrier concentration to be made. As in the lattice vibrational analysis, the experimental technique is Fourier Transform Spectroscopy. As an added bonus, this method with appropriate analysis, can yield the layer thickness.

3.3.2 Hall Measurements

The temperature dependence of the mobility has been measured using the van der Pauw configuration of the Hall technique. Contacts were formed

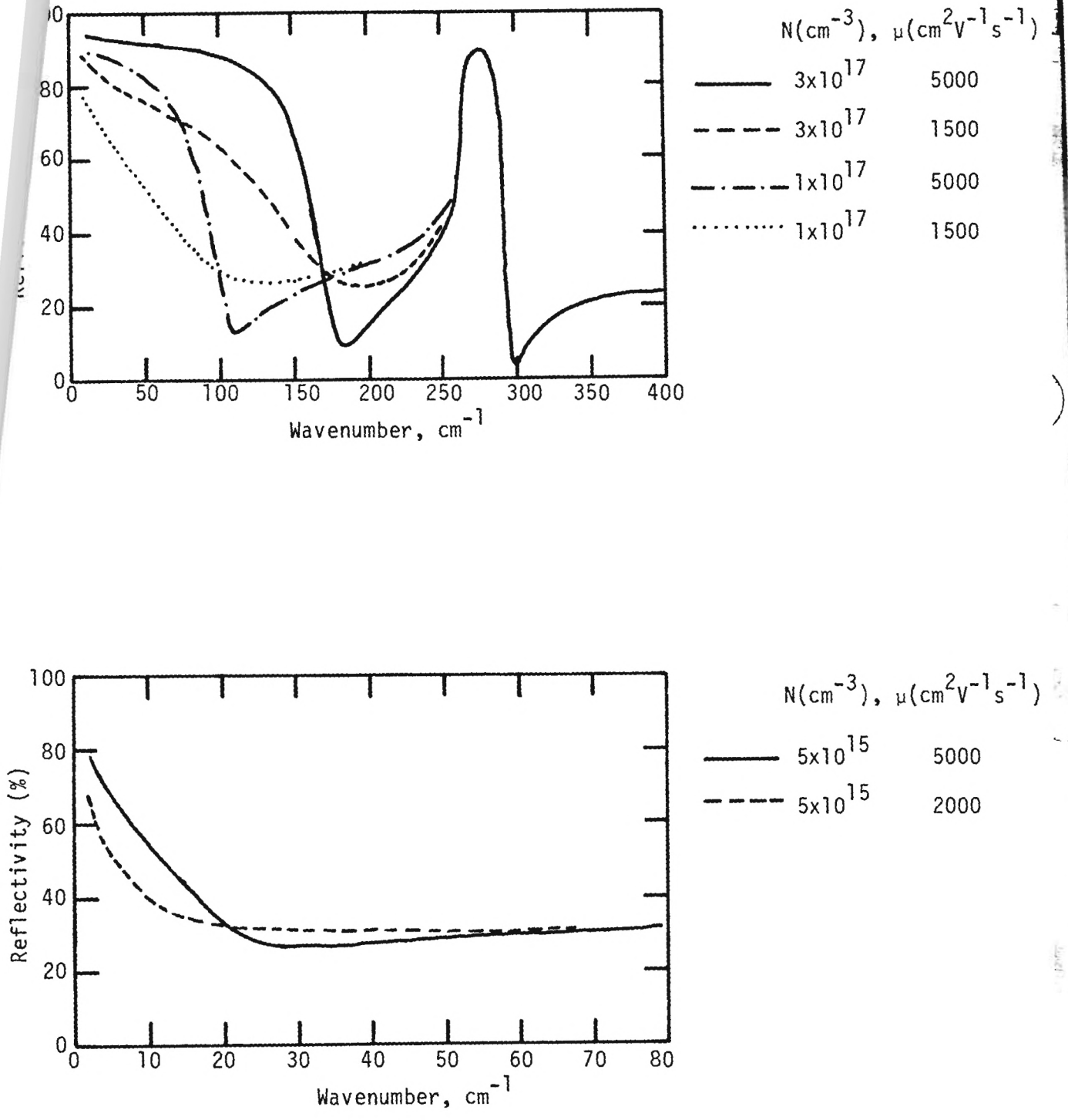

Figure 9. Infrared Reflection spectra for GaAs showing various free-carrier plasma contributions. Lattice contribution is identical for all cases.

by evaporating Au-Ge (88:12) pads; usually it was found that good ohmic contact could be obtained without any alloying. The results for two samples are shown in Figure 10. The relatively flat response shows the significant effect of alloy scattering. This has been typical of most of the n-type $In_{1-x}Ga_xAs_yP_{1-y}$ samples grown by MBE. The carrier concentration of D0926-II, unintentionally n-type, ranged from $1.9 \times 10^{17} cm^{-3}$ at 105 °K to $2.8 \times 10^{17} cm^{-3}$ at 300 °K.

3.3.3 Summary

It is still not routine to make consistently high quality electrical measurements of the mobility and carrier concentration. There are inherent problems in producing good ohmic contacts. These difficulties are being addressed in two ways. Firstly, the complete Hall measurement set-up is being reevaluated and short term improvements, especially for room temperature contacting, have already been incorporated. In the long term a completely new, fully automated Hall apparatus is being designed. This will consist of a Lakeshore Cryogenic cryostat, small electro-magnet and microprocessor control. New contacting procedures are being evaluated to reduce errors arising from uncertain contacts.

The second procedure involves the use of optical techniques. In addition to the analysis of infrared reflectivity, as detailed in Section 3.3.1, the electroreflectance measurement may also be used to obtain carrier concentration, as deduced from signal strengths.

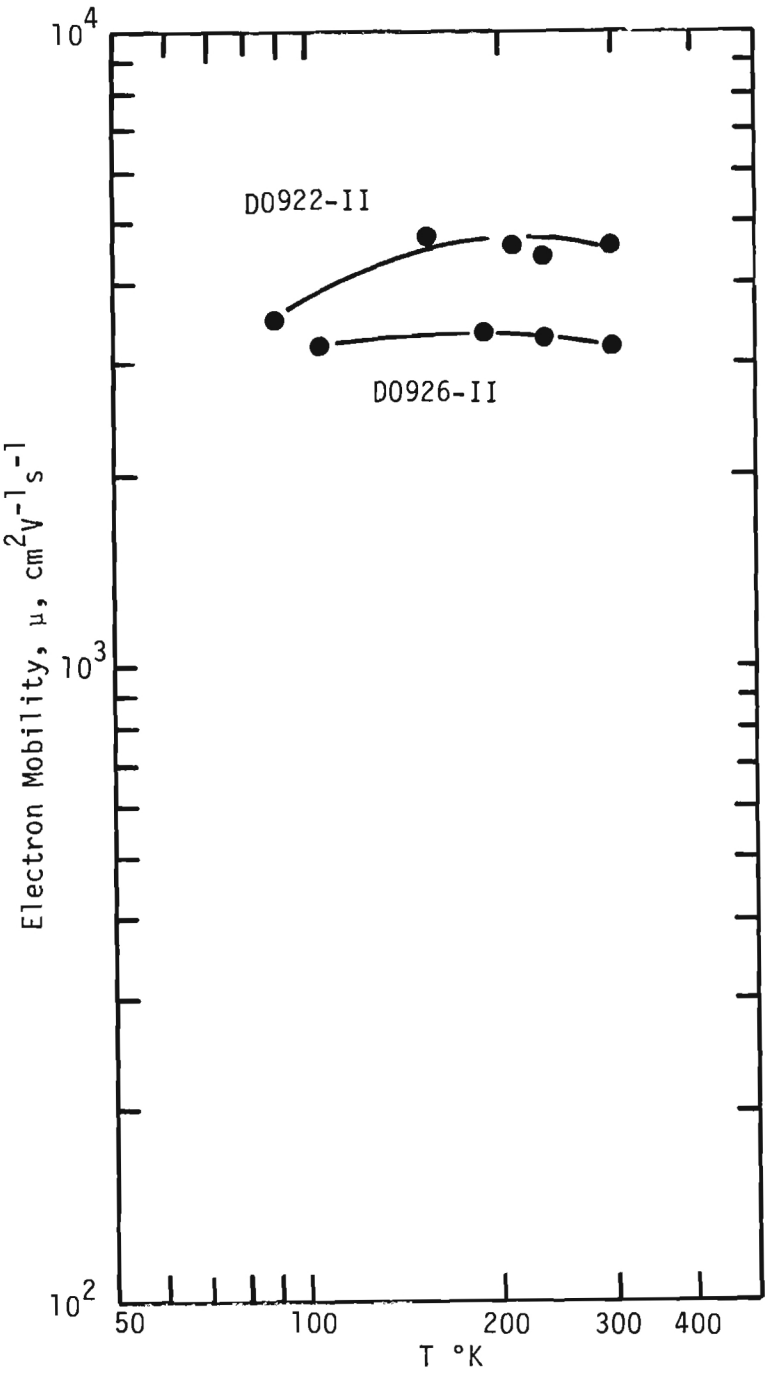

Figure 10. Temperature dependence of Hall mobility for two similar $In_{1-x}Ga_xAs_yP_{1-y}$ layers on InP.

4.0 REFERENCES

1. "Special Issue on Quaternary Compound Semiconductor Materials and Devices - Sources and Detectors." IEEE J. Quantum Electronics, QE17, pp. 117 - 284, (1981).

2. C. J. Neuse, "III-V Alloys for Optoelectronic Applications," J. Electron, Mater., 6, pp. 253-293 (1977).

3. D. Botez, "InGaAsP/InP Double Heterostructure Lasers: Simple Expression for Wave Confinement, Beamwidth, and Threshold Current over Wide Ranges in Wavelength (1.1 - 1.65 μm)," IEEE J. Quantum Electron 17, pp. 178-186, (1981).

4. S. R. Forrest, "Performance of $In_xGa_{1-x}As_yP_{1-y}$ Photo-diodes with Dark Current Limited by Diffusion, Generation Recominbation, and Tunneling," J. Quantum Electron 17, pp. 217-226, (1981).

5. S. Arai and Y. Suematsu, "1.11 - 1.67 μm (100) GaInAsP/InP Injection Lasers Prepared by Liquid Phase Epitaxy," IEEE J. Quantum Electronics QE16, pp. 197-205, (1980).

6. G. H. Olsen, C. J. Nuese, and M. Ettenberg, "Low-threshold 1.25 μm vapour grown InGaAsP CW lasers," Appl. Phys. Lett 34, pp. 262-264, (1979).

7. M. A. Littlejohn, J. R. Hauser, and T. H. Glisson, "Velocity-field characteristics of $Ga_{1-x}In_xP_{1-y}As_y$ quaternary alloys," Appl. Phys. Lett. 30, pp. 242-244, (1977).

8. Y. Takeda, M. A. Littlejohn, and J. R. Hauser," Electron Hall mobility in $Ga_xIn_{1-x}As_yP_{1-y}$ calculated with two-longitudinal optical-phonon model," Appl. Phys. Lett. 39, pp. 620-621, (1981).

9. R. E. Nahory, M. A. Pollack, W. D. Johnston, Jr., and R. L. Varnes, "Band Gap versus composition and demonstration of Vegard's Law for $In_{1-x}Ga_xAs_yP_{1-y}$ Lattice-matched to InP," Appl. Phys. Lett. 33 pp. 659-661, (1978).

10. R. L. Moon, G. A. Antypas, and L. W. James, "Bandgap and Lattice Constant of GaInAsP as a function of Alloy Composition," J. Electron Mater., 3, pp. 635 - 644, (1974).

11. F. H. Pollack, "Modulation spectroscopy as a technique for semiconductor characterization," Proceedings of the Society of Photo-Optical Instrumentation Engineers, Vol. 276, pp. 142-156, (1981).

12. P. M. Laufer, F. H. Pollack, R. E. Nahory and M. A. Pollack, "Electroreflectance Investigation of $In_{1-x}Ga_xAs_yP_{1-y}$ Lattice-matched to InP," Solid State Commun., 36, pp. 419-422, (1980).

13. K. Oe, Y. Shimoda, and K. Sugiyama, "Lattice deformation and misfit dislocation in GaInAsP/InP double-heterostructure layers," Appl. Phys. Lett 33, pp. 962-964, (1978).

14. P. M. Amirtharaj, G. D. Holah, and S. Perkowitz, "Far Infrared spectroscopic study of $In_{1-x}Ga_xAs_yP_{1-y}$," Phys. Rev. B.21, pp. 5656-5661, (1980).

QUARTERLY PERFORMANCE AND STATUS OF FUNDS

Level of Effort

Categories	1 August 1981 - 31 October 1981	Cumulative Total (Man months)
Principal Research Engineer/Scientist	0.2	0.2
Senior Research Engineer/Scientist	2.2	2.2
Research Engineer/Scientist	0.2	0.2
Assistant Research Engineer/Scientist	0.4	0.4
Graduate Research Assistant	-	-
Co-op, Student	-	-
TOTAL	3.0	3.0

Financial Status

1 August 1981 - 31 October 1981	Cumulative Total Expended
$19,298	$19,298

Total Contract Funding (through 30 April 1982)	$99,982

A-2951

BINARY, TERNARY AND QUATERNARY HETEROJUNCTIONS OF III-V SEMICONDUCTORS GROWN BY MOLECULAR BEAM EPITAXY

(A003)

Quaterly Report No. 3

G. D. Holah, E. L. Meeks, and F. L. Eisele

Engineering Experiment Station
Georgia Institute of Technology
Atlanta, Georgia 30332

Report for Period 1 November 1981 - 31 January 1982

Contract No. N00014-81-K-2007

Prepared for:

Naval Research Laboratory
Washington, D.C. 20375

TABLE OF CONTENTS

LIST OF TABLES

LIST OF ILLUSTRATIONS

1.0 INTRODUCTION

This report summarises the research carried out during the third quarter of a program directed towards the preparation and characterization of binary and quaternary III-V semiconductors grown by molecular beam epitaxy. Of specific interest is the application of these materials to the fabrication of diode lasers,[1] detectors[2] and microwave devices[3] which can take advantage of the various novel properties of the materials. In the case of the quaternary layers of $In_{1-x}Ga_xAs_yP_{1-y}$ these properties include the capability of simultaneously adjusting the electronic bandgap whilst at the same time maintaining good lattice match to either InP or GaAs substrates.[4]

1.1 Objectives of Third Quarter

a) To establish a flux monitoring scheme which would enable the fluxes of the individual ovens to be continuously monitored during growth.

b) Grow GaAs layers on specially prepared substrates such that the structures may be fabricated into FET devices.

1.2 Results

a) An electron impact ionization flux monitor has been installed in front of one oven in the MBE system. The system was tested and found to correlate very well with temperature measurements of the same oven. The ion current and cell temperature tracked essentially identically over a large temperature range for both increasing and decreasing temperature. Changes in ion current of three orders of magnitude were easily determined.

b) MBE n-GaAs layers of thickness near 3000Å and with concentrations between 4×10^{16} and 2×10^{17} cm^{-3} have been grown on specially prepared substrates provided by NRL. These

structures are suitable for processing into FET devices. Due to the restriction of being allowed to etch only a small layer (300Å) of GaAs from the substrates, the usual clean/etch procedure had to be modified. Initially there were problems associated with growth of whiskers on the surface which were associated with a lack of cleanliness of the surface. Additional problems have been encountered during mounting of the substrate on the heater. An etching procedure for the rear surface has been formulated which is similar to that for the regular substrates. However problems still exist in getting the indium to bond the substrate to the heater. This will certainly give rise to poorer quality layers. A number of layers have however been grown with mobilities and carrier concentrations suitable for fabrication into FET devices. These have been delivered to NRL and are awaiting processing.

1.3 Plans for Next Quarter

- o Growth of p-InP and fabrication of ohmic contacts
- o Growth of higher mobility layers of $In_{1-x}Ga_aAs_yP_{1-y}$ on InP substrates
- o Growth of n-InP buffer layers on n-InP substrates.
- o Growth of structure suitable for processing into diode lasers near 1.4 μm.

2.0 FLUX MONITOR FOR MBE SYSTEM

2.1 Single Oven Flux Monitor

One of the major problems associated with the growth of $In_{1-x}Ga_xAs_yP_{1-y}$ using MBE is the difficulty of achieving the accurate control of the fluxes from the various ovens necessary to be able to predetermine the composition coefficients x and y. Thus far the flux has been measured for each oven prior to growth and the temperature needed to establish that particular flux has been kept constant during the growth, ideally of course it is the flux which should be kept constant. By monitoring the fluxes before and after growth, changes in the fluxes have been observed. In order to compensate for this, the temperatures of some of the ovens has been judiciously raised during growth. It would clearly be of great benefit if the flux of each oven could be monitored during growth and this information used to control the temperature of the oven.

As a first step towards achieving this, a prototype single oven flux monitor has been installed and tested in the MBE system. A diagram of the monitor and its location is shown in figure 1.

The electron impact ionization flux monitor uses a 100 eV electron beam to ionize a fraction of the neutral molecular beam emerging from a growth oven. The positive ions formed are then collected and the resultant current monitored. The measured current remains proportional to the molecular beam flux as long as the density of gas in the molecular or atomic beam is large compared to the background gas pressure but is not so large as to permit multiple electron scattering events. These conditions are usually satisfied immediately in front of a growth oven under normal MBE growth conditions.

Electrons are emitted from the heated filament and accelerated by a relatively strong electric field to form a broad, diverging electron beam. These electrons, with a typical energy of 100 eV, then pass through a 95% transmitting grid and into a much weaker deccelerating field. The electron beam continues to diverge and gradually decreases in energy as it passes directly in front of an MBE growth oven. The electron beam is perpendicular to the oven flux and sufficiently broad

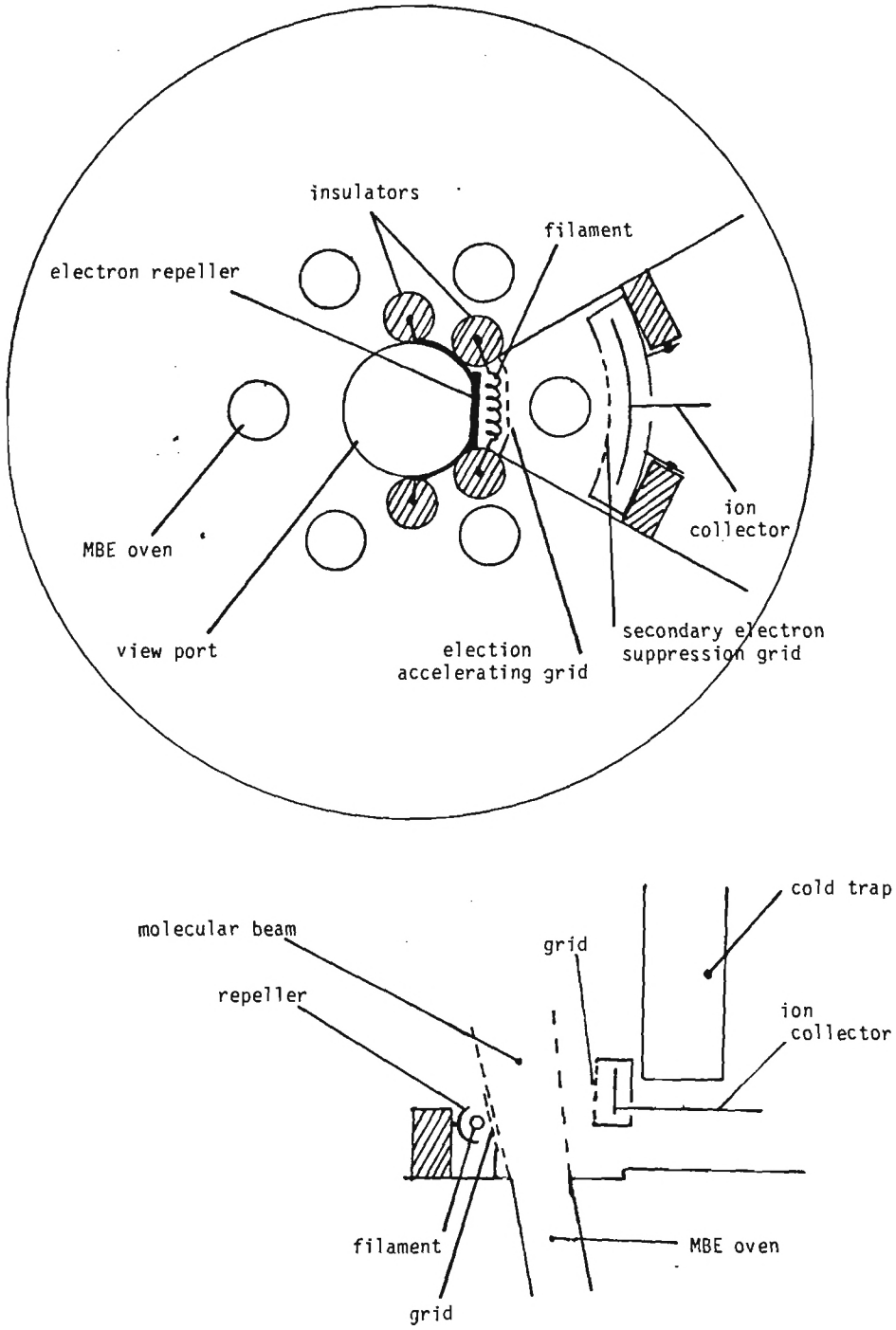

Figure 1. Schematic showing location and construction details of ionization gauge flux monitor.

to pass through virtually all of it.

Except under extreme conditions, about one electron in 10^3 will participate in an ionizing collision with the gas in front of the growth oven. A typical range of molecular densities in front on an MBE growth oven is 10^{10} - 10^{13} molecules/cm^3. Assuming a large ionization cross-section of 10^{-15} cm^2 results in an electron mean free path of at least 100 cm even for the highest growth beam density considered. Thus only a one percent non-linearity would occur under fairly extreme conditions. Most of these electrons, along with those that did not cause ionization, will then pass out of the growth beam and hit the conductive sides of the monitoring assembly. The positive ions produced by the electron beam (which account for at most 0.1% of the total growth beam and can be decreased by several orders of magnitude by decreasing electron beam current) are then accelerated towards a collection plate by the same field which deccelerates the electron beam. These ions then pass through a 95% transmitting grid and are collected on a plate which is maintained at a sufficiently negative potential to prevent the collection of electrons from the monitoring beam. The ion collection plate is surrounded by, but electrically isolated from, a metal housing which prevents electrons or ions from reaching it from all directions expect from the side closest to the growth beam. Thus the ion current is characteristic of the flux from one specific oven. Electrons are prevented from reaching the grid (which encloses this side of the housing) by its electrical potential, which is more negative than either the electron filament or the collection plate. Thus, only positive ions from one direction, and hence one oven, can reach the collection plate; secondary electrons which could be ejected from the collection plate are suppressed by the grid which is in front of it.

The typical electron beam current is about 10^{-3} amps and ion current ranges from 10^{-9} to 10^{-6} amps. The primary limitation of this device for low flux measurements is that of background pressure. Positive ions are formed by electron bombordment of background gas just as they are formed from the growth beam. Thus, if the density of the growth beam approaches the background gas density, a correction for the background gas must be made.

The initial testing of this monitoring system was performed in front of an indium growth oven in one of our MBE growth systems. A plot of the positive ion current versus indium oven temperature is shown in Figure 2.

This flux monitor can be used either directly to control the growth oven or in conjunction with a temperature controller to maintain a constant flux as the oven load is depleted. The long term stability of this monitoring system is increased by using the positive ion current dividied by the electron emission current instead of using the ion current along. Low flux measurements are further improved by monitoring positive ion current from beyond the growth beam path so that the current due to ionization of background gases can be subtracted.

2.2 Summary

It has been demonstrated that continuous flux monitoring during MBE growth is possible at least for a single oven. Further testing is required to determine the ultimate sensitivity and selectivity of the monitor especially when used in a multi-oven configuration. Feedback control of the oven temperature by the flux rate has to be verified initially for a single oven and then for a multi-oven geometry.

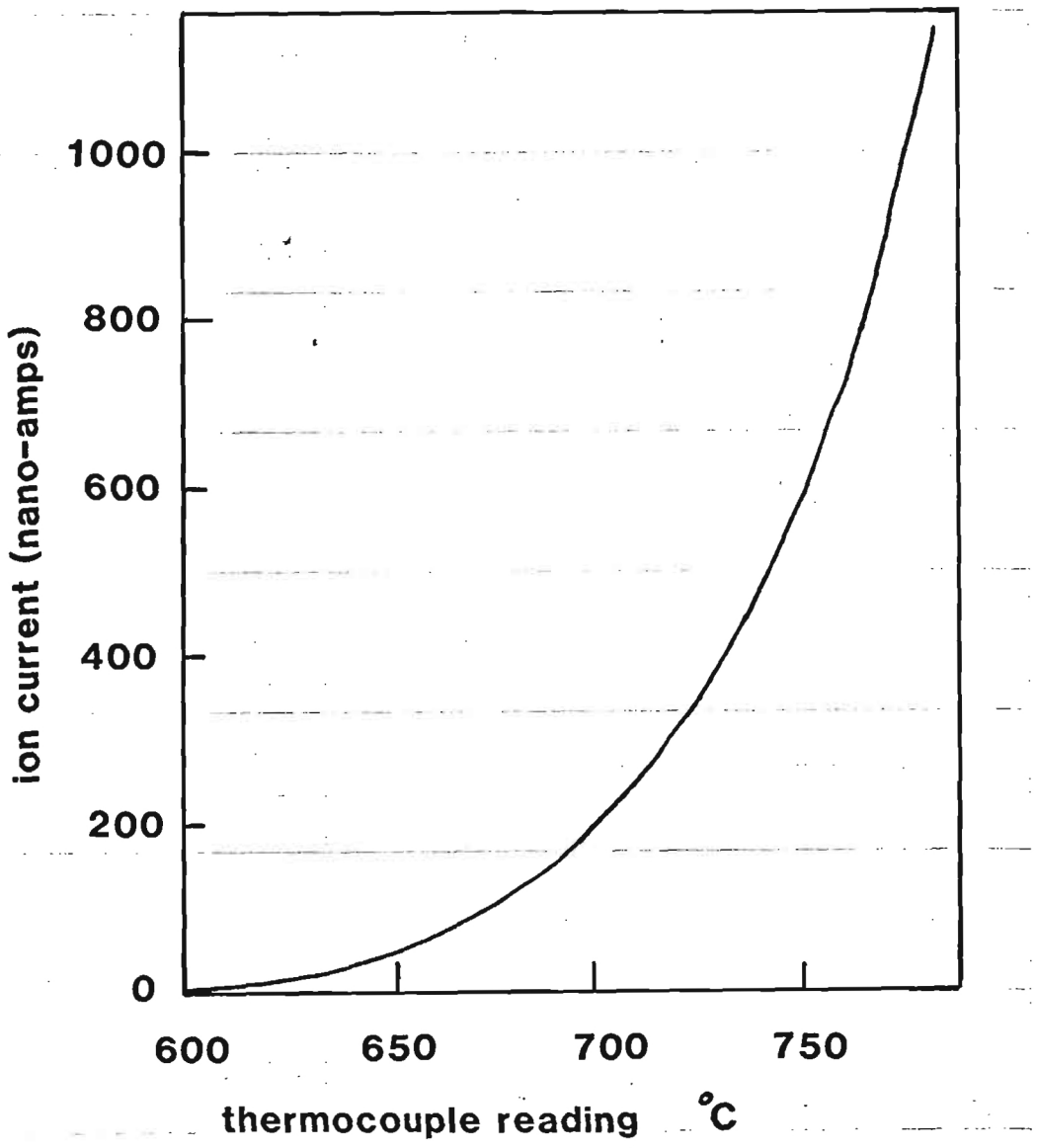

Figure 2. Curve of ion current versus thermocouple reading for ionization gauge flux monitor.

3. GROWTH OF GaAs ON PREPARED SUBSTRATES FOR FET FABRICATION

3.1 Introduction

Selective molecular beam epitaxy is a planar process which lends itself readily to the production of various high speed logic devices especially FET structures. Very recently[5] the simultaneous deposition of single crystal and polycrystalline GaAs has been used to fabricate a number of devices. This section reports efforts on similar growth procedures using patterned samples provided by NRL. In addition to MBE growth in windows opened by selective etching of grown oxide layers on GaAs, MBE layers were also deposited on samples which had regions defined by ion implantation.

3.2 Substrate Preparation

The procedure normally used to prepare substrates suitable for MBE growth could not be used for these specially prepared substrates since the etches would remove the patterned region. For the ion implanted samples, the implanted depth was only about 3000Å which would be removed by the regular etch. The oxide patterned substrates also could not be etched extensively since significant undercutting of the GaAs would occur which would severely degrade any device potential. It was decided to aim for a removal of about 300Å of GaAs.

The etching rates of the Bromine-Methanol 1% etch was measured and found to be about 2.5 μm/min. Figure 3 shows the results of the present study together with previously reported data for GaAs[6] and InP[7]. The strength was reduced by a factor of 10 which gave an etching rate of 3000Å/min. Finally, an etch of 0.01% Bromine-Methanol for 30s seemed to given the required etch. The Tencor Thickness Monitor used to measure the depth of the etched step was used at its highest sensitivity, and the generated curve contained appreciable fluctuations. The $5:1:1/H_2SO_4:H_2O_2:H_2O$ etching step in the normal preparation procedure was removed completely. The preparation procedure included the standard organic solvent stages followed by the Br:Meth etch and then washing in deionized water.

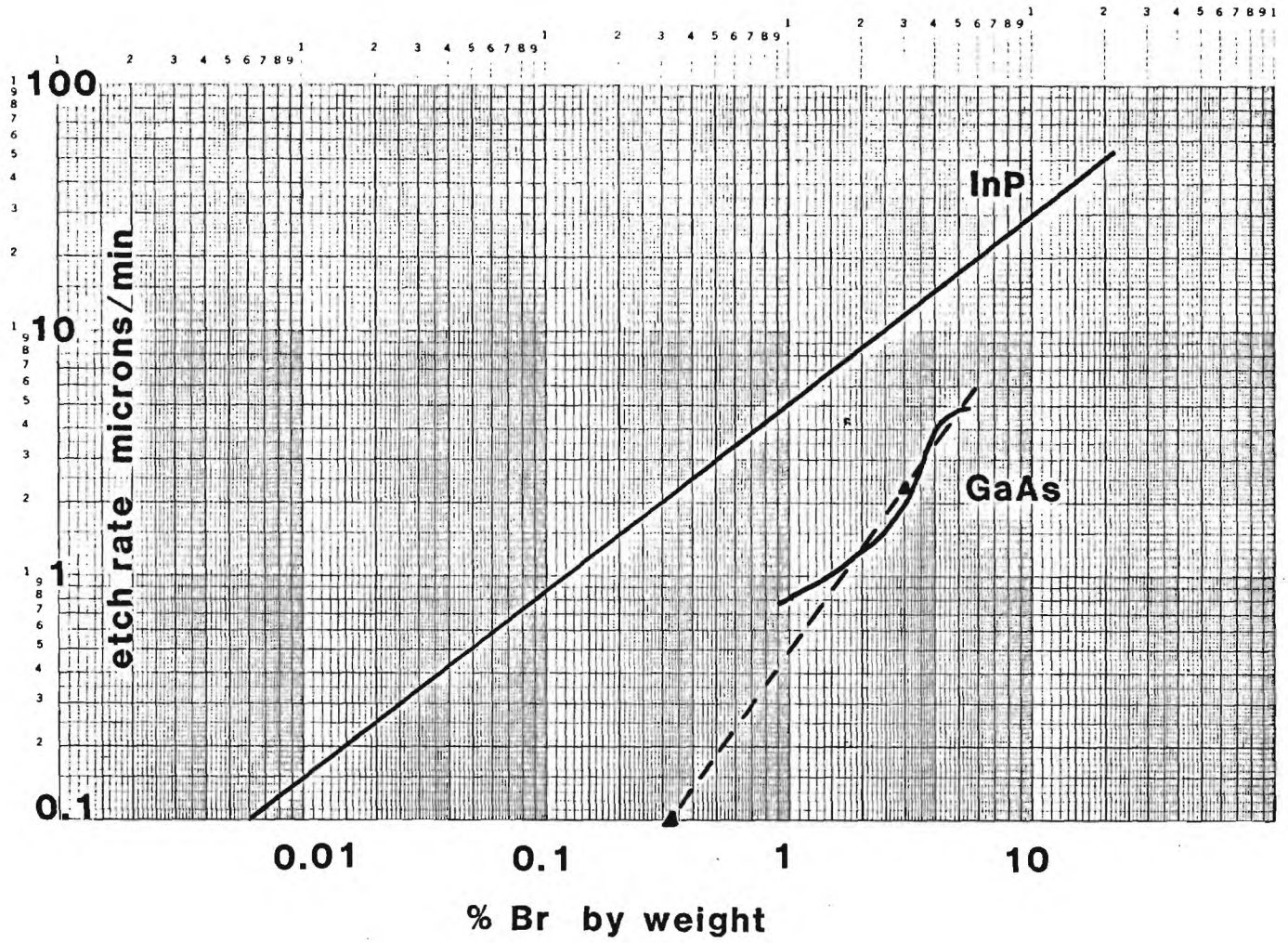

Figure 3. Etching rate of Bromine-Menthanol etches for (100) InP and GaAs versus etchant composition. --- represents present results, solid lines are from ref. 6 for GaAs and 7 for InP.

Problems in getting the substrate to adhere to the sample holder were immediately encountered. It was extremely difficult to get the molten indium to adhere to the substrate rear surface. A number of the initial samples supplied by NRL were degraded during this period due to excess indium getting on the front surface while mounting the substrate. The problem was initially attributed to the relatively unetched rear surface. To overcome this, the front surface of the sample was stuck to a glass slide using black wax and the near surface etched using the H_2SO_4:H_2O_2:H_2O etch followed by a 1% Br:Meth etch. Although this improved the tinning level of the substrate considerably, difficulties still occur and this presently represents the major problem area. No difficulty has been encountered with any other substrate, so the problem is clearly associated with the prepared sample in some as yet unknown way. There is also the possibility that the substrates may not have been sufficiently flat.

3.3 Growth Conditions

The important parameters for an FET structure are layer thickness and carrier concentration. These were specified to be 3000Å and 1 x 10^{17} cm^{-3} respectively. The growth rate for the MBE system, using Ga and As as sources, was 1 µm/hr. Si was used as the n-type dopant. The dopant level as a function of Si oven temperature had been determined from calibration runs on 1 µm thick samples and is shown in figure 4. In order to measure the thickness and carrier concentration of the layer, an extra piece of plain GaAs was inserted adjacent to the patterned sample and the thickness and Hall measurements made on that piece.

It was found that the thickness followed the previous calibration runs exactly, but the carrier concentration was always less than that expected from the calibration runs. The reasons for this are not certain at the moment, but the difference in the layer thicknesses may be a factor. It is probable that the effect of carrier depletion near the substrate/film interface has a significant effect on the average carrier concentration for the thin film whilst being relatively unimportant for the thicker films.

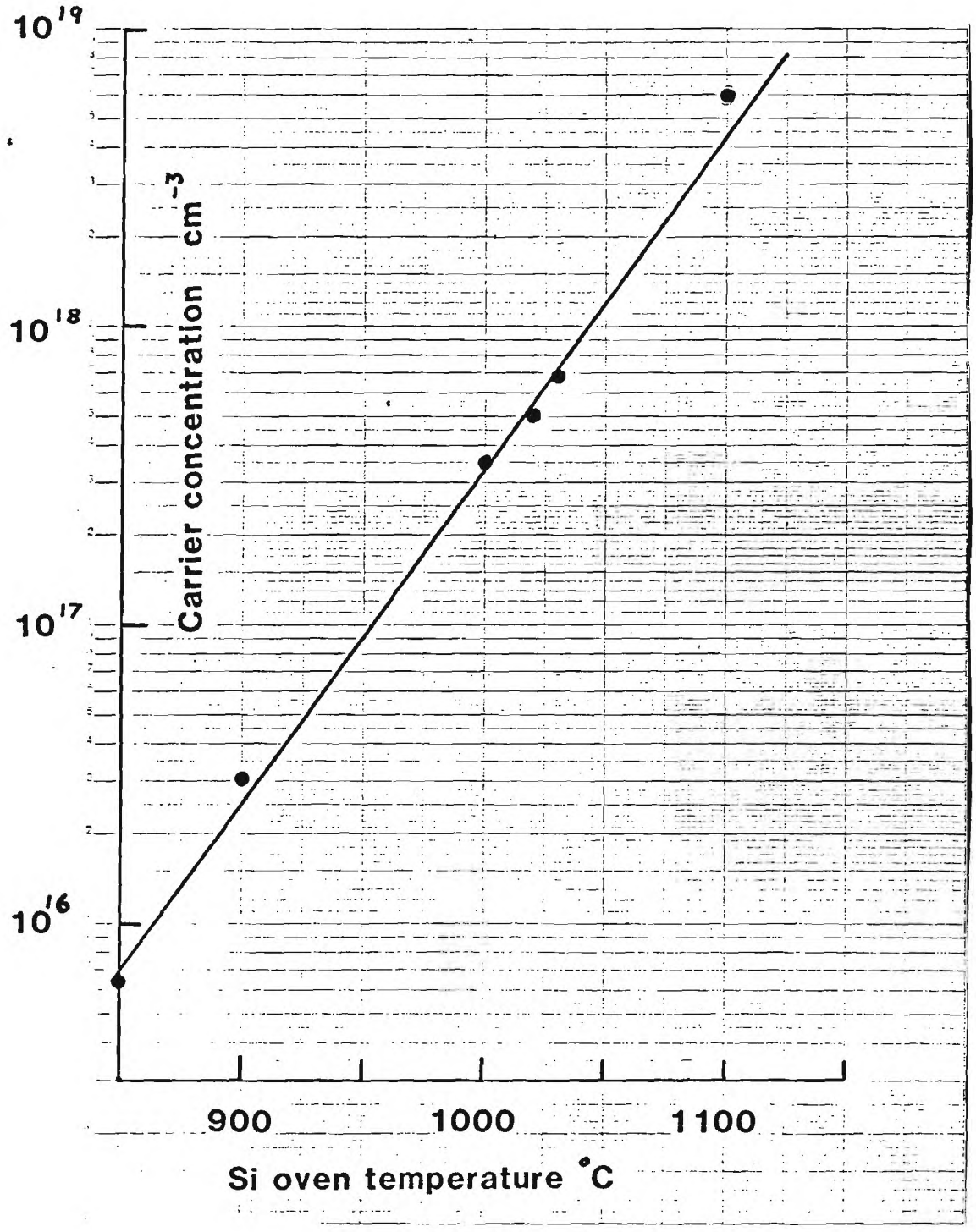

Figure 4. Carrier concentration versus Si oven temperature for MBE grown GaAs. Thickness of samples ~ 1 μm.

Typical MBE growth conditions were: substrate temperature 580°C, Ga pressure 4×10^{-7} torr and As pressure 1.6×10^{-6} torr. The Si oven temperature expected for a concentration of 10^{17} cm^{-3} is 990°C, however, temperatures between 950 and 1000°C were used. Growth rates are typically 1 μm/hr; for the 3000A thick layers grown, this required 19 minutes growth time. The substrate is heated under an incident arsenic flux at all times.

Presently the layer is grown without a buffer layer; however, future runs may incorporate an undoped 0.5 μm or thicker buffer layer.

3.4 Results on MBE Grown GaAs Layers

3.4.1 Electrical Measurements

In order to make Hall-van der Pauw measurements, as well as thickness measurements, a piece of Cr-doped GaAs was placed next to the sample on the substrate holder and the measurements were made on that piece. There may therefore be some discrepancy between the actual characteristics of the sample and the data reported here. Any difference is most probably due to difficulties of bonding the sample onto the substrate holder as discussed earlier. This may give rise to a different effective substrate temperature, and hence growth rate, or to a temperature variation across the sample thereby leading to inhomogeneity. Additionally, the surface may not be completely free of contaminants. In fact some of the earlier results showed the presence of whiskers which typifies surface contamination. Later samples were essentially devoid of whiskering except on the polycrystalline areas. Presumably this is due to the lack of cleaning and etching of the oxide layer.

Room temperature Hall data for four runs are shown in table 1 together with the film thickness d and temperature of the Si doping oven. The samples corresponding to these runs have been delivered to NRL and are awaiting processing.

Table 1

Sample	Run No.	($cm^2V^{-1}2^{-1}$)	$n(cm^{-3})$	d(m)	(T_{Si})
VI4/1	E0304-III	4100	3.5×10^{16}	.36	950
VI4/4	E0317-III	3300	3×10^{16}	.30	970
VI4/6	E0330-III	3600	3.5×10^{16}	.33	990
VI4/7	E0401-III	3500	1.6×10^{17}	.38	1000

The Hall data have been corrected for the error introduced by using relatively large contacting pads.[9] For these samples, no further correction for assymmetry was necessary, except for sample VI4/4. The defined Hall Resistances for this sample varied by more than a factor of 60 for the two orthogonal directions. To interpret this data in order to obtain meaningful measurements is not straightforward. The usual correction factor, van der Pauws f factor, relates to a difference in the Hall resistances which is due to a geometrical assymmetry which is not applicable in the present case. Probably the simplest way to analyze the data is just to use the lowest Hall resistance and attribute the difference as due to contact problems. If this is done a mobility for VI4/4 greater than 5000 $cm^2V^{-1}s^{-1}$ is obtained. The number given in the table is the average of the two Hall resistances without consideration of the differences and should be taken as being somewhat pessimistic.

The data obtained for VI4/7 is very similar to data obtained elsewhere for a similar system but with an undoped GaAs buffer layer.[5] It is clear therefore from the Hall data that the MBE layers are of as good quality in terms of mobility as may be expected. The ability to control the thickness is also indicated in Table 1. The variation in depostion time was between all samples was less than two minutes which lead to a spread of 800Å in layer thicknees. This suggests that the layer can be controlled to about 100Å. The dopant level is the most difficult parameter to control and, as seen from table 1, Si oven temperatures from 950 to 990 did not appear to change the concentration significantly. However, sample VI4/7 has approximately the correct value of concentration.

Table 1

Sample	Run No.	($cm^2V^{-1}2^{-1}$)	$n(cm^{-3})$	d(m)	(T_{Si})
VI4/1	E0304-III	4100	3.5×10^{16}	.36	950
VI4/4	E0317-III	3300	3×10^{16}	.30	970
VI4/6	E0330-III	3600	3.5×10^{16}	.33	990
VI4/7	E0401-III	3500	1.6×10^{17}	.38	1000

The Hall data have been corrected for the error introduced by using relatively large contacting pads.[9] For these samples, no further correction for assymmetry was necessary, except for sample VI4/4. The defined Hall Resistances for this sample varied by more than a factor of 60 for the two orthogonal directions. To interpret this data in order to obtain meaningful measurements is not straightforward. The usual correction factor, van der Pauws f factor, relates to a difference in the Hall resistances which is due to a geometrical assymmetry which is not applicable in the present case. Probably the simplest way to analyze the data is just to use the lowest Hall resistance and attribute the difference as due to contact problems. If this is done a mobility for VI4/4 greater than 5000 $cm^2V^{-1}s^{-1}$ is obtained. The number given in the table is the average of the two Hall resistances without consideration of the differences and should be taken as being somewhat pessimistic.

The data obtained for VI4/7 is very similar to data obtained elsewhere for a similar system but with an undoped GaAs buffer layer.[5] It is clear therefore from the Hall data that the MBE layers are of as good quality in terms of mobility as may be expected. The ability to control the thickness is also indicated in Table 1. The variation in depostion time was between all samples was less than two minutes which lead to a spread of 800Å in layer thicknees. This suggests that the layer can be controlled to about 100Å. The dopant level is the most difficult parameter to control and, as seen from table 1, Si oven temperatures from 950 to 990 did not appear to change the concentration significantly. However, sample VI4/7 has approximately the correct value of concentration.

3.4.2 Surface Characteristics

All of the GaAs monitor samples appeared highly reflecting. The main samples however had a variety of defects which presumably therefore are due to a specific sample-related cause and not due to growth conditions.

Intially, the degree of the cleaning etch was reduced relative to the more usual procedure and this resulted in extensive whiskering over large parts of the surface. The presence of these whiskers is directly related to the presence of contaminants or other defects on the surface. Growth on plain substrates requires significant etching to achieve a surface sufficiently clean for epi growth. The normal preparation typically removes 10 to 20 μm, which cannot be used in the present case which is limited to 300Å. It is important therefore that since the substrates cannot be etched after the patterned regions are fabricated, they must be etched in 5:1:1/ $H_2H_2SO_2$:H_2O_2:H_2O prior to this process. The very light 0.01% Br:Methanol etch used on the prepared wafer, which removes about 300Å in 30s, may be insufficient to produce a good surface for growth.

A selection of optical micrographs is shown in figures 5,6,7 and 8. Nominally, the clean/etch process was identical in all cases. A further variable may be due to indium spillover incurred when bonding the sample to the holder. These micrographs generally are of areas not obviously contaminated with spillover of In or scratches inadvertently made when wetting the sample.

Figure 5 shows a 200X micrograph of E0304-III, VI4/1. The crystalline area is essentially free of whiskers and other defects; significant whiskering appears just outside this window. This high whisker density does not extend into the polycrystalline region and therefore suggests a localization of defects.

Figure 6 shows sample E0317-III VI4/4 at a magnification of 125x. The localization of whiskers in this case is very much reduced. Very little whiskering is evident in either the window or oxide regions. Visually this appeared to be one of the better samples; unfortunately, the Hall data for this sample was the most unreliable.

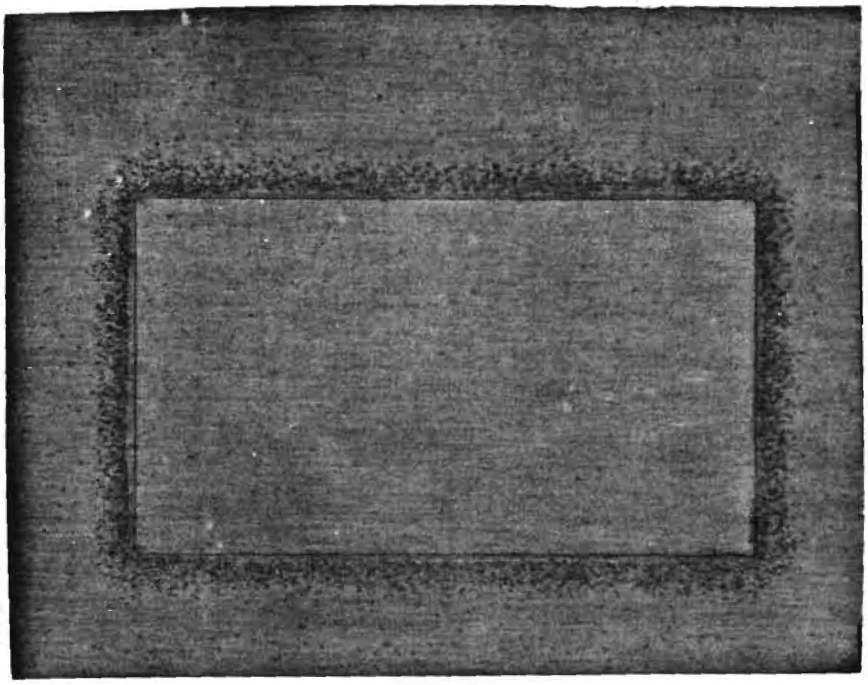

Figure 5. Optical micrograph of one window and surrounding oxide layer for sample VI4/1, Run E0304-III. Substrate temperature 560°C.

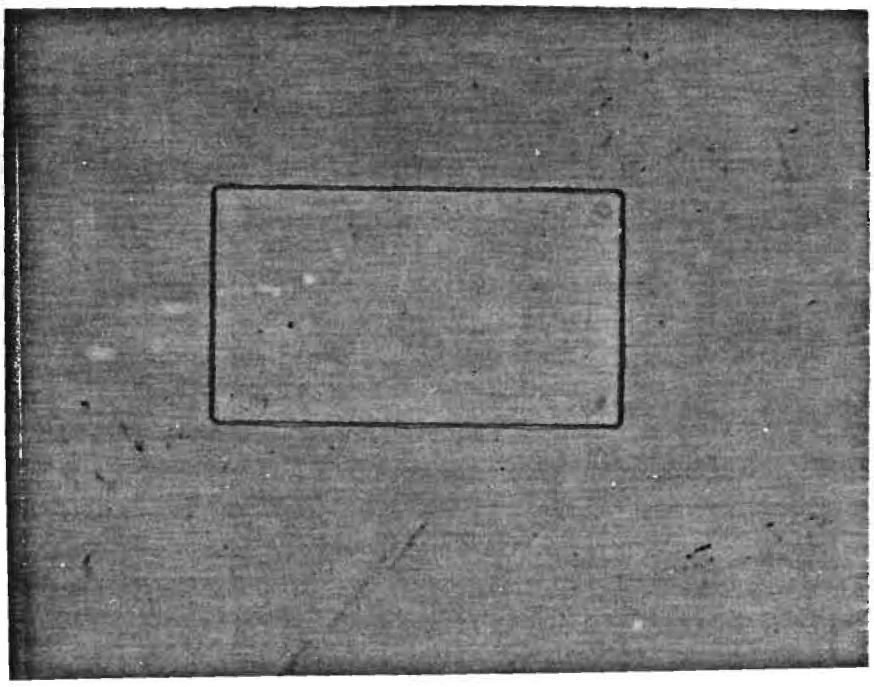

Figure 6. Optical micrograph of one window and surrounding oxide layer for sample VI4/4, Run E0317-III. Substrate temperature 560°C.

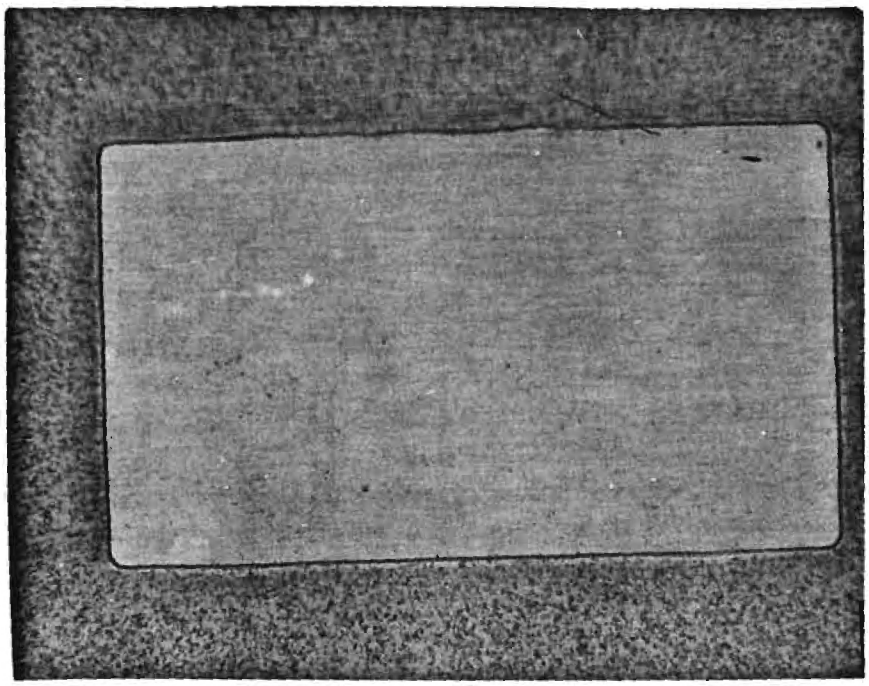

Figure 7. Optical micrograph of one window and surrounding oxide layer for sample VI4/6, Run E0330-III. Substrate temperature 560°C.

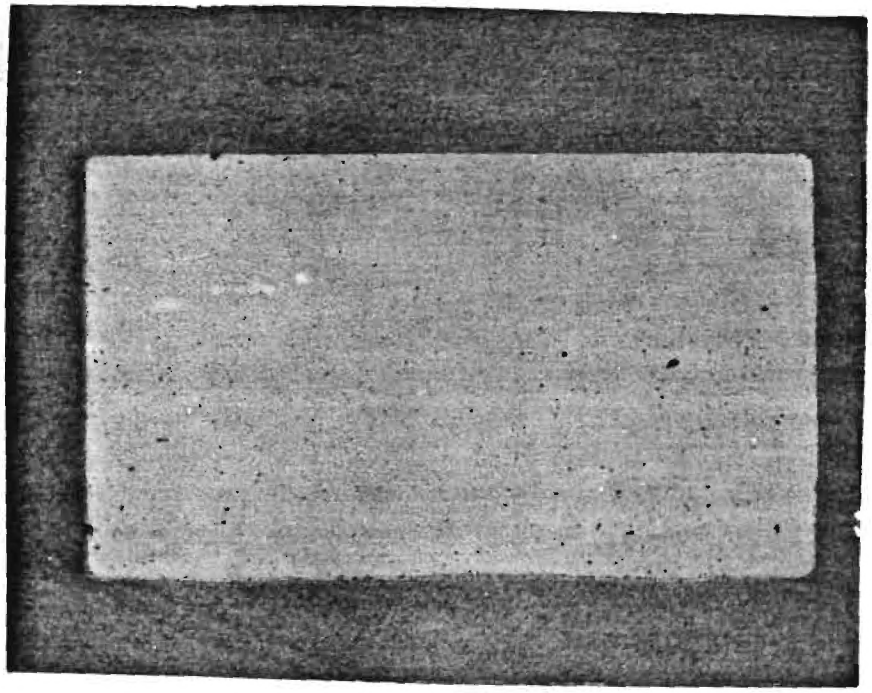

Figure 8. Optical micrograph of one window and surrounding oxide layer for sample VI4/7, Run E0401-III. Substrate temperature 560°C.

The micrographs shown in figures 7 and 8 of samples E0330-III, VI4/6 and E0401-III, VI4/7 are somewhat similar. There is a uniform whisker defect within the oxide regions and little indication of clustering around the edges of the window. The window region is relatively free of defects.

All the above figures represent the best part of each sample but are nevertheness an indication of the quality of layers achievable using selective molecular beam epitaxy.

3.4.3 Growth on Ion Implanted GaAs

In addition to MBE growth on the patterned oxide layered substrates, some growths were also made on ion implanted GaAs. The objective was to determine if selective implantation could be used to generate regions of damage which would then give rise to high resistivity regions of GaAs when a layer is grown using MBE. Non implanted area would have good crystalline growth. In this way a pattern of high resistivity GaAs with windows of high mobility GaAs suitable for FET fabrication could be achieved. Unfortunately the high temperature of the GaAs substrate during growth essentially anneals out the implanted damage and all the films grown on these implanted areas showed good crystallinity.

3.5 Summary

The results discussed in the previous section are the outcome of a number of test runs to establish operating conditions. These have now been established as far as the growth of a suitable layer is concerned. However, two problems which may be interrelated, still remain. These are:

1) Presence of whiskers due to inadequate surface etching - this may be solved by either etching the substrate before pattern definition and/or by light etching immediately prior to growth using an H_2SO_4 based etch rather than the 0.01% Br:CH_3OH presently used.

2) Etching of the wafer prior to pattern definition in a $5:1:1/H_2SO_4:H_2O$ etch may also help overcome the problems in tinning and bonding the sample to the substrate holder.

It should be pointed out that of the eight sections cut from wafer VI/4, four were degraded by overflow and scratches which occurred during the bonding stage.

4.0 REFERENCES

1. See, for example, "Special Issue on Quaternary Compound Semiconductor Materials and Devices-Sources and Detectors" IEEE J. Quantum Electronics Q.E. 17 pp. 161-207, (1981) and "Special Issue on the 1980 International Semiconductor Laser Conference" IEEE J. Quantum Electronics QE 17 pp. 597-671, (1981).

2. See, for example, "Special Issue on Quaternary Compound Semiconductor Materials and Devices - Sources and Detectors" IEEE J. Quantum Electronics Q.E. 17 pp. 217-284, (1981).

3. M. A. Littlejohn, J. R. Hauser, and T. H. Glisson, "Velocity-field characteristics of $Ga_{1-x}In_xP_{1-y}As_y$ quaternary alloys." Appl. Phys. Lett. 30 pp. 242-244, (1977).

4. R. L. Moon, G. A. Antypas, and L. W. James, "Bandgap and Lattice Constant of GaInAsP as a function of alloy composition, J. Electron. Mater., 3 pp. 635-644, (1974).

5. H. M. Levy, G. M. Metze, D. W. Woodard, W. O. Camp. R. C. Tiberio, C.E.C. Wood, and L. F. Eastman, "GaAs Integrated Circuits by Selective Epitaxy and Electron Beam Lithography." Solid State Technology 24, pp. 127-130, (1981).

6. Y. Tarui, Y. Komiya, and Y. Harada, "Preferential Etching and Etched Profile of GaAs" J. Electrochem. Soc. 118 pp. 118-122, (1971).

7. S. Adachi, H. Kawaguchi, and G. Iware "InGaAsP/InP Planar-Stripe Lasers with Chemically Etched Mirrors", J. Electrochem. Soc. 129 pp. 883-886, (1982).

8. L. J. van der Pauw, "A method of measuring the resistivity and Hall Coefficient on Lamellae of arbitrary shape" Philips Technical Review 20 pp. 220-224, (1958/59).

QUARTERLY PERFORMANCE AND STATUS OF FUNDS

Level of Effort

Categories	1 November 1981-31 January 1982	Cumulative Total (Man months)
Principal Research Engineer/Scientist	0.13	0.33
Senior Research Engineer/Scientist	2.92	5.12
Research Engineer/Scientist	0.5	0.7
Assistant Research Engineer/Scientist	0.45	0.85
Graduate Research Assistant	-	-
Co-op, Student	-	-
TOTAL	4.0	7.0

Financial Status

1 November 1981 - 31 January 1982	Cumulative Total Expended
29,759	49,057

Total Contract Funding (through 30 April 1982)	$99,982

BINARY, TERNARY AND QUATERNARY HETEROJUNCTIONS OF III-V SEMICONDUCTORS GROWN BY MOLECULAR BEAM EPITAXY

(A0004)

Quaterly Report No. 4

G. D. Holah

Engineering Experiment Station
Georgia Institute of Technology
Atlanta, Georgia 30332

Report for Period 1 February 1982 - 30 April 1982

Contract No. N00014-81-K-2007

Prepared for:

Naval Research Laboratory
Washington, D.C. 20375

TABLE OF CONTENTS

LIST OF TABLES

LIST OF ILLUSTRATIONS

1.0 INTRODUCTION

1.1 Background

This is the fourth quarterly report on a research program directed primarily towards the growth and characterization of quaternary layers of $In_{1-x}Ga_xAs_yP_{1-y}$ grown by molecular beam epitaxy. The program was initially of one year duration but due to staffing changes work on the program was initiated in August 1981 and not April 1981 as originally intended. For this reason the fourth quarterly does not represent the final achievements of the program.

The initial objectives of the program emphasized the application of the quaternary alloys to high frequency microwave devices such as FETS and TEDS which would exploit the potentially high low field mobilities and peak velocities expected from these materials.[1] More recent studies[2] suggest that the original calculation which gave rise to this optimism may have been somewhat misleading, and present calculations do not indicate that significant improvements may be expected. However, there is still some speculation and possibly hope that submicron structures of these materials, operating in the velocity overshoot regime, may offer some advantages relative to GaAs and InP.[3] However, as yet no measurements of the velocity-field curves for these quaternary materials have been made. Such a program of measurement would clearly be of great importance and interest.

Due to the aforementioned reasons, there has been a slight change of emphasis of the programs objectives, and the current direction is towards fabricating a structure which can be processed into a diode laser emitting near 1.55 μm, a region of great importance for optical fiber communication. Accordingly, the bulk of the work reported here is concerned with the component steps towards the fabrication of a double heterostructure laser.

At the present time the conventional silica-based optical fibers have their minimum loss and minimum dispersion near 1.55 μm and 1.3 μm. Due to the fundamental absorption peak of silica near 2 μm, most fiber optic systems will probably operate near 1.3 μm except for long distance systems using 1.55 μm single mode lasers. These latter wavelengths will be particular important for undersea communication systems. There is

the possibility in the future that ultra-low-loss fibers in the 2 μm to 6 μm region may become available and would necessitate even longer wavelength lasers and detectors.

The quaternary system $In_{1-x}Ga_xAs_yP_{1-y}$ is unique in that it can be lattice matched to InP and GaAs over a wide range of composition and hence bandgap. In terms of diode lasers near 1.5 μm it can be grown lattice matched to InP. Diode lasers have already been grown using the well-established liquid phase and vapor phase epitaxy techniques, however MBE offers certain advantages when the integration of lasers, detectors and transistors in a single monolithic package is considered. Of particular importance is the potential to change doping profiles and composition much more abruptly than is possible with LPE and possibly VPE.

The growth of a laser structure such as that shown in figure 1 requires the deposition of n- and p-type layers of InP. In order to be able to obtain a set of growth parameters for the p- and P^+- InP layers, a procedure for forming ohmic contacts has to be realized so that the electrical parameters can be measured. Part of the effort during this report period was therefore directed towards a study of Au:Mn as a possible ohmic contact alloy to p-type InP.

Some brief consideration of diode laser design will help to comprehend the orientation of the research reported here. For all intents and purposes semiconductor lasers are fabricated solely from direct bandgap materials. Indirect gap material such as silicon would require the involvement of a lattice vibration during the recombination process which lowers the transition probability significantly. This would necessitate very high currents to compensate for the low transition probability. Having decided upon the active medium by the virtue of the required wavelength it is also necessary to be able to confine both the emitted photons and the carriers to this active medium otherwise the lasing efficiency falls. The laser medium is therefore sandwiched between a lower refractive index materials for photon confinement and a higher energy bandgap to confine the electrons and holes. Fortunately the empirical relationship between energy gap and refractive index is such that these conditions (of high bandgap and low refractive index) are always satisified. This relationship[4] can be

InGaAsP DIODE LASERS

Double-heterostructure

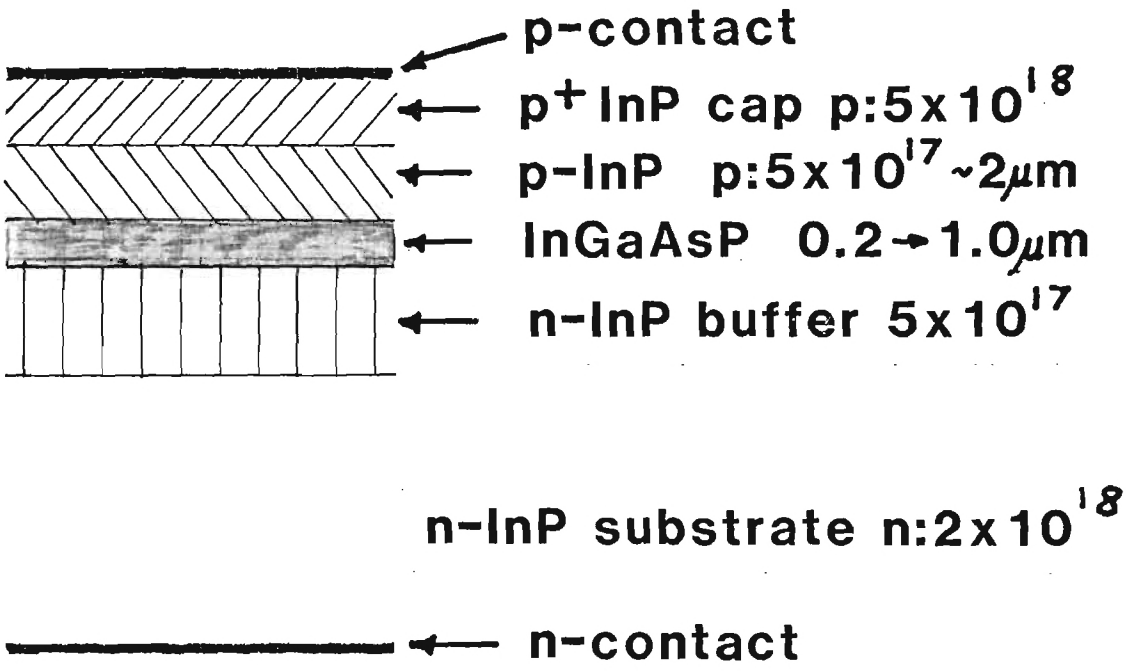

Figure 1

written as

$$E_g = \frac{108}{n^4}$$

For the quaternary alloy system, InP is an ideal choice of lower index higher bandgap material. Since the bandgap of the quaternary can be varied, the efficiency of carrier confinement, and hence the magnitude of leakage current, will change. The longer the emission wavelength the lower the leakage current when InP is used as the confining layer.

Barriers for hole and electron confinement are achieved by having a sandwich consisting of p^+-type InP:InGaAsP:n^+-type InP. The fabrication of the double-heterostructure diode laser with InGaAsP as the active layer therefore requires, in addition to the growth of the InGaAsP layers, layers of n^+- and p^+-type InP. Some effort was to expended in determining growth procedures for these layers. Before the p^+-type layers can be evaluated, a reproducible technique for forming ohmic contacts onto p-type InP has to be established. This task has been undertaken and some success achieved with Au:Mn alloys. This work is still underway, more measurements are needed before a completely consistent set of procedures is realized.

1.2 Objectives of Fourth Quarter

In consideration of the previous discussions the main objectives of this quarter have been directed towards the necessary steps for eventual MBE diode laser fabrication. These are:

- Growth of MBE InGaAsP with composition such that the bandagp and hence laser emission wavelength is near 1.55 μm.
- Generation of a procedure for producing ohmic contacts on p-type InP.
- Growth of p-type and n-type InP of correct carrier concentration required as buffer and confining layers (see figure 1).

1.3 Results of Fourth Quarter

- o InGaAsP MBE films have been grown with the bandgap at 1.55 μm. Lattice matching to the InP substrate, as measured from x-ray rocking curves has been substantially improved over previous MBE samples. Infrared absorption has been used to establish the bandgap and hence composition parameter. Hall measurement indicate that the mobilities have been generally increased. Values of 4600 $cm^2V^{-1}s^{-1}$ for the mobility have been achieved.

- o Ohmic contacts have been established on p-type InP using evaporated Au:Mn (92:8). The general consistency was not good but contacts were produced which demonstrated good ohmic behavior.

- o Good quality n^+ films of InP have been grown using Sn as the n-type dopant. A mobility of 1900 $cm^2V^{-1}s^{-1}$ and an electron concentration of 2×10^{18} cm^3 was achieved.

1.4 Plans for Next Quarter

- o Growth of p-type InP
- o Install plating process for fabrication of ohmic contacts
- o Grow InP/InGaAsP/InP structure suitable for processing into diode lasers at 1.55 μm.
- o Fabricate and test InGaAsP diode lasers grown by molecular beam epitaxy.

2. OHMIC CONTACTS TO P-TYPE InP

2.1 Introduction

A simple double-heterostructure diode laser using InGaAsP has the structure shown in figure 1. As mentioned in the previous section the purpose of the InP layers is two fold:

1) to confine the electrons and holes to the active region

2) to confine the lasing radiation to the active region.

The second purpose, radition confinement, is achieved via differences in the dielectric constant. The first purpose requires bandgap differences and a specific doping profile. Such a system is shown in fig. 2. The n^+-n junction, A, for the valence band serves to confine holes and the n-p^+ junction confines electrons. The situation shown is for forward bias. The dopant type and level of the active layer is not crucial as long as it is not very heavily doped. If the active layer is less than a diffusion length thick it is possible to inject equal concentration of holes and electrons up to 10^{18} - 10^{19} cm^{-3}.

Typical carrier concentrations for the n^+ and p^+ InP regions are 10^{18} cm^{-3}. n-type dopants for InP are relatively straightforward, as is the preparation of ohmic contacts. Tin has been found to be a suitable n-type dopant, and the Au:Ge/Ni/Au system produces good ohmic contacts to n-type InP. The situation for p-type InP is not quite as satisfactory. Contacting systems which have been used for p-type InP have included Au-Zn,[6] Au-Mg, Au-Cd,[7] In-Zn,[7] and In-Cd.[7] The success of these systems has not been completely satisfactory. Although Au-Zn seems to produce the best ohmic contacts so far, these have only been realized by a plating process. Plating[8] was found to be beneficial since the high vapor pressure of Zn makes it difficult to control the thickness of the zinc layer. Furthermore, Zn is harmful to vacuum systems.

Au:Be, sequentially evaporated (Be first), has been shown[9] to give good ohmic contacts to p-type InP. However due to the toxicity of Be, it was decided to investigate whether or not some less undesirable procedure could be found. It was proposed therefore, in order to produce a contacting system that could be produced by evaporation, to examine Au-Mn as a possible ohmic contact to p-type InP.

Figure 2

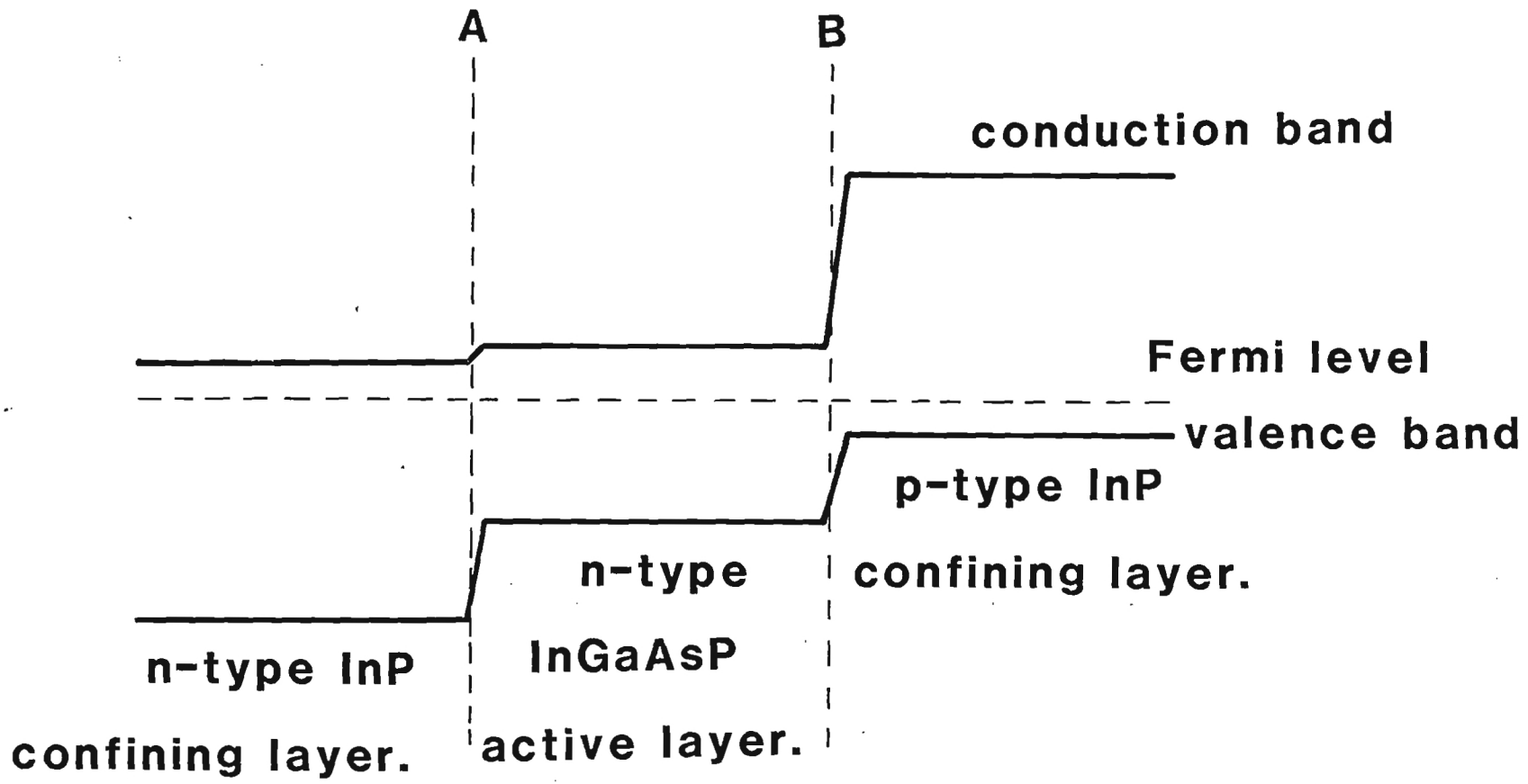

Energy band diagram of double-heterostructure diode laser.

2.2 Contacts to p-Type InP using Au-Mn Alloys

The metals were evaporated using separate boats for the Mn and Au. The initial tests were performed using a 95% Au: 5% Mn alloy, with the Mn being evaporated first. The total weight of Au + Mn was 50 mg. The substrates were either Zn doped InP or Zn^+ doped InP. Values for the carrier concentrations are not available but are probably in the region $1- 2 \times 10^{18}$ cm^{-3}. Following the deposition the contacts are alloyed in forming gas at 450^oC for various lengths of time.

The contacts were made by evaporating through our regular Hall sample mask. The behavior of the contacts were determined from I-V curves.

The bulk samples were prepared by either cleaning in organic solvents or by cleaning and then etching. The etch was a standard InP etch. Generally there was little difference in the ohmic properties of cleaned and cleaned/etched samples. The minimum alloying time at 450^oC was three minutes. Times shorter than three minutes exhibited I-V curves inferior than those of longer times. Presumably this is due to the diffusion time of the Mn into the InP. A series of I-V curves after various alloying times is shown in fig. 3. The contacts are clearly symmetric but non-linear. The final curve after annealing for six minutes at 450°C did become linear with a contact-contact resistance of 30Ω. Although not perfect this was sufficiently encouraging to repeat the procedure on an MBE p-type InP film.

Fig. 4 show the I-V curves obtained using a Au(90):Mn(7) contact alloy on p-type InP MBE sample D0920-II after annealing for 4 mins at 450^oC in hydrogen. This shows a contact-contact resistance of 7.5 Ω. The contacts were not consistent however. Figure 4 also shows a two I-V curves for this system which represent the characteristics of various pairs of the four contacts. The key signifies which of the four contacts are being studies. Good linearity and ohmic behavior, at least under conditions pertaining to the Hall measuring conditions of 1 mA current and voltages typically $\leq$ 1V, is achieved, but only for one pair of contacts.

Follwing a discussion with Brad Roos of NRL contacts were fabricated from similar alloy ratios but with simultaneous evaporation

after 1 minute anneal.

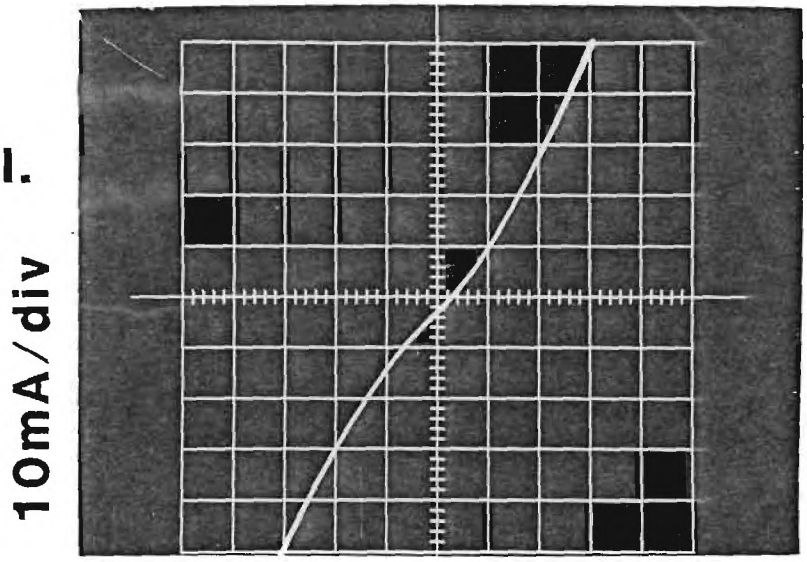

fter 2 minute anneal.

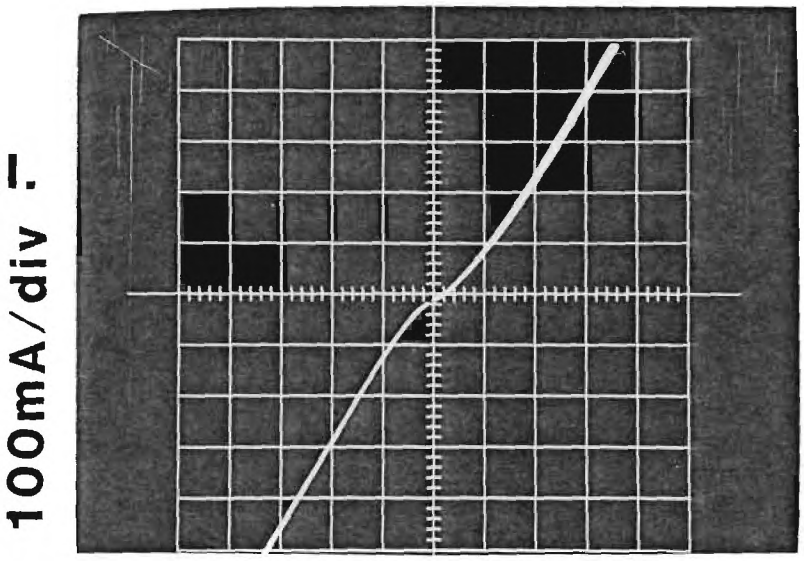

after 4 minute anneal.

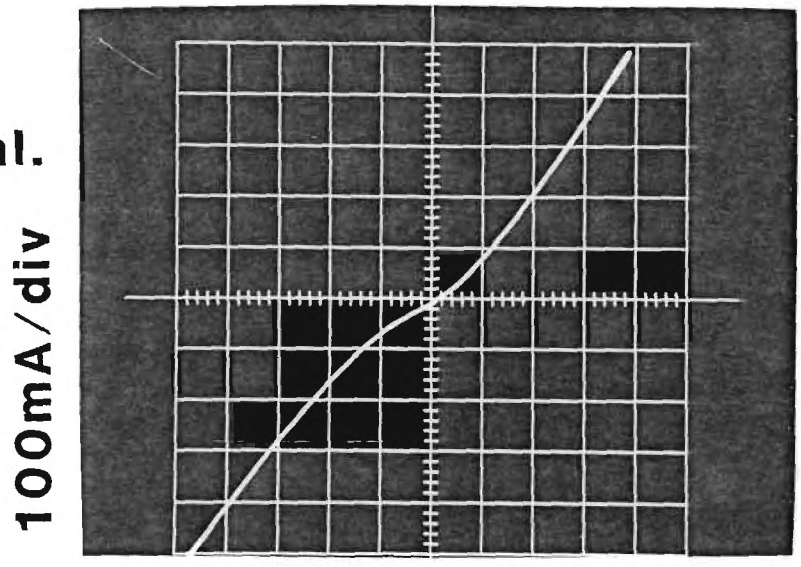

Figure 3

I-V curves for Au:Mn contacts on p-type InP.

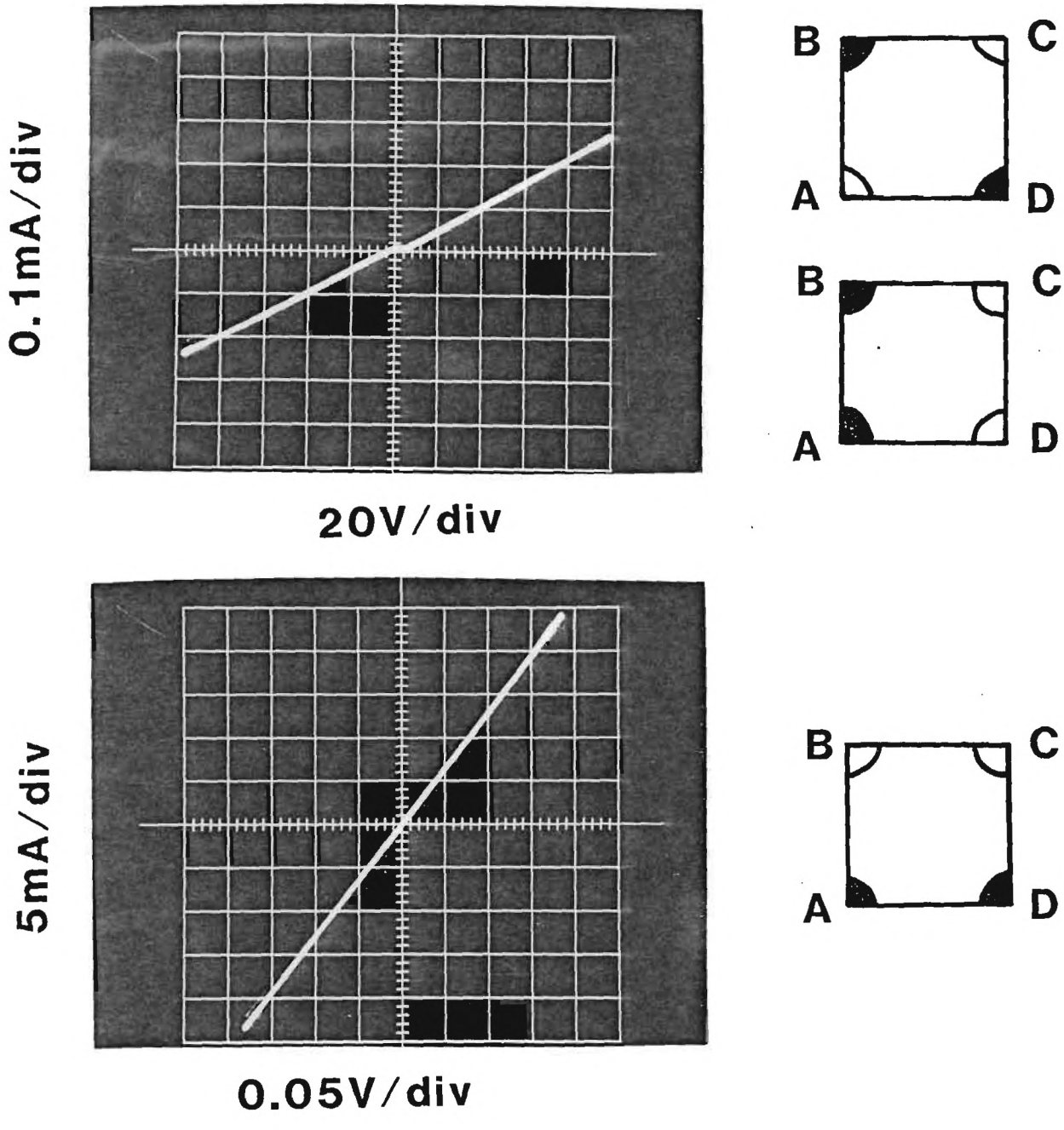

I-V curves for Au:Mn(90:7) contacts on p-type InP(Mn doped) D0929-II

contacts annealed in hydrogen at 450 C for 4 mins.

Figure 4

from the same boat. Contrary to results reported with Au:Zn alloys no improvement was observed with the Au:Mn system. However, it was not possible to pursue this technique further since the amount of p-type InP material available at that time was very small. It is possible that further studies may have shown some improvement.

At this time a paper on the fabrication of ohmic contacts on p-type InP using a Au and Zn periodic plating procedure together with photolithographica defintion of the contact area was published.[8] This technique produces the lowest resistance contacts and is ideally suited for fabricating contacts on a complete diode laser structure since the photolithographic process can be used to define the contact geometry and hence the lasing area.

Further effort on contacting will be aimed at setting up a direct plating facility.

2.3 Summary

A procedure for fabricating ohmic contacts on p-type InP has been devised using Au-Mn alloys. Some success was achieved and ohmic behavior was exhibited for some contacts, however the contacts were not consistent and the procedure in this respect is not a signficiant improvement over other reported techniques. However, if an evaporation procedure is required for contacts, the Au:Mn system is comparable to Au-Zn and less harmful to vacuum systems. Further studies will undoubtedly improve the inconsistencies found in the contact quality.

3. MBE GROWTH OF InGaAsP WITH BANDGAPS NEAR 1.5 MICRONS

3.1 Introduction

As mentioned in Chapter 1, the $In_{1-x}Ga_xAs_yP_{1-y}/InP$ system is the only material combination which will allow the bandgap and hence the possible lasing wavelegnth to be adjusted to the optimum conditions for silica-based optical fibers. Thus far, the lasing systems have been grown using mainly LPE and less frequently VPE. The objective of this part of the program is to determine the growth conditions of an $In_{1-x}Ga_xAs_yP_{1-y}$ film with a bandgap near 1.55 μm which is lattice matched to InP. Minimum dispersion in the fibers occurs at 1.3 μm and so this wavelength is the optimum for distortionless signal transmission. The wavelength of minimum attenuat ion is 1.55 μm and has particular relevance for longdistance communications, especially undersea communications including hydrophonic detection of ships.

3.2 Growth of MBE InGaAsP

The films which have been previously grown[10] and characterized were grown using a elemental Ga oven as the Ga source in addition to the Ga emanating from the GaAs oven. The present runs have been performed using only the GaAs oven as the source for both Ga and As. The deposition parameters and electrical and electrical measurements are given in table 1.

Prior to growth the Fe-doped InP substrate is thermally cleaned at $560^{o}C$ in an arsenic passivation flux for 45s. The substrate is then cooled and an Auger spectrum of the surface taken to ensure that removal of oxygen has been achieved. The Auger spectra of the surface at various temperature is shown in the fig. 5 and verifies that all the oxide layer has been removed after cleaning at $500^{o}C$. The substrate has to be moved into the interlock chamber of the MBE system for the Auger spectrum. Following this step, the substrate is returned to the growth chamber and heated to the growth temperature under a passivating arsenic flux. Typical partial pressures and oven temperatures are In, 1.8×10^{-7} torr at $770^{o}C$; InP, 9×10^{-7} torr at $650^{o}C$; and GaAs, 4.2×10^{-7} torr at $350^{o}C$. These settings, along with a substrate temperature near $510^{o}C$ gave a growth rate of 0.65 μm/hr.

ROOM TEMPERATURE HALL DATA

SAMPLE	MOBILITY	CONCENTRATION	THICKNESS	SUBSTRATE TEMP.
E0326-II	4630 $cm^2V^{-1}s^{-1}$	$4.8 \times 10^{16} cm^{-3}$	0.65μm	510 C
E0401-II	4200 $cm^2V^{-1}s^{-1}$	1.25 z $10^{17} cm^{-3}$	0.64μm	510
E0405-II	3160 $cm^2V^{-1}s^{-1}$	$1.5 \times 10^{17} cm^{-3}$	0.66μm	500
E0407-II	3900 $cm^2V^{-1}s^{-1}$	$3 \times 10^{16} cm^{-3}$	0.66μm	520

Bandgap for all samples about 0.8 eV, lattice matching implies x = 0.41, y = 0.86, wavelength = 1.55 microns

Table 1

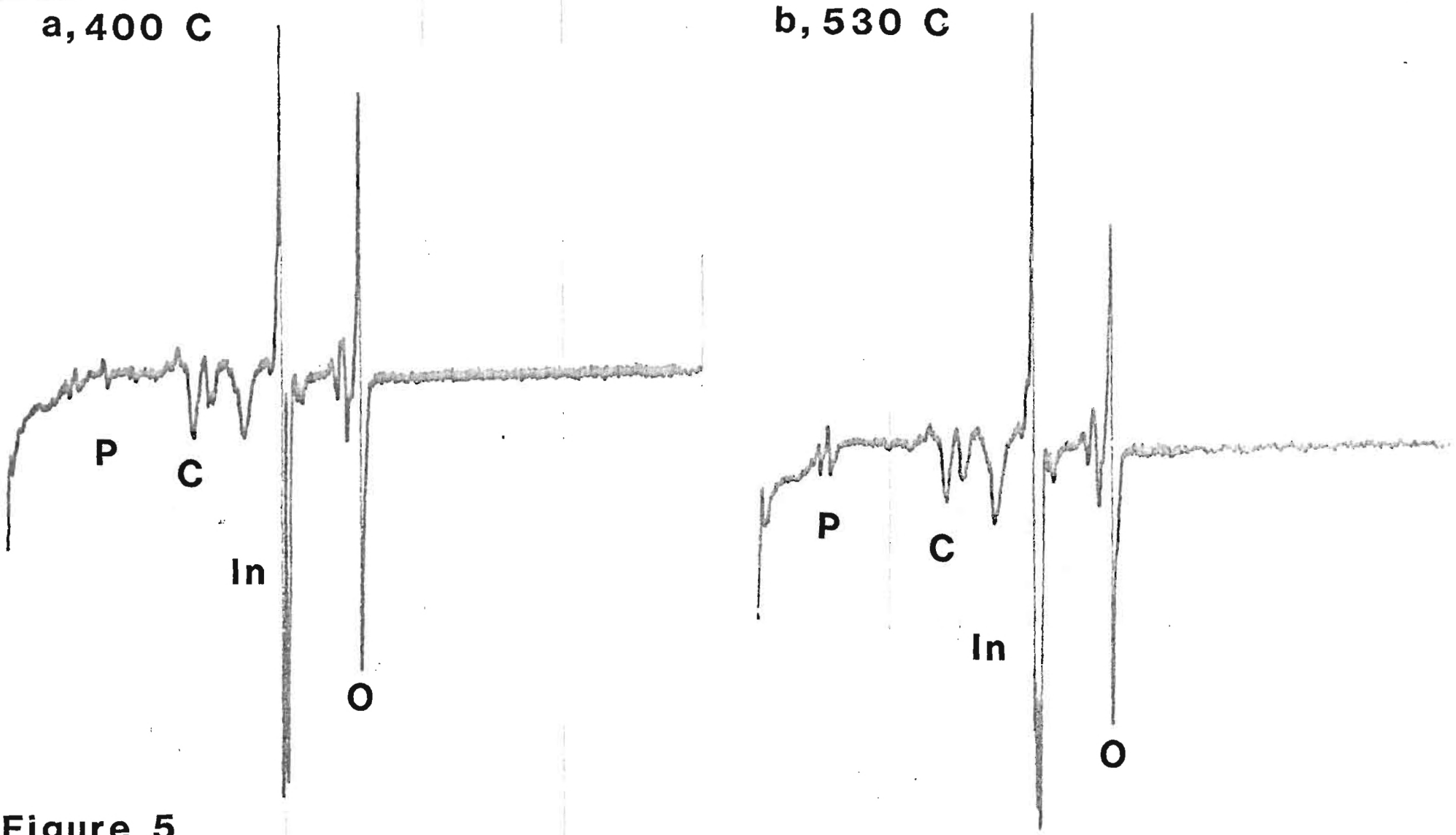

Figure 5

Auger spectra of InP substrate after thermal cleaning at various temperatures for 45s with arsenic passivation flux.

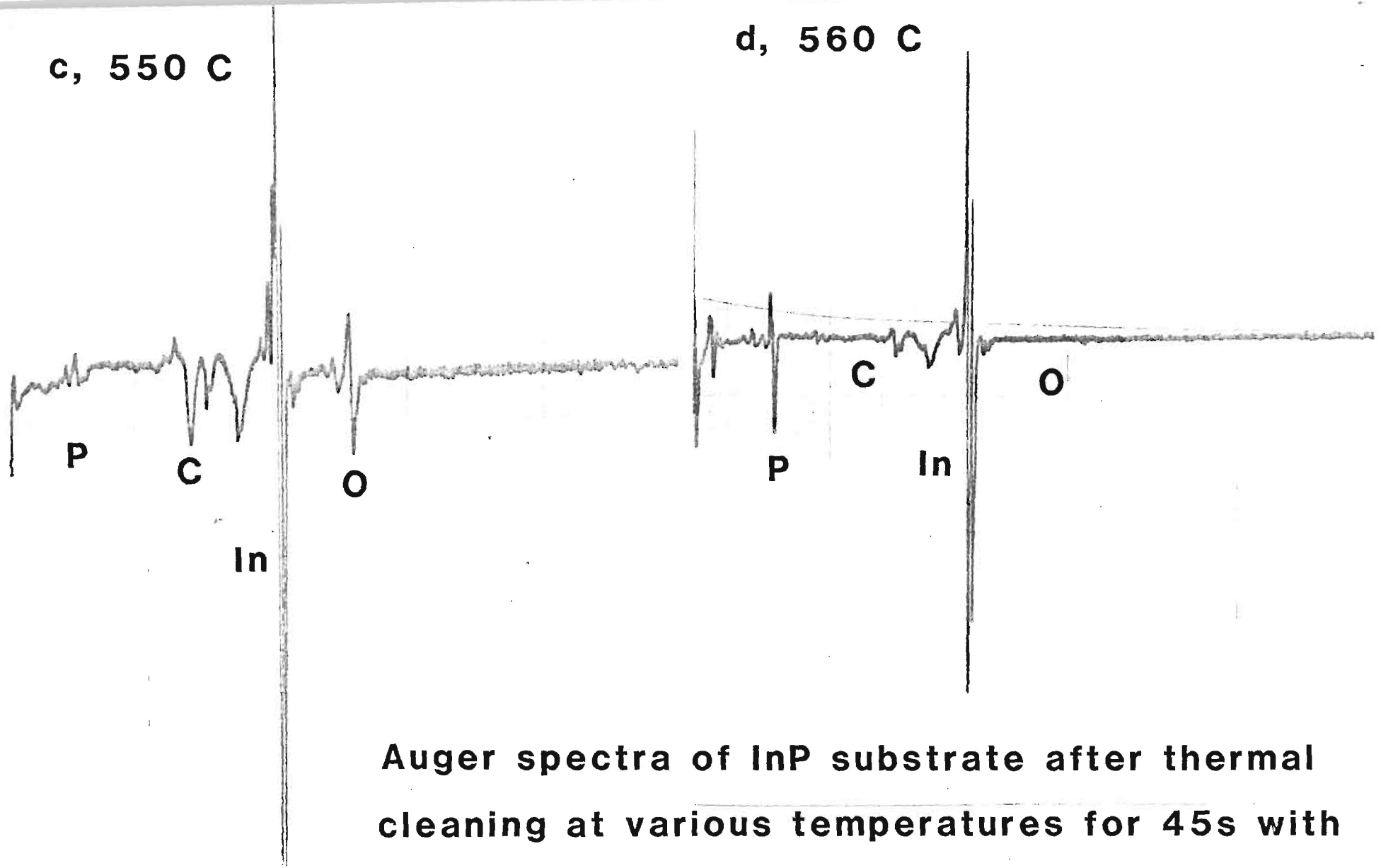

Auger spectra of InP substrate after thermal cleaning at various temperatures for 45s with arsenic passivation flux.

Figure 5

3.3 Layer Analysis

The MBE layers have been characterized using infrared absorption, x-ray rocking curves, optical microscopy and Hall measurements. Samples are currently at NRL awaiting photoluminescence measurements and fabrication into FET structures. Reflection electron diffraction measurements are usually made to ensure smooth surfaces and good epitaxial growth. Unfortunately the Georgia Tech facility has been under repair for some time and is still not back on line at the time of writing. These data will be reported in the next quaterly report.

The composition has been determined using a combination of x-ray rocking curves and infrared absorption.

3.3.1 X-ray Rocking Curves

In order to ascertain whether the MBE film is lattice matched to the InP substrate, the most direct technique is to perform x-ray diffraction from the film and substrate simultaneously. This procedure removes the necessity of making an absolute measurement of the diffraction angle. The present measurements have utilized the $\{400\}$ reflections of Cu $K\alpha_1$, and $K\alpha_2$ lines. For the $\{400\}$ reflections the lattice parameter of the film is given by

$$a_o = \frac{2\lambda}{\sin[\Delta\Theta + \sin^{-1}(\frac{2\lambda}{a_s})]}$$

where λ is the x-ray wavelength

$\Delta\Theta$ is the angle between the diffraction peaks from the film and from the substrate, and

a_s is the lattice constant of the substrate.

All that is necessary therefore is to measure $\Delta\Theta$ since λ and a_s are known and hence a_s can be measured. X-ray rocking curves for sample E0326-II are shown in fig. 6 which shows the diffraction peaks from both the MBE layer and, for comparison, the back surface of the InP substrate. From this figure it is clear that, to within the precision of the x-ray equipment, the film is very well matched to the substrate, with only a very slight assymmetrical broadening observed. This is a substantial improvement over previous samples.

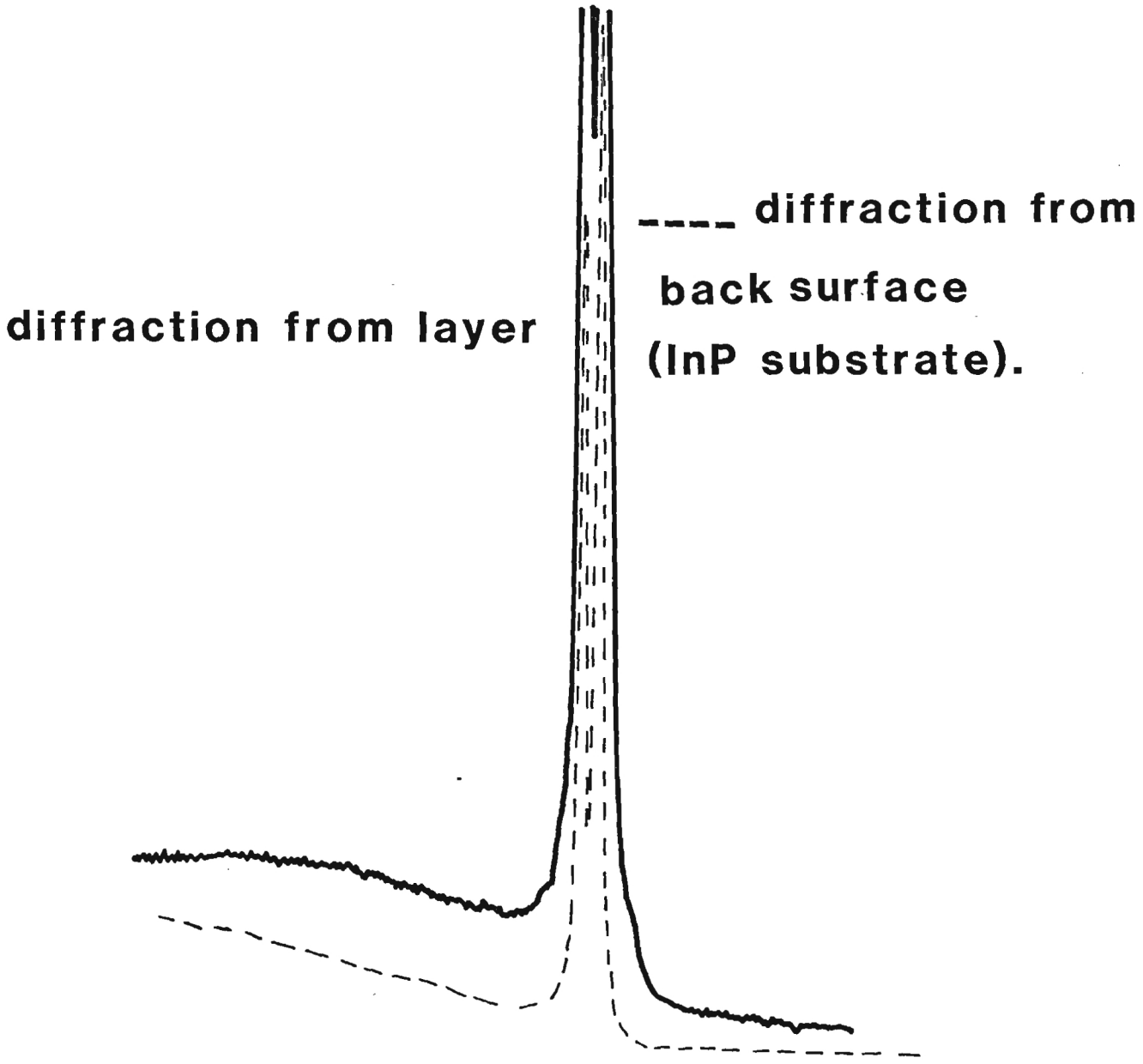

X-ray rocking curves for InGaAsP

MBE layer E0326-II

Figure 6

Having established that good lattice-matching has been achieved and hence that the ratio of the composition variables, y/x, is approximately 2.1, then a measurement of bandgap energy is sufficient to determine x and y uniquely.

Ideally the best way to measure the bandgap precisely is to make electroreflectance studies, however the system at Georgia Tech is yet not operational and there was insufficient time to enable outside workers, e.g. Pollack and co-workers at Brooklyn, to do the measurements. A less precise method, but much simpler to set up, is infrared transmission.

3.3.2 Infrared Transmission

Infrared transmission measurements have been made at room temperature for four samples and the results are shown in fig. 7. These are the transmission values of the InP substrate plus the film ratiod against the transmission of an InP sample of comparable thickness. The spectra have been individually normalized with respect to the maximum transmission. The apparent trailing of the edge to shorter wavelengths is consistent with absorption coefficients of 10^4 cm^{-1} for very thin films. For example, the transmission of a slice of material of thickness d and absorption coefficient α is given by

$$T = e^{-\alpha d}$$

Reflection effects can be taken into account and a plot of α vs. Ev. as shown in fig. 8 obtained. This shape is typical of a direct gap semiconductor and can be analyzed to give an energy gap of 0.8 ± 0.02 eV. This corresponds to a wavelength of 1.55 ± 0.4 m which is esentially the desired wavelength. The y value is 0.86 and x is 0.41 for this lattice matched energy gap.

3.3.3 Hall Measurements

The four MBE grown InGaAsP films have been characterized for their electrical properties at room temperature using van der Pauw-Hall measurements. Contact pads were formed on the unintentionally doped n-type material by evaporating sequentially Au:Ge/Ni/Au alloy. The Au:Ge ratio was 88:12. The contact pads were alloyed for 20s at $450^{o}C$ in

Infrared transmission of MBE InGaAsP layers on InP substrates.

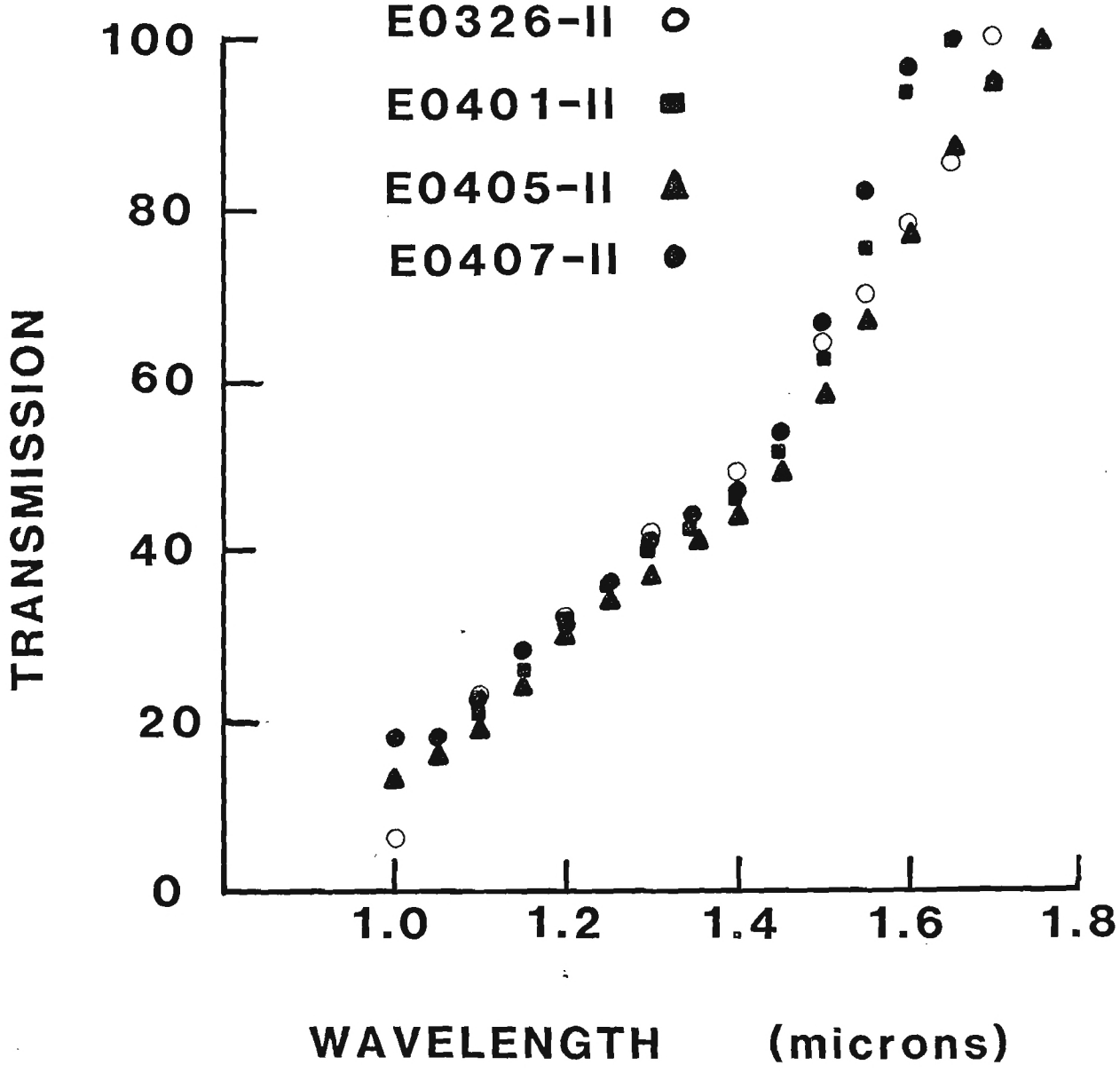

Figure 7

Absorption coefficient vs. energy for MBE InGaAsP layer E0326-II.

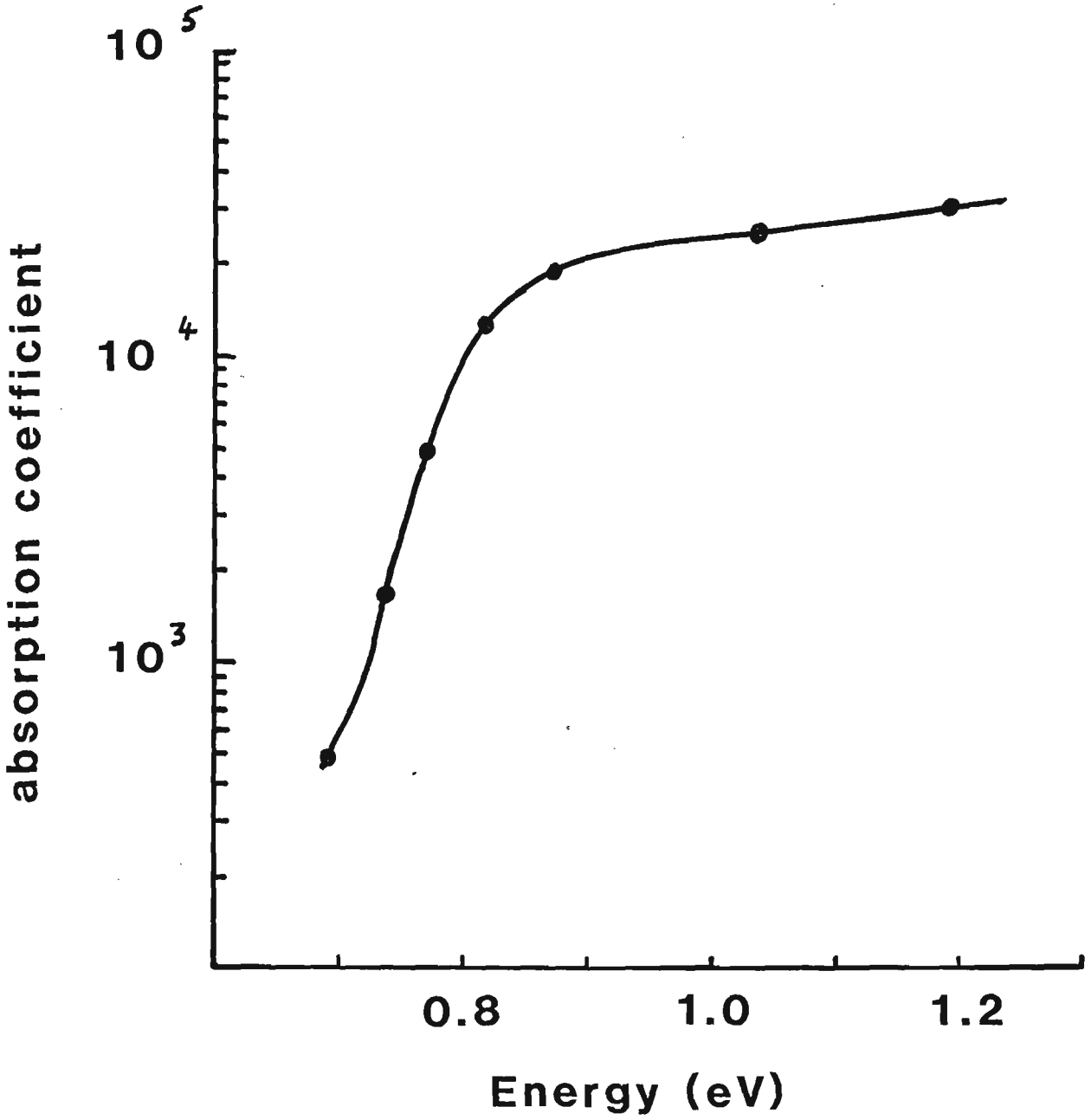

Figure 8

forming gas. Contact was achieved by pressure mounted probes. The results are given in Table 1.

The mobility of 4600 $cm^2V^{-1}s^{-1}$ measured for sample E0326-II is the highest yet reported for an MBE InGaAsP film. This value has been corrected for finite contact pad size.[11] The values of mobility measured for these MBE samples compare very favorably with those of LPE and VPE samples of the same electron concentration and composition. At the present time, the carrier concentration of the MBE samples, although substantially lower than previous MBE samples, still tends to be somewhat higher than the electron concentrations of LPE[12] and VPE[13]. VPE samples can be in the range 0.3 - 1.4 x 10^6 cm^{-3} and for LPE, values down to 1.3 x 10^{16} cm^{-3} can be achieved. The lowest value for an MBE sample is the 3 x 10^{16} cm^{-3} of the present work.

Table 1 also gives the substrate temperature T_s and, if E0401-II is excluded, it would appear that as T_s is increased the carrier concentration is decreased. The mobilities seem to peak at 510°C. These data may be insufficient to draw any meaningful conclusions, however as will be discussed in the next section, the surface morphology of the samples was also dependent upon temperature and signficiant differences occured even for the small range in T_s of 500 - 520°C.

3.3.4 Surface Morphology

The four samples discussed above were grown with different substrate temperatures. The temperatures ranged from 500°C to 520°C. The results of the Hall measurements for the different samples are given in table 1. There is insufficient data to draw unabbiguous conclusions but it would appear that the highest mobilities occur at a substrate temperature of 510°C. It would also seem that the carrier concentration is reduced as the substrate temperature is increased, although the two samples at 510°C have carrier concentrations which differ by a factor of two so one should be wary of drawing too rigid a conclusion.

Further information can be obtained using optical microscopy. Fig. 9 show optical micrographs of the four epilayers under a magnification of 200X. It is obvious that the lowest substrate temperature has yielded the film with the least density of defects. All three other samples exhibit a regularly shaped and oriented defect whose size and

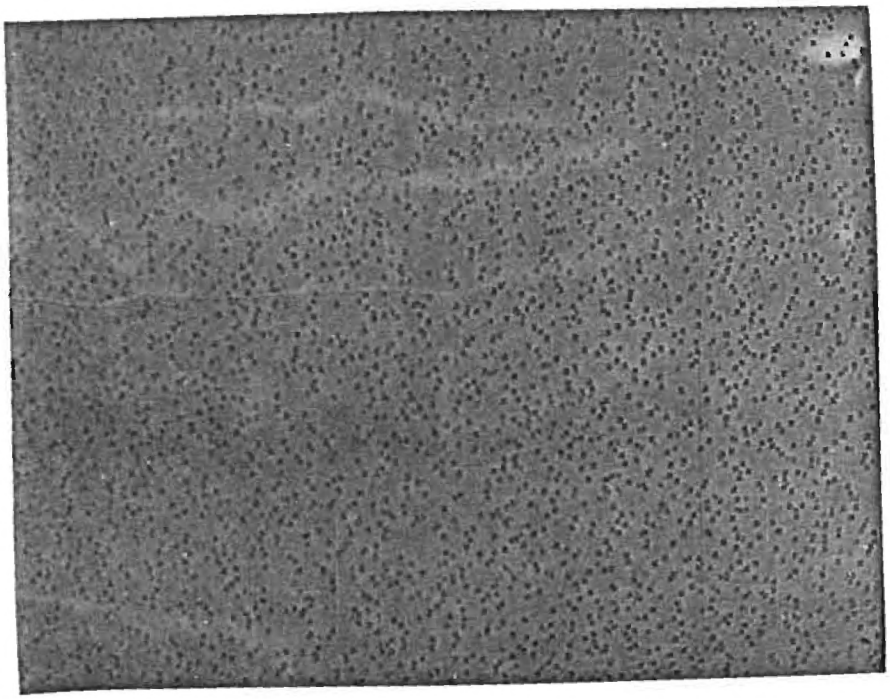

UNDER FOOT

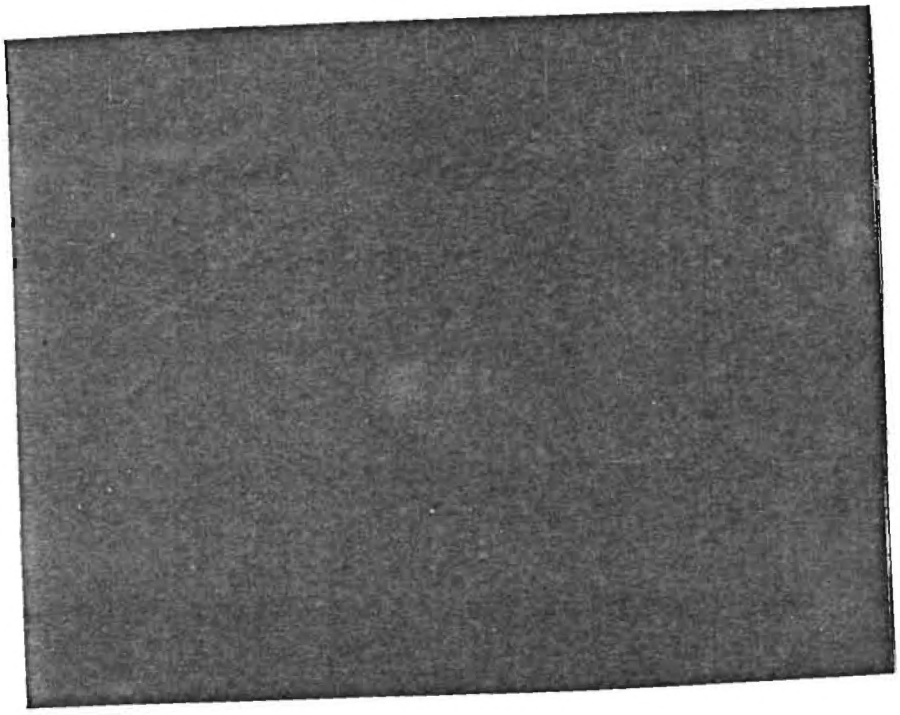

MBE LAYER

InGaAsP LAYER E0326 MAGN. 200X

T(sub):510 C

Figure 9a

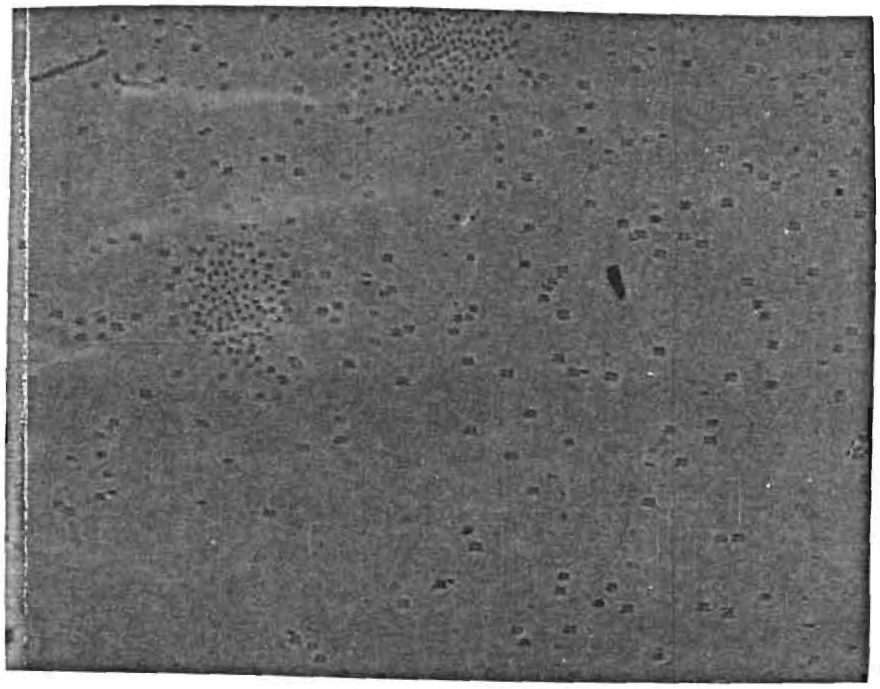

UNDER FOOT

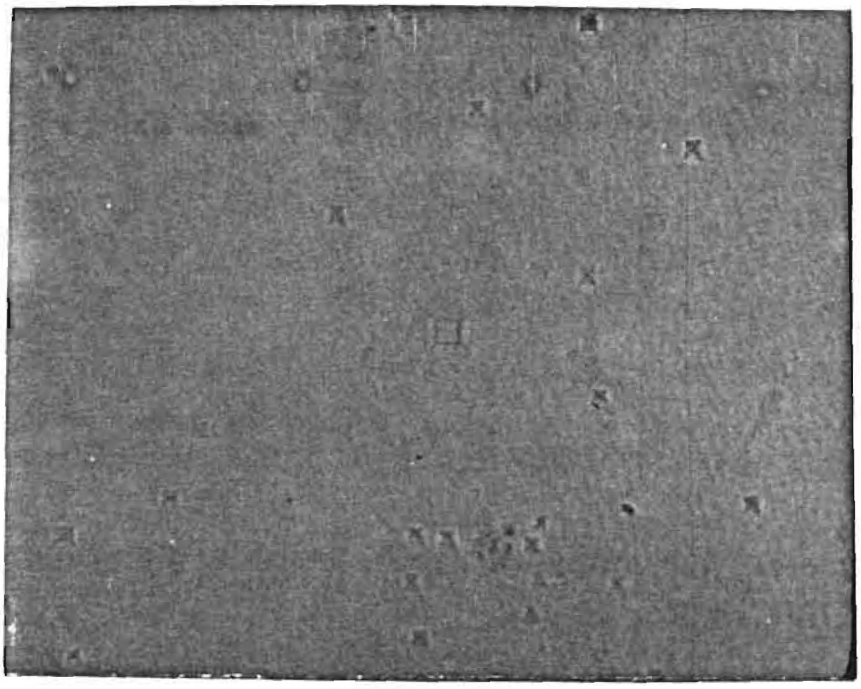

MBE LAYER

InGaAsP MBE LAYER E0401 MAGN. 200X

T(sub):510 C

Figure 9b

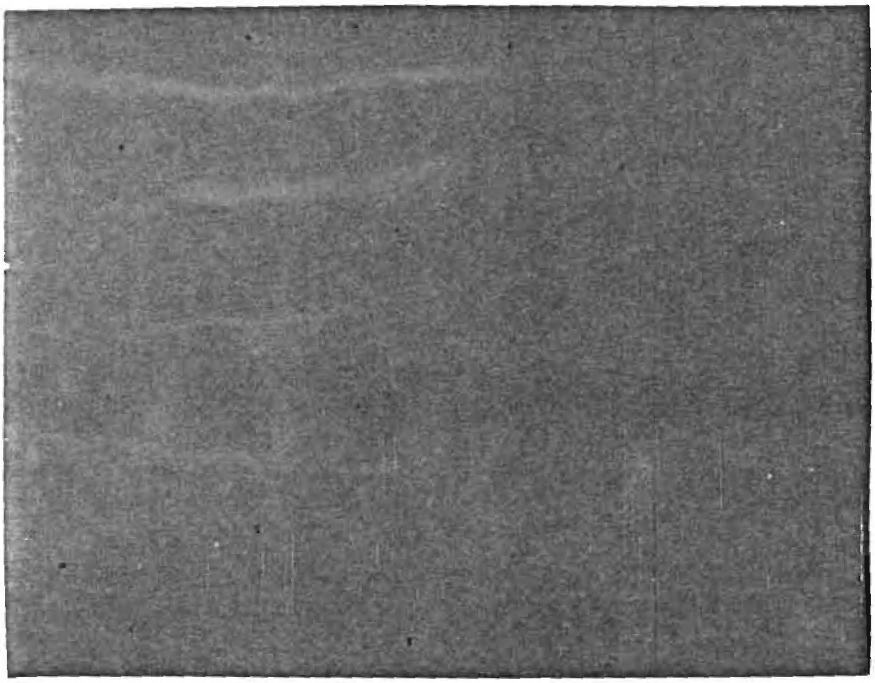

MBE LAYER

UNDER FOOT

InGaAsP MBE LAYER E0405 MAGN. 200X

T(sub):500 C

Figure 9c

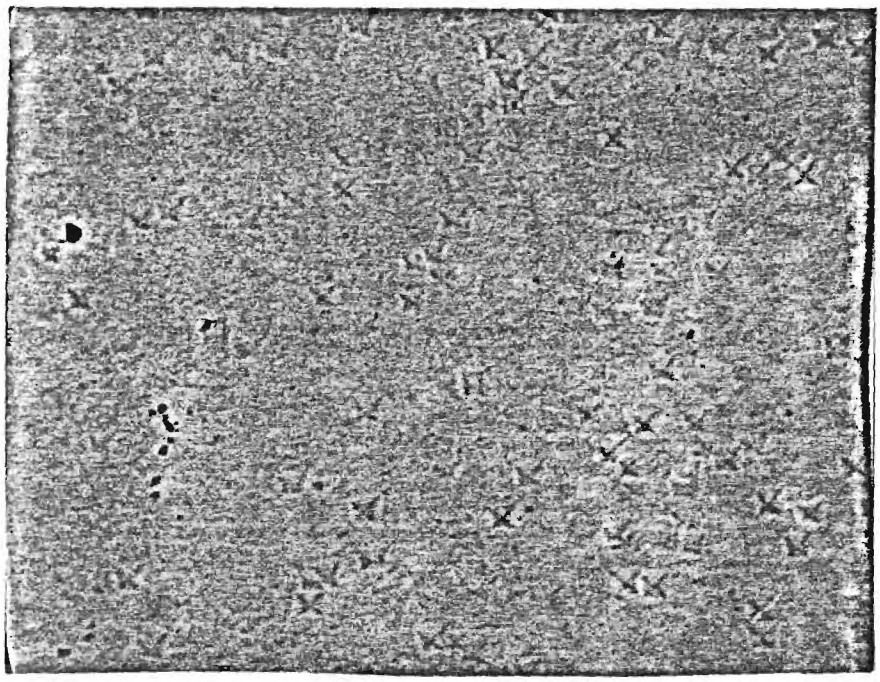

InGaAsP MBE LAYER E0407 MAGN. 200X

T(sub):520 C

Figure 9d

density seem to increase with substrate temperature. A scan across part of E0326-II using the Tencor step profiler is shown in figure 10 which determines that the defects are projections with heights up to 2000Å (the film thickness is 6500 Å). The defects have a square cross-section with a tapered profile, being widest at the base. They all have the same orientation.

Since part of the substrate is obscurred during growth by the foot which is used for thickness measurements, it is possible to examine the substrate surface without the growth of an epilayer. An optical micrograph of the area under the foot on sample E0326-II is shown in fig. 9a. Similar-looking defects to those on the film are observed. They have the same shape and orientation. Interestingly, for sample E0405-II fig. 9c, which was grown at 500°C and which showed essentially zero defects on the film, there is some evidence of defects under the foot. These defects tend to grow along imperfections, scratches etc. Also very interesting is the fact that a Tencor scan of the area under the foot, fig. 11, shows that the defects under the foot consist, not of projections, but pits with depths up to 400 Å.

Presumably what is happening is that the high substrate temperature causes phosphorous depletion which in turn induces the formation of pits in the substrate, especially near surface or crystalline imperfection. These pits then becomes a source for preferential growth, giving rise to the projections observed in the film.

In spite of the defect density and size being greater for T_s = 510°C than for T_s = 500°C, the mobilities are better for the higher T_s. Surface appearance therefore does not necessarily correlate with electrical quality.

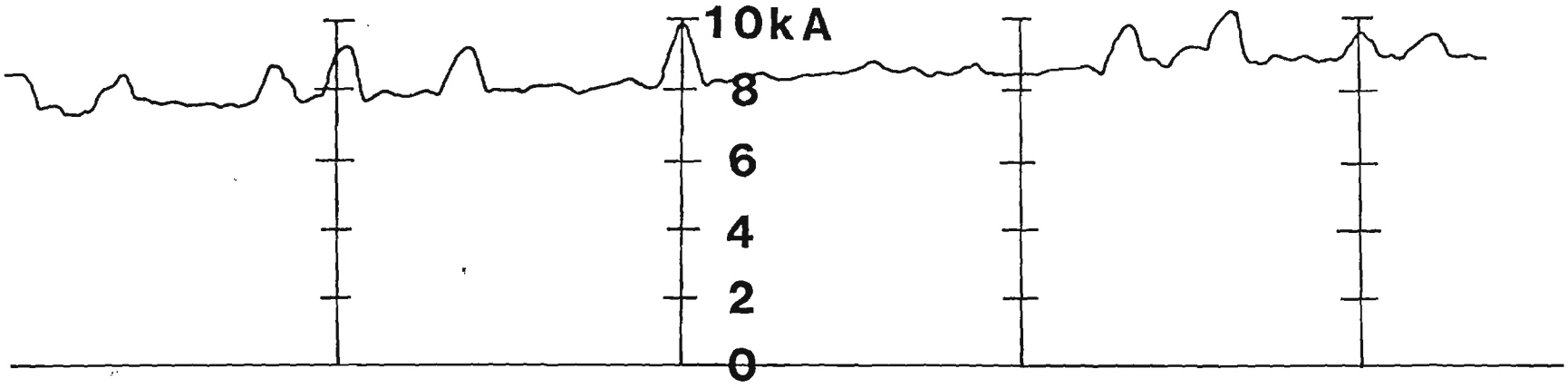

Figure 10

Tencor scan across MBE InGaAsP film.

Scan shows projections up to 2000A in height.

Projections have square horizontal cross-section and triangular vertical cross-section.

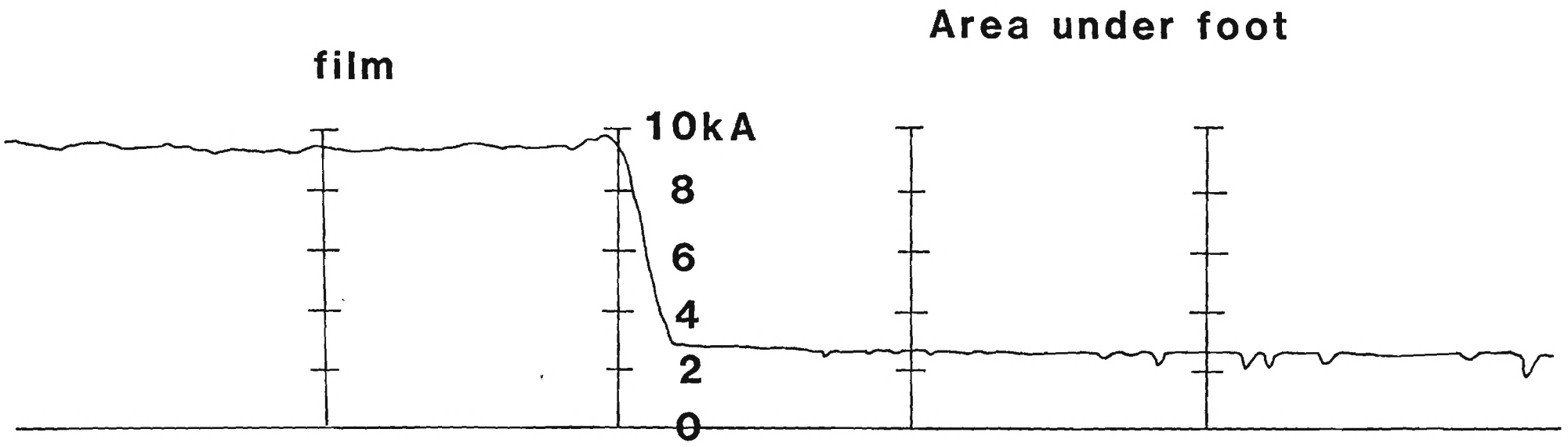

Tencor scan from film to foot of MBE InGaAsP on InP substrate

Foot scan shows presence of pits up to 400A deep.

Pits have square horizontal cross-section and triangular vertical cross-section.

Figure 11

4. MBE GROWTH OF INTENTIONALLY-DOPED n-TYPE InP

As discussed earlier in section 1, the InGaAsP/InP double-heterostructure diode laser requires both n-type and p-type InP confining layers. This section is concerned with the growth of a suitably-doped n-type InP layer by MBE.

4.1 Growth of InP by Molecular Beam Epitaxy

Although InP is a potentially very important material for the fabrication of high-frequency microwave devices, relatively little work has been reported on the growth of InP by MBE. Growth has been achieved using both InP[14,15] and red phosphorous[16,17,18] sources; substrate temperatures between 350 and 510°C have been used. The lowest carrier concentration which has been achieved are 2×10^{16} cm^{-3} with mobilities of 3,500 $cm^2V^{-1}s^{-1}$ at room temperature.[18] As the substrate temperature is increased the ratio of phosphorous to indium has to be increased in order to compensate for the loss of phosphorous from the surface. This situation has already been encountered in the growth of InGaAsP films on InP and as mentioned previously, the loss of phosphorous could be the origin of the surface features observed in InGaAsP grown at temperatures above 500°C. However, the defects reported by Norris and Stanley[14] for $T_s > 410$°C consisted of whiskers anchored to In droplets. In our situation the defects were more regularly shaped and occurred at much higher temperatures.

The question of surface-cleaning has recieved some attention. Norris and Stanley[14] have used argon ion sputtering followed by annealing to remove the oxygen and carbon layers. The reason for using ion cleaning was the supposition that heat cleaning of the InP substrate could not remove the contaminant due to the low noncongruent evaporation temperature. However as shown in an earlier section, and verified by Auger analysis, heat cleaning at temperatures up to 560°C under an arsenic passivation flux is successful.

This section is a brief discussion of the growth of unintentionally-doped n-type InP using In and InP as the sources. The general growth conditions, and procedures are similar to those already detailed for InGaAsP and will not be repeated here. The results for four films are

given in table 2. With the exception of film E0610-II, the mobilities at room temperature are about 2000 $cm^2V^{-1}s^{-1}$ with carrier concentration 1 - 2 x 10^{17} cm^3. Although the background carrier concentration is rather higher than hoped for, these values are consistent with other reported work. One factor worth mentioning is the relatively slow growth rate. The temperatures of the ovens used gave rise to a growth rate of 0.4 μm per hours. Higher oven temperatures will be needed to increase the growth rate.

Having established a set of growth conditions for InP it was necessary to increase the electron concentration up to 2 x 10^{18} cm^{-3}, as required for the confinement layer on an InGaAsP/InP double-heterostructure laser. The information on suitable dopants in the literature is very sketchy but tin has been used with some degree of success although the present seems to be the first reported Hall measurement on Sn-doped InP. A Sn oven was incorporated into the MBE system and a preliminary growth run at an oven temperature of 640°C was made. At this temperature the pressure differential was too small to be measured by the ion gauge. The electrical characteristics for this film are also shown in table 2. The growth conditions were those established for the undoped InP growths. This film has been the only doping result obtained in the time frame covered by this report but shows that the conditions were almost ideal, with an electron concentration of 2.2 x 10^{18} cm^{-3} and a mobility of 1900 $cm^2V^{-1}s^{-1}$ at room temperature being achieved.

4.2 Summary

This brief section has shown that unintentionally-doped and Sn-doped InP layers have been successfully grown using MBE. The necessary growth condition for material suitable for incorporation into DH lasers have been established.

ROOM TEMPERATURE HALL DATA

SAMPLE	MOBILITY $cm^2V^{-1}s^{-1}$	CONCENTRATION cm^{-3}	THICKNESS μm	SUBSTRATE TEMP. °C
E0528-II	1600	1.3×10^{17}	0.7	510
E0610-II	1100	4×10^{17}	0.25	510
E0611-II	2300	2.5×10^{17}	0.56	510
E0624-II	2500	2.3×10^{17}	0.36	510
*E0625-II	1900	2×10^{18}	0.4	520

*Sn-doped

Table 2

5.0 REFERENCES

1. M.A. Littlejohn, J. R. Hauser, and T. H. Glisson, "Velocity-field characteristics of $Ga_{1-x}In_xP_{1-y}As_y$ quaternary alloys," Appl. Phys. Lett. 30 pp. 242-244, (1977).

2. D. K. Ferry, "Materials Considerations for Advances in Submicron VLSI" Advances in Electronics and Electron Physics Edited by C. Marton, Academic Press, New York, 1982.

3. S. Bandy, Y. Chai, R. Chow. T. Gibbs, C. Hooper, C. Nishimoto and P. Stonestrom. "Submicron FETS Using Molecular Beam Epitaxy" Final Report. Contract N00014-77-C-0655. Office of Naval Research.

4. N. M. Ravindra and V. K. Srivastava, "Variation of Refractive Index with Energy Gap in Semiconductors" Infrared Physics 19, pp. 603-604, (1979).

5. Unpublished work at Georgia Tech.

6. L. M. Schiavone and A. A. Pritchard, "Ohmic Contacts for moderately resistive p-type InP," J. Appl. Phys. 46, pp. 452-453, (1975).

7. F. A. Thiel, D. D. Bacon, E. Buehler, and K. J. Bachmann," Contacts to p-type InP," J. Electrochem. Soc. 124, pp. 317-318 (1977).

8. K. Tabatabaie-Alavi, A. N. M. M. Choudhury, N. J. Slater, and C. G. Fonstad. "Very low resistance ohmic contacts on p-type InP by direct plating," Appl. Phys. Lett. 40, pp. 398-400, (1982).

9. G. Y. Robinson, "A Study of Metal-Semiconductor Contacts in InP", RaDC Report No. TR-81-169, 1981.

10. G. D. Holah, E. L. Meeks, F. L. Eisele and D. W. Covington, "Growth and Characterization of $In_{1-x}Ga_xAs_yP_{1-y}$ and GaAs using Molecular Beam Epitaxy," Final Report, Contract No. N00173-79-C-0033, Naval Research Laboratory, (1982).

11. L. J. van der Pauw. "A Method of Measuring Specific Resistivity and Hall Effect in Discs of Arbitrary Shape," Phillips Res. Repts. 13 pp. 1-9, (1958).

12. P. K. Bhattacharaya, J. W. Ku, S. J. T. Owen, G. H. Olsen, and S. H. Chiao, "LPE and VPE $In_{1-x}Ga_xAs_yP_{1-y}$/InP: Transport Properties, Defects,and Device Considerations," I.E.E.E. J. Quantum Electron. QE-17, pp. 150-160, (1981).

13. G. H. Olsen and T. J. Zamerowski, "Vapor-Phase Growth of (In,Ga)(As,P) Quaternary Alloys" I.E.E.E. J. Quantum Electron, EQ-17, pp. 128-138, (1981).

14. M. T. Norris and C. R. Stanley, "Substrate Temperature limits for epitaxy of InP by MBE," Appl. Phys. Lett. 35 pp. 617-620, (1979).

15. Y. Kawamura, M. Ikeda, H. Asahi, and H. Okamoto, "Photoluminescence of undoped (100) InP homoepitaxial films grown by molecular beam epitaxy," Appl. Phys. Lett. 35 pp. 481-483, (1979).

16. R. F. C. Farrow, "Growth of indium phosphide films from In and P_2 beams in ultra high vacuum," J. Phys. D: Appl. Phys. 7, pp. L121-L124, (1974).

17. Y. Matsushima, Y. Hirofuji, S. Gonda, S. Mukai, and M. Kinata, "Molecular Beam Epitaxial Growth of InP," Jpn. J. of Appl. Phys. 15, pp. 2321-2325, (1976).

18. J. H. McFee, B. I. Miller and K. J. Bachmann, "Molecular Beam Epitaxial Growth of InP," J. Electrochem. Soc. 124, pp. 259-272, (1979).

QUARTERLY PERFORMANCE AND STATUS OF FUNDS

Level of Effort

Categories	1 February 1982 30 April 1982	Cummulative Total (Man months)
Principal Research Engineer/Scientist	0.11	.44
Senior Research Engineer/Scientist	2.88	8.0
Research Engineer/Scientist	0.44	1.1
Assistant Research Engineer/Scientist	0.65	1.5
Graduate Research Assistant	-	-
Co-op, Student	-	-
TOTAL	4.04	11.4

Financial Status

1 February 1982 - 30 April 1982	Cummulative Total Expended
$25,958	$73,849

Total Contract Funding (through 30 April 1982) Extension to 31 August 1982	$99,982

A-2951

FINAL REPORT
PROJECT A–2951

BINARY, TERNARY AND QUATERNARY HETEROJUNCTIONS OF III-V SEMICONDUCTORS GROWN BY MOLECULAR BEAM EPITAXY

By

G. D. Holah, E. L. Meeks, and F. L. Eisele

Prepared for

NAVAL RESEARCH LABORATORY
WASHINGTON, D.C. 20375

Under

Contract No. N00014–81–K–2007

November 1982

GEORGIA INSTITUTE OF TECHNOLOGY
A Unit of the University System of Georgia
Engineering Experiment Station
Atlanta, Georgia 30332

GT EES

1982

BINARY, TERNARY AND QUATERNARY HETEROJUNCTIONS OF III-V SEMICONDUCTORS GROWN BY MOLECULAR BEAM EPITAXY

FINAL REPORT

G. D. Holah, E. L. Meeks, and F. L. Eisele

A-2951

Engineering Experiment Station
Georgia Institute of Technology
Atlanta, Georgia 30332

November 1982

Contract No. N00014-81-K-2007

Prepared for:

Naval Research Laboratory
Washington, D.C. 20375

PREFACE

This report describes work primarily performed at the Georgia Institute of Technology Engineering Experiment Station under Contract No. N00014-K-2007 during the period May 1st 1981 through 31 August 1982. Funding for the program is provided by the Naval Electronics Systems Command. The Scientific Officers responsible for the technical administration of the program are Dr. John E. Davey and Dr. Harry Dietrich of the Naval Research Laboratory.

SUMMARY

This report describes the technical accomplishments of a one-year basic research program directed towards a study of the quaternary III-V alloy system $In_{1-x}Ga_xAs_yP_{1-y}$ grown by molecular beam epitaxy. The objectives were to grow layers of $In_{1-x}Ga_xAs_yP_{1-y}$ and InP suitable for processing into double heterostructure diode lasers. Layers of $In_{1-x}Ga_xAs_yP_{1-y}$ have been grown lattice matched to InP with bandgaps near 1.55 μm and with electron mobilities of 4600 $cm^2V^{-1}s^{-1}$ which are the highest reported to date. InP films suitable for confinement layers in a diode laser have been grown and Sn has been shown to be a suitable n-type dopant. Preliminary data suggests that Be will be a useful p-type dopant.

The layers have been analyzed using infrared absorption, photoluminescence, electroreflectance, x-ray diffraction, reflection electron diffraction and Hall measurements. The photoluminescent data are the first reported for $In_{1-x}Ga_xAs_yP_{1-y}$ grown by MBE and indicate that lasing quality material has been grown.

TABLE OF CONTENTS

TABLE OF CONTENTS (Cont'd)

LIST OF TABLES

LIST OF ILLUSTRATIONS

1.0 INTRODUCTION

1.1 Background

Quaternary and ternary compound semiconductors have been subject of considerable interest for a number of years due to their application in laser diodes[1] and sources for optical fiber communications. The bandgap energy[2] and hence the lasing wavelength of the quaternary III-V alloy $In_{1-x}Ga_xAs_yP_{1-y}$ can be adjusted by varying the composition parameters x and y. At the same time the quaternary can be lattice matched[3] to both InP and GaAs. By keeping the y/x ratio near 2.1, $In_{1-x}Ga_xAs_yP_{1-y}$ can be grown lattice matched to InP and by adjusting the absolute values of x and y it can be grown with bandgaps between 1.1 μm and 1.6 μm whilst still lattice-matched to InP. This covers the region of low loss and low dispersion of the silica-based optical fibers presently used in optical telecommunications. These quaternary alloys therefore find important applications as sources and detectors for optical communications. Commercial diode lasers using $In_{1-x}Ga_xAs_yP_{1-y}$ (henceforth this will be written without the composition, i.e. as InGaAsP) have been available for some time. Photodetectors, such as avalanche photodiodes,[4] using InGaAsP, although at a much earlier stage of development than diode lasers, have also been fabricated. Thus far, these devices have been processed from epitaxial films grown by liquid-phase epitaxy[5] (LPE) or vapor-phase epitaxy[6] (VPE); no device has yet been fabricated from material grown using molceular beam epitaxy (MBE).

Recently, theoretical calculations have suggested that carrier peak velocities and low field mobilities[7] for InGaAsP/InP should be higher than those of GaAs, InP and InGaAs. If this were indeed the case experimentally, then the InGaAsP/InP system would find important

application in microwave devices such as MESFETS and TED devices. Much interest was generated by these calculations and in fact were part of the rationale for the proposal of the present program. It became increasingly obvious however that large discrepancies existed between measured and calculated mobilities and velocities.[8] These discrepancies were resolved when new calculations showed that much lower values of mobility and velocity were to be expected.[9] The initial calculations used extrapolated values for the Γ_{LX} energy gap which were eventually found to be too high. When this value was finally measured it was about 25% lower than predicted; the lower value enabled inter-valley scattering to occur at a much earlier stage, thereby reducing the mobilities and velocities.

Although the application in microwave and millimeter-wave devices of InGaAsP will probably not be as signficiant as thought earlier, the application to optical fiber telecommunications is undisputed, and this is reflected by the very large numbers of research papers being published. Furthermore, the future possibilities of totally integrated opto-electronic circuits using InGaAsP/InP systems may well prove to be of signficant importance. Presently, however, the direct importance of InGaAsP remains as diode laser and detector material for devices operating near 1.3 μm and
1.55 μm.

In spite of the proven optical device applications of InGaAsP, very little effort has been reported on the growth using molecular beam epitaxy. The most comprehensive study,[10] for which the present program is essentially a follow-on, demonstrated epitaxial growth on both InP and GaAs substrates. The lattice-matching and composition control in that study was not optimised, and hence it was not possible to grow

material of the highest quality and with a predetermined bandgap. This program was successful however in growing the best MBE material available at that time. The present program has successfully addressed both of these problems.

1.2 Present Status of MBE Growth of InGaAsP

There have been three reported attempts to grow InGaAsP using MBE. Cho[11] used a Ga and In mixture in one effusion cell GaAs and GaP mixed in another effusion cell as the As and P source together with an additional elemental phosphorous cell. The sticking coefficients of phosphorous and arsenic depend upon the amounts of Ga and In incident on the InP substrate as well as the substrate temperature, whereas Ga and In have unity sticking coefficients for the range of substrate temperatures commonly used. The ratio of P_2:As_2 from the GaAs-GaP cell could be adjusted via the cell temperature. At a cell temperature of 905^{o}C the P_2:As_2 flux ratio was 8:1, rising to 16:1 at 900^{o}C. Since phosphorous has a lower sticking coefficient than arsenic at the substrate temperatures used (~ 400^{o}C), it was found necessary to use a P_2:As_2 flux ratio of 40:1 to give a final composition ratio P:As of 3:1. Cho also reported that material doped with Sn was n-type with a carrier concentration and mobility at room temperature of 5 x 10^{16} cm^{-3} and 1650 $cm^{2}V^{-1}s^{-1}$ respectively although undoped values were not given. Foxon et al[12] reported a film grown on a GaAs substrate using As_4 and P_4 sources. No further information was reported however except to state that x-ray diffraction yielded a broad curve which suggested vertical and/or horizontal spatial compositional inhomogeneity.

The most comprehensive study prior to the present program was undertaken at Georgia Tech[10] with support from Naval Electronics Systems

Command under contract No. N00173-79-C-0033. This program which was not wholly concerned with quaternary growth by MBE, and also included growth of InP, GaAs and InGaAs, reported the growth of InGaAsP MBE films on both GaAs and InP substrates using a variety of sources. The group V sources were either GaAs or As as an As source and InP as the P source. The best material was grown using GaAs and InP as As_2 and P_2 sources respectively. The highest mobility obtained for undoped InGaAsP films was 2126 $cm^2V^{-1}s^{-1}$ with a carrier concentration of $1.6 \times 10^{17} cm^{-3}$ at room temperature. During a period when this program overlapped with the present program, the mobility figure was increased to 4000 $cm^2V^{-1}s^{-1}$ for a similar carrier concentration. However, good compositional control was not achieved. The 4000 $cm^2V^{-1}s^{-1}$ mobility value approached the values achieved using LPE.

1.3 Program Objectives

The objectives outlined in the original statement of work involved the growth and characterization of InGaAsP/InP heterojunctions with emphasis on millimeter and microwave devices. In light of the discussion in section 1.1, the following objectives were finalized after discussion with NRL staff.

1. Improve growth and characterization of InGaAsP/InP
2. Establish a flux monitoring scheme to continuously monitor fluxes emerging from the various ovens during growth.
3. Grow selected epitaxial GaAs layers on specially prepared substrates for FETs.
4. Grow films of InGaAsP with bandgaps at 1.5 μm
5. Grow InGaAsP/InP structure suitable for processing into double-heterostructure diode laser. In addition to task 4, this

would include investigating suitable n- and p-type dopants for InP.

1.4 Principal Results

- o An optical characterization facility has been set up to allow more detailed material analysis.
- o A flux monitor based upon an electron impact ionization gauge has been tested for one oven and shown to be a feasible monitoring technique
- o InGaAsP films have been grown on InP which show improved lattice matching and increased mobility. Reproducibility of the growth runs has been verified.
- o InGaAsP with bandgaps at 1.5 μm have been grown with room temperature mobilities exceeding 4600 $cm^2V^{-1}s^{-1}$ and with carrier concentrations near $5 \times 10^{16} cm^{-3}$. This material is as good as or better than corresponding liquid phase epitaxial films.
- o Sn has been established as a suitable n-type dopant for InP.
- o Be has been studied as a possible p-type dopant for InP and initial results indicate potential use.
- o Selected epitaxial MBE n-layers of GaAs have been grown on specially prepared NRL substrates with thicknesses and concentrations suitable for FET processing.
- o A laser structure was not grown, although the conditions for growth of all the layers had been established, due to a serious system malfunction which resulted in growth being curtailed for several weeks towards the end of the time period covered by the contract.

2.0 GROWTH AND ANALYSIS OF MBE FILMS

2.1 System

Most of the films discussed in this report contain phosphorous which is potentially a severe contaminant to ion pumps and vacuum systems in general. Because of this, two MBE systems have been used during this program, one to grow InGaAsP and InP and the other being restricted to only GaAs. Since both systems are very similar, differing mainly in dimension, only the InGaAsP-InP MBE system will be discussed in any detail.

A schematic of the MBE system is shown in figure 1. There are two distinct pumping areas. The main growth chamber and an interlocked sample loading chamber can be isolated and pumped independently; the main chamber is pumped by a cryopump and the interlock by an ion pump. During growth there is no isolation and both pumping systems work together. Initial roughing of either chamber, which can be accomplished independently, is achieved using a rotary pump followed by sorption pumping. All parts of the system, including both pumps, can be baked out at temperatures up to 200^{o}C. The loadlock chamber allows substrates to be loaded without opening the growth chamber, thereby reducing the possibility of system contamination. The growth chamber is only opened for source replenishment. The fast pumping speed of the cryopump is especially beneficial since, as will be discussed later, the InP oven rapidly depletes of phosphorous, which therefore necessitates frequent opening of the growth chamber for source replenishment. The cryopump minimizes pump down times. Six graphite effusion cells are mounted inside a water-cooled cryoshroud. A further cryogenic panel completely surrounds the region between, and including, the sources and substrate to prevent contamination due to materials desorbing from the chamber

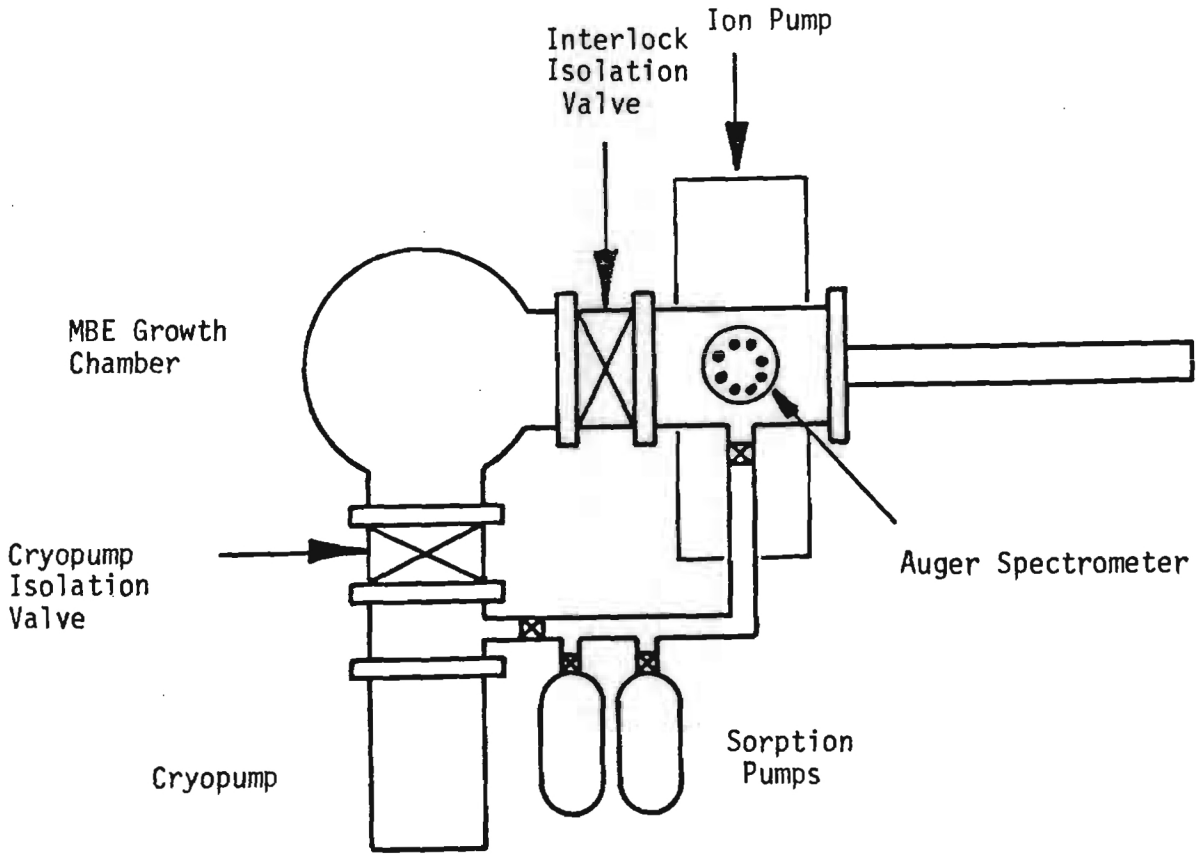

Figure 1

Figure 1. Schematic of MBE Quaternary Growth System.

walls.

At the bottom of the growth chamber is an optical viewing port which enables the layer to be evaluated visually during growth. If the layer does not maintain a mirrorlike surface, the growth can be terminated therby reducing waste of ovenloads. This port can also be used with a laser, either for surface analysis using reflection measurements or for possible laser annealing during growth.

An ion gauge immediately behind the substrate position is used to determined the flux rates from each oven. The temperature of each oven is adjusted until the required partial pressure due to molecules from that oven is achieved. Individual shutters enable each oven to be monitored independently.

The substrate is mounted on the substrate holder using indium solder. The holder is heated radiantly from the rear and the substrate temperature monitored by a thermocouple mounted adjacent to the substrate. The substrate is moved within the system from the loadlock into the growth chamber using a magnetic drive.

The ovens and substrate are normally held at an elevated temperature, approximately 50% of growth temperature, between runs to prevent contamination due to absorption of foreign material. With the system under these 'idling' conditions and with full cryogenic pumping, base pressures down to 5×10^{-10} torr have been achieved after bakeout of about 12 hours. Automatic overnight bakeout is routinely used.

It is clearly of utmost importance for the substrate to have as clean a surface as possible immediately prior to growth. For InP substrates the most common technique is to sputter-clean followed by thermal annealling to remove damage introduced by the sputter process.

From studies at Georgia Tech[10] it has been found sufficient to use a thermal clean process. An Auger spectrometer has been installed on the interlock chamber and a spectrum of the surface contaminants is obtained immediately after loading the substrate. The substrate is then heated to 560^{o}C under either an arsenic or phosphorous stabilising flux, preventing a depletion of phosphorous which would otherwise occur since the substrate cleaning temperature is well above the congruent evaporation temperature. An Auger spectrum is obtained after thermal cleaning. Heating the substrate at 560^{o}C for 45s removes all traces of oxygen and carbon. Typical Auger spectra before and after thermal cleaning are shown in figure 2, and confirm the complete removal of oxygen and carbon as surface contaminants.

As indicated in section 1.1 various sources of phosphorous may be used for MBE growth. The two most common being InP which is a source of P_2[13], and elemental red phosphorous which produces P_4.[14] Both sources have been used with varying degrees of success. For InP MBE films the highest mobility material grown has used InP as a dimer phosphorous source. This work at Georgia Tech[15] achieved room temperature mobilities near 3800 $cm^2V^{-1}s^{-1}$ compared to 3500 $cm^2V^{-1}s^{-1}$ which is the highest reported using P_4. The evaporation of indium from InP is sufficiently small so as to make no contribution to the overall In concentration. There is however, a major problem with using InP in that the phosphorous depletes so rapidly. Using the standard ovens in our MBE system, approximately 1 cm diameter by 3 cm long, total growth times of 5-6 hrs. with maximum film thicknesses of no more than 4 microns are obtained. A larger oven was constructed and tested but the increased surface area of the load seemed to increase the formation of P_4 and, in

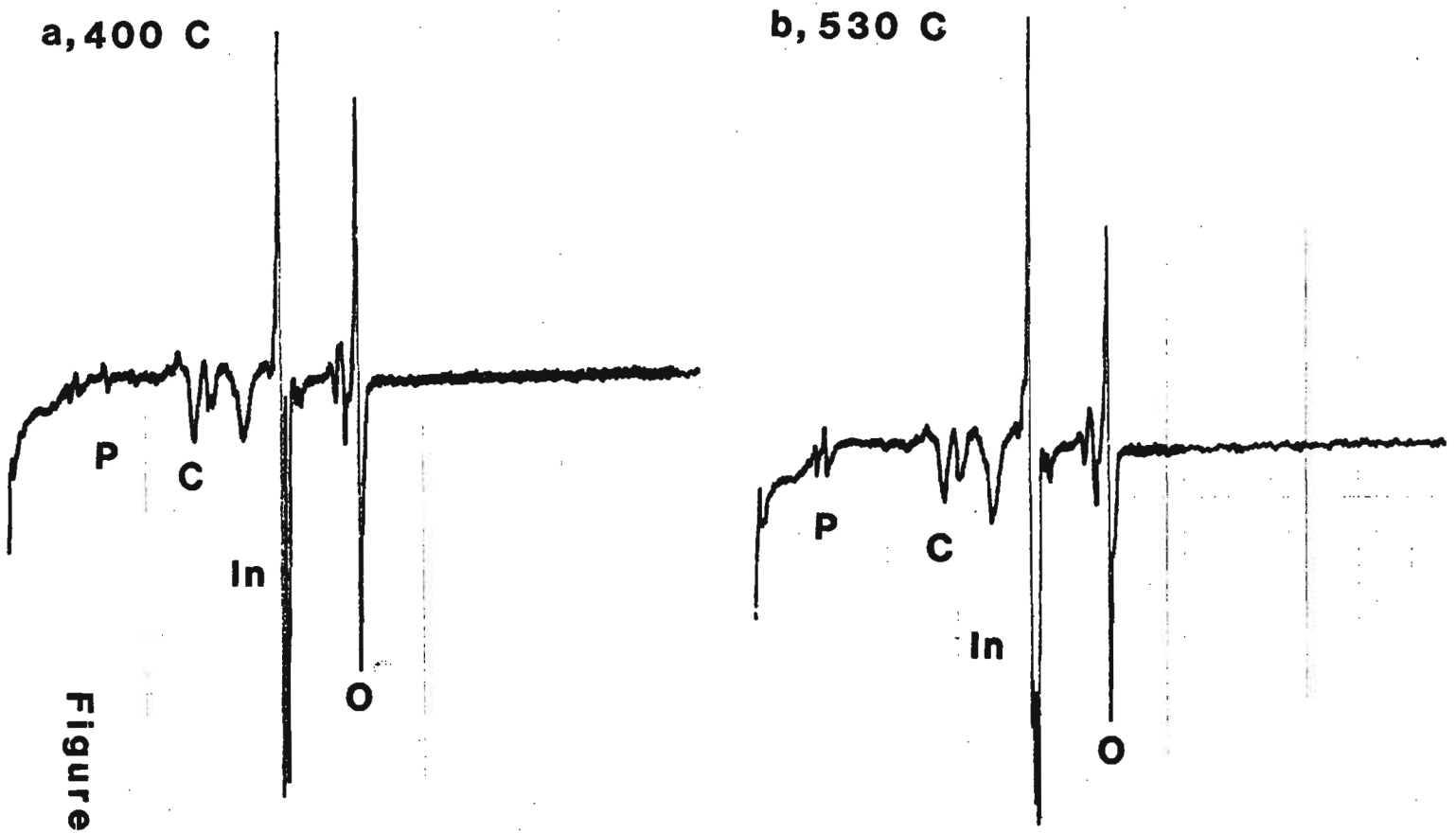

Figure 2a

Auger spectra of InP substrate after thermal cleaning at various temperatures for 45s with arsenic passivation flux.

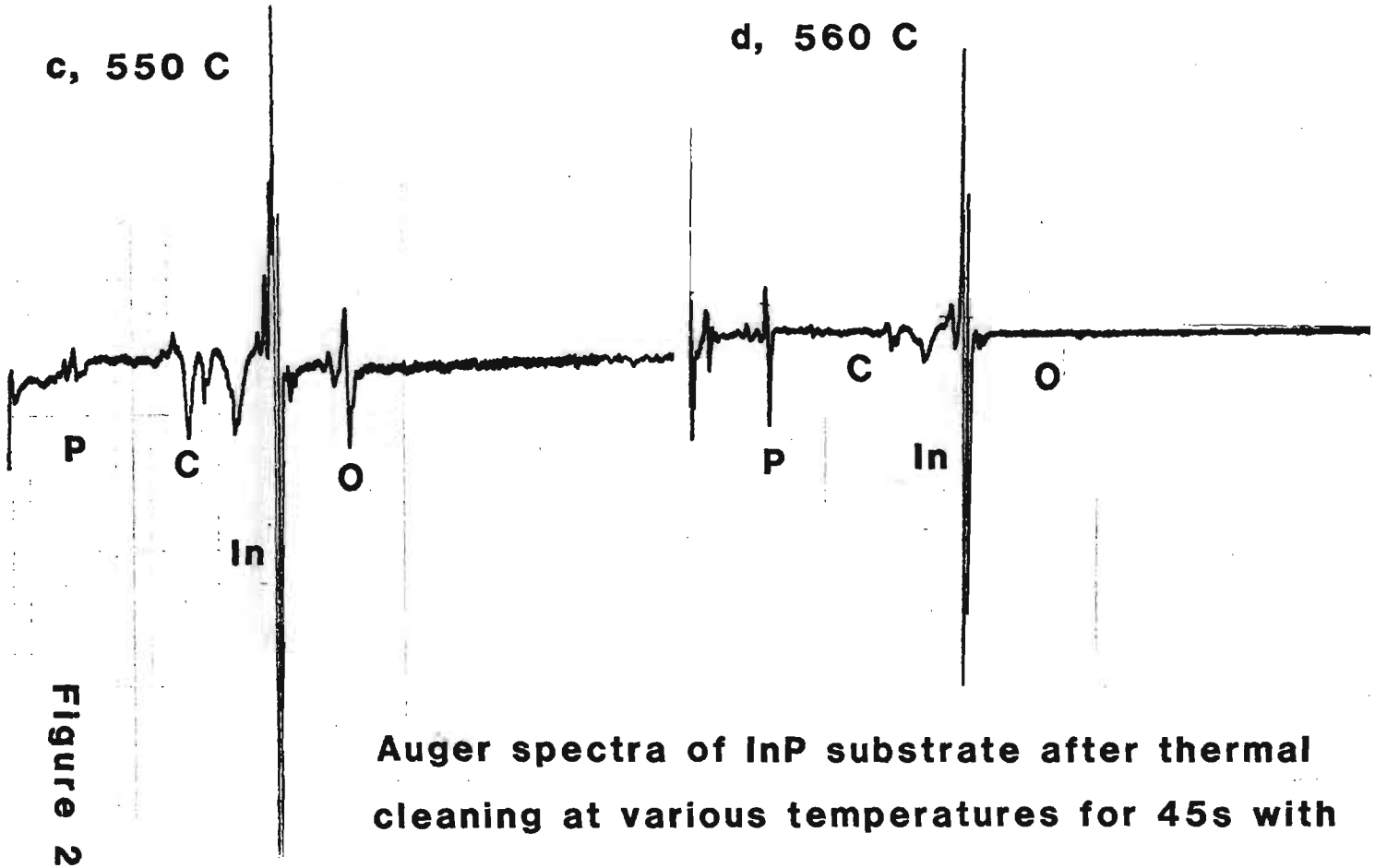

Figure 2b

Auger spectra of InP substrate after thermal cleaning at various temperatures for 45s with arsenic passivation flux.

spite of some reported success in using P_4 at other laboratories, no films of any resonable quality have been grown at Georgia Tech using P_4. All the films grown here have therefore used InP as the phosphorous source with the frequent replenishment, and hence increased chance for contamination being tolerated. For the future, a new oven using elemental red phosphorous will be tested whereby P_4 can be cracked into P_2, hopefully this will solve the problem.

GaAs is a useful source of arsenic; however, in this case the group III element does make a significant contribution to the overall Ga flux and must be considered. In fact for some of the InGaAsP films it was found possible to dispense with the Ga oven and use just the Ga coming from the GaAs oven.

The main advantage in using binary oven loads for As and P sources is that the evaporation temperatures are higher than those of the elements where high vapor elements lead to relatively low oven temperatures which can make flux control somewhat difficult. The flux control of the group V element is not quite as crucial in binary growth since there is almost always an excess of the group V. However in the quaternary system it is essential to be able to control the relative fluxes of the two group V elements as well as the total flux. For this reason all quaternary growths reported here have used binary sources since it was easier to control the flux rates. It is intended to test and install continuous flux monitors for each oven which should further improve control of the composition.

2.2 Single Oven Flux Monitor

One of the major problems associated with the growth of $In_{1-x}Ga_xAs_yP_{1-y}$ using MBE is the difficulty of achieving the accurate

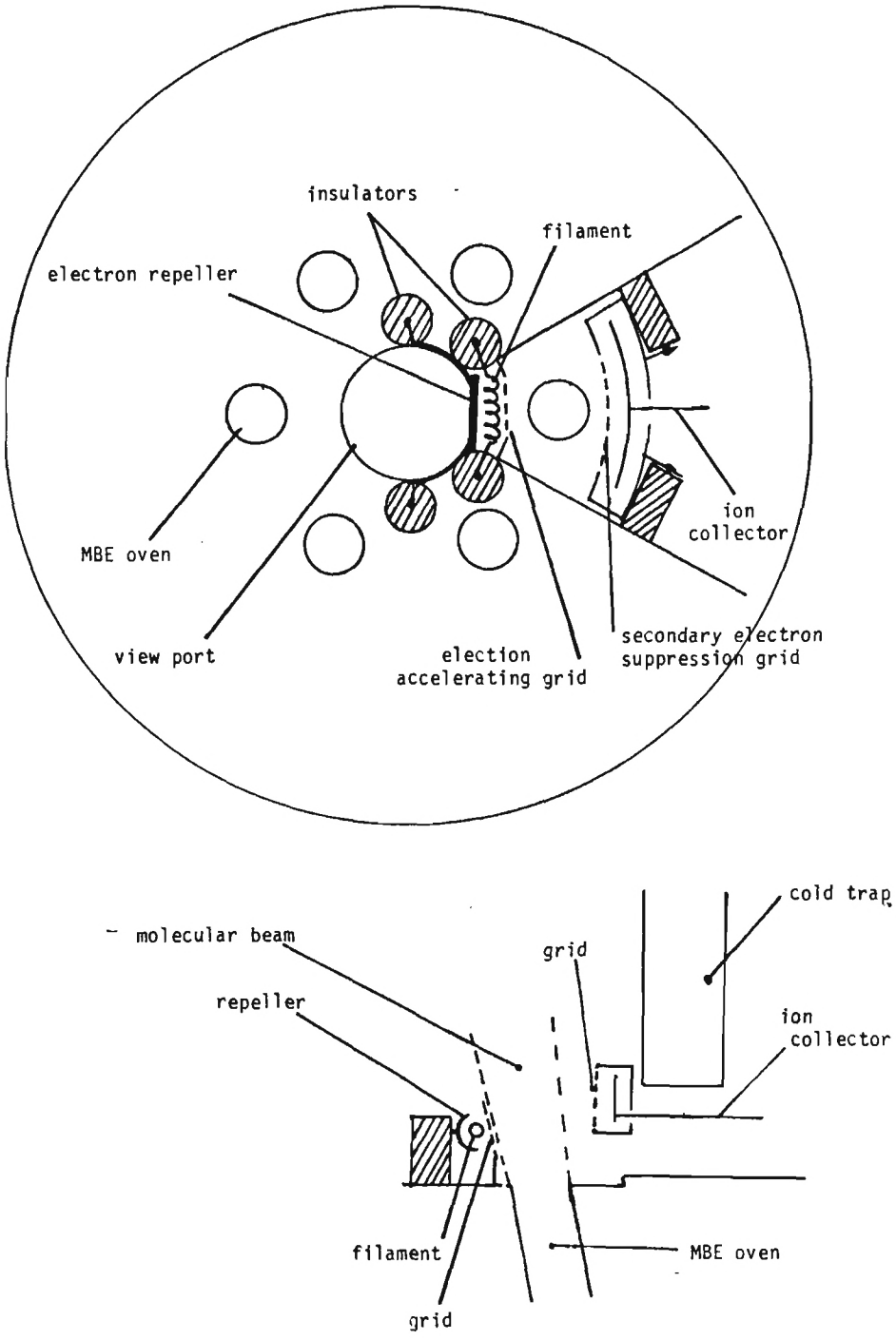

Schematic showing location and construction details of ionization gauge flux monitor.

Figure 3

control of the fluxes from the various ovens necessary to be able to predetermine the composition coefficients x and y. Thus far the flux has been measured for each oven prior to growth and the temperature needed to establish that particular flux has been kept constant during the growth, whereas ideally of course it is the flux which should be kept constant. By monitoring the fluxes before and after growth, changes in the fluxes have been observed. In order to compensate for this, the temperatures of some of the ovens, especially InP, have been judiciously raised during growth. It would clearly be of great benefit if the flux of each oven could be monitored during growth and this information used to control the temperature of the oven.

As a first step towards achieving this, a prototype single oven flux monitor has been installed and tested in the MBE system. A diagram of the monitor and its location is shown in figure 3.

The electron impact ionization flux monitor uses a 100 eV electron beam to ionize a small fraction of the neutral molecular beam emerging from a growth oven. The positive ions formed are then collected and the resultant current monitored. The measured current remains proportional to the molecular beam flux as long as the density of gas in the molecular or atomic beam is large compared to the background gas pressure but is not so large as to permit multiple electron scattering events. These conditions are usually satisfied immediately in front of a growth oven under normal MBE growth conditions.

Electrons are emitted from the heated filament and accelerated by a relatively strong electric field to form a broad, diverging electron beam. These electrons, with a typical energy of 100 eV, then pass through a 95% transmitting grid and into a much weaker deccelerating

field. The electron beam continues to diverge and gradually decreases in energy as it passes directly in front of an MBE growth oven. The electron beam is perpendicular to the oven flux and sufficiently broad to pass through virtually all of it.

Except under extreme conditions about one electron in 10^3 will participate in an ionizing collision with the gas in front of the growth oven. A typical range of molecular densities in front on an MBE growth oven is 10^{10} - 10^{13} molecules/cm^3. Assuming a large ionization cross section of 10^{-15} cm^2, results in an electron mean free path of at least 100 cm even for the highest growth beam density considered. Thus, only a one percent non-linearity would occur under fairly extreme conditions. Most of these electrons, along with those that did not cause ionization, will then pass out of the growth beam and hit the conductive sides of the monitoring assembly. The positive ions produced by the electron beam (which account for at most 0.1% of the total growth beam and can be decreased by several orders of magnitude by decreasing the electron beam current) are then accelerated towards a collection plate by the same field which deccelerates the electron beam. These ions then pass through a 95% transmitting grid and are collected on a plate which is maintained at a sufficiently negative potential to prevent the collection of electrons from the monitoring beam. The ion collection plate is surrounded by, but electrically isolated from, a metal housing which prevents electrons or ions from reaching it from all directions expect from the side closest to the growth beam. Thus, the ion current is characteristics of the flux from one specific oven. Electrons are prevented from reaching the grid (which encloses this side of the housing) by its electrical potential, which is more negative than either the electron filament or the collection plate. Thus, only positive ions

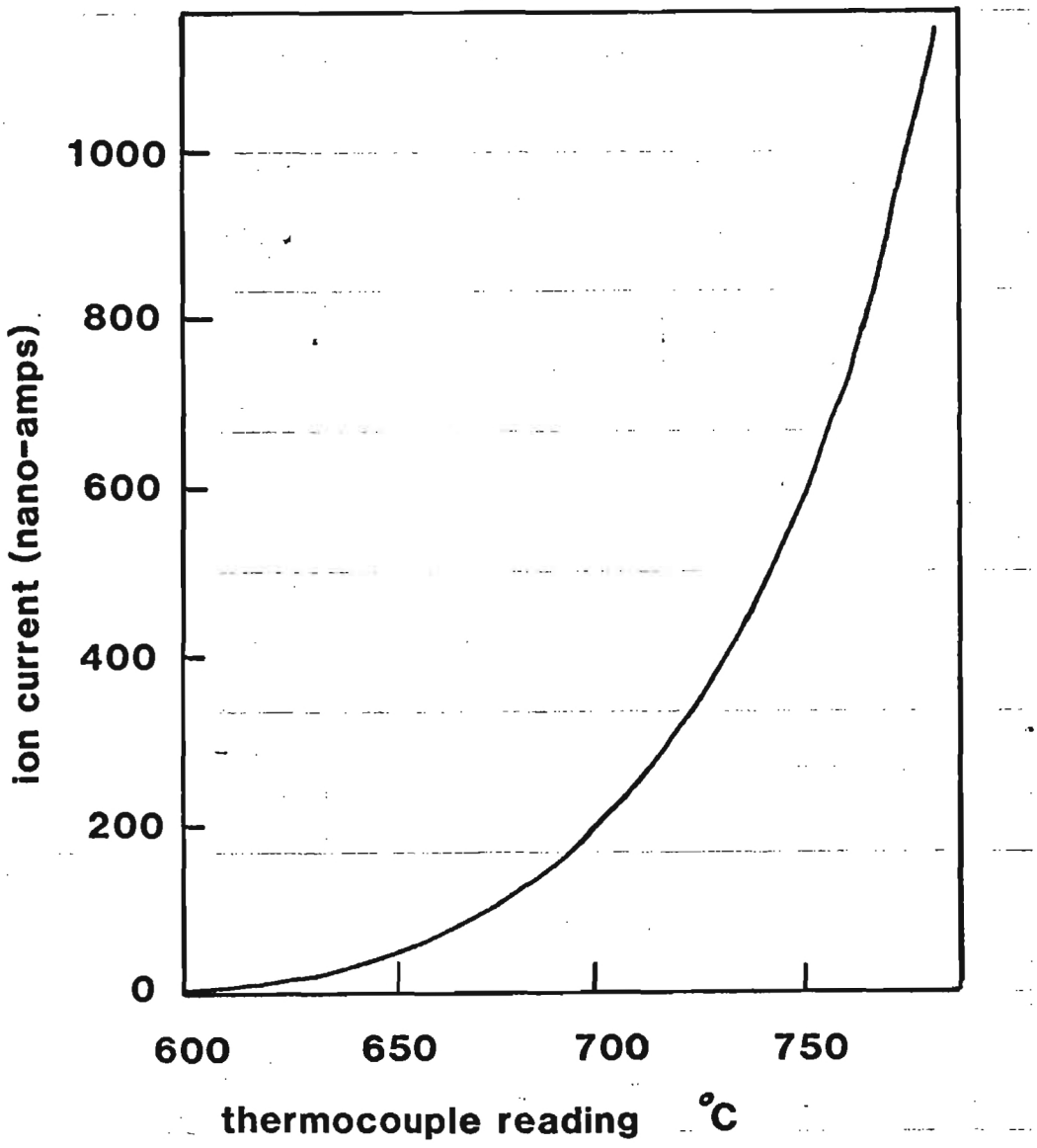

Curve of ion current versus thermocouple reading for ionization gauge flux monitor.

Figure 4

from one direction, and hence one oven, can reach the collection plate; secondary electrons which could be ejected from the collection plate are surpressed by the grid which is in front of it.

The typical electron beam current is about 10^{-3} amps and ion current ranges from 10^{-9} to 10^{-6} amps. The primary limitation of this device for low flux measurements is that of background pressure. Positive ions are formed by electron bombordment of background gas just as they are formed from the growth beam. Thus, if the density of the growth beam approaches the background gas density, a correction for the background gas must be made.

The initial testing of this monitoring system was performed in front of an indium oven in the MBE growth system. A plot of the positive ion current versus indium oven temperature is shown in figure 4.

This flux monitor can be used either directly to control the growth oven or in conjunction with a temperature controller to maintain a constant flux as the oven load is depleted. The long term stability of this monitoring system is increased by using the positive ion current divided by the electron emission current instead of using the ion current alone. Low flux measurements are further improved by monitoring positive ion current from beyond the growth beam path so that the current due to ionization of background gases can be subtracted.

2.3 Analysis of Layers

Analysis of the quaternary layers is directed towards two objectives. The first, which is common to all MBE films, is the quality of the films which can be expressed in terms of parameters such as carrier mobility, carrier concentration, photoluminescence efficiency,

surface smoothness and epitaxial growth. The second parameter of great concern in the quaternary systems is that of composition, the ability to adjust the relative amounts of In, Ga, As, and P such that they produce a semiconductor with the correct bandgap and at the same time be lattice matched to the InP substrate. A variety of techniques have been used during the course of this program to evaluate the aforementioned factors.

The 'quality' of the films can be adequately expressed in terms of the carrier mobility and concentration. These were determined directly using van der Pauw-Hall measurements. Reflection electron diffraction has been used to verify epitaxial growth and to evaluate surface smoothness. Optical methods are very powerful analytical tools and techniques such infrared absorption, photoluminescence and electroreflectance have been used to determine bandgap energies as well as to estimate the quality of the films. The only direct way to determine lattice-matching is to use x-ray diffraction and this technique has also been used. The composition can then be deduced from the bandgap measurements together with the lattice-matching measurements.

2.3.1 X-ray Rocking Curve

The most direct way to determine the lattice match between the film and substrate is to perform x-ray diffraction studies from the film and substrate simultaneously. This technique uses the diffraction from the substrate as an internal calibration and hence removes the necessity of making an absolute measurement of the diffraction angle. For the {400} reflection the lattice parameter of the film is given by

$$a_o = \frac{2\lambda}{\sin(\Delta\theta + \sin^{-1}(\frac{2\lambda}{a_s}))}$$

where λ is the x-ray wavelength

$\Delta\theta$ is the angle between the diffraction peaks from the film and substrate, and

a_s is the lattice constant of the substrate.

Since λ and a_s are known, a measurement of $\Delta\theta$ is sufficient to enable a_o to be calculated.

The lattice constant of $In_{1-x}Ga_xAs_yP_{1-y}$ is a function of the compositional parameters x and y and is expressed by[3]

$$a_o(x,y) = 01894y - 0.4184x + 0.0130xy + 5.8696$$

Lattice matching to InP is achieved by maintaining the y/x ratio 2.1.

2.3.2 Bandgap Measurements

The most important attribute of the quaternaries, which has determined its widespread application to optical communication systems as sources and detectors, is the ability to adjust the fundamental bandgap and hence the lasing wavelength of a diode laser by a suitable choice of composition parameters. The fundamental bandgap energy can be expressed by:[2]

$$E_g(x,y) = 1.35 - y + 1.4x - 0.33xy - (0.758 - 0.28y)x\ (1-x) - (0.101 - 0.109x)y\ (1-y)$$

If both the bandgap energy and lattice constant are known, the composition parameters can be calculated. The solutions to the lattice constant and energy gap equation are shown graphically in figure 5 as

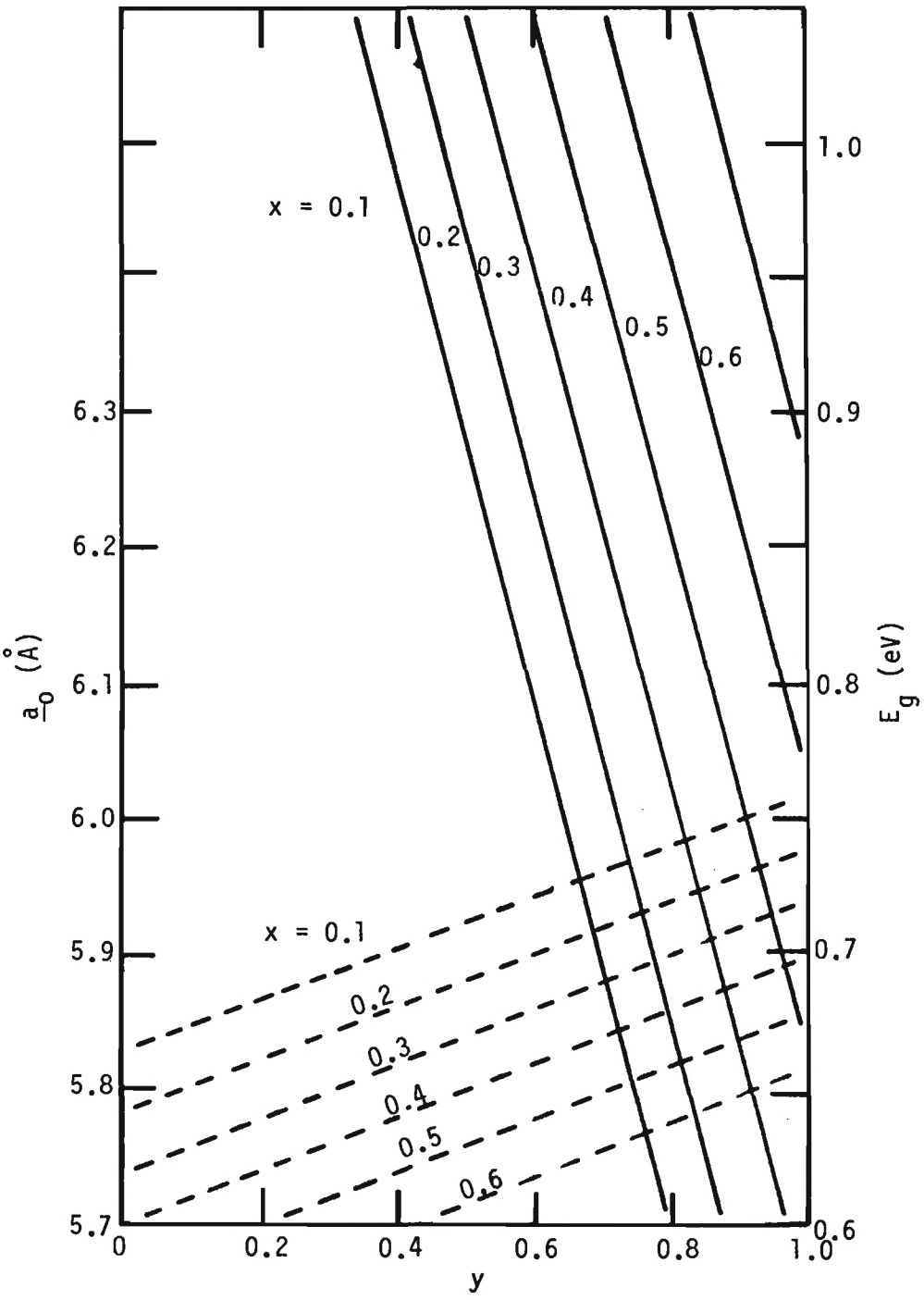

Bandgap (——) and lattice constant (---) of $In_{1-x}Ga_xAs_yP_{1-y}$ as functions of x and y.

Figure 5

functions of both x and y.

There are a variety of optical techniques which can be used to determine the bandgap energy; these techniques include infrared transmission, photoluminescence and electroreflectance. The simplest technique is infrared transmission which measures directly the absorption of the sample in the vicinity of the bandgap.

The transmission of radiation through a sample of thickness d, reflectivity R, and absorption coefficient α is given by:

$$T = \frac{(1-R)^2 e^{-\alpha d}}{1 - R^2 e^{-\alpha d}}$$

For an approximate estimate it is usually allowable to assume $R << 1$ and hence $T \approx e^{-\alpha d}$. The situation of a thin film on a substrate is somewhat more complex and allowance has to be made for the optical properties of the substrate as well as possible interference effects between film and substrate. The shape of the spectrum can be analyzed to yield the bandgap energy.

A more precise technique is to use electroreflectance which is one form of modulation spectroscopy. In modulation spectroscopy the optical spectrum either reflection or absorption of a solid is modulated in some way by a periodic variation of the measurement environment, e.g. electric field, magnetic field, temperature, wavelength or polarization of the incident light. The modulation gives rise to sharp, differential-like optical features in the region of critical points in the electronic energy band structure. Normally there is very little change in the reflection or transmission associated with a critical point (higher band gap for example) and so it is difficult to observe. Using phase-sensitive detection at the modulation frequency, it is possible to

observe changes in reflectance as small as 10^{-6}. Signals are only observed where there is a change, however small, in reflection with modulation field.

Electroreflectance uses an electric field to change the optical properties of the semiconductor. Basically, the electric field modifies the band structure through a Franz-Keldysh effect and hence the optical properties also change. Electroreflectance enables not only the fundamental bandgap E_0 to be determined more precisely, due to its derivative property, but also the higher bandgaps, E_1 and E_2, together with spin-orbit splittings. The energies E_0, E_1, and E_2 correspond to different wavelengths and different absorption coefficients and so in principle it is possible to use this technique for depth profiling. Additionally, if the line shapes of the electroreflectance spectra are carefully analyzed, both carrier concentration and mobility may be deduced. The width of the lines depends upon the mobility and the height of the signal is a relatively simple function of carrier concentration.

The technique is essentially quite simple: an audio-frequency modulated voltage (~1V) is placed across the sample. The incident white light is chopped relatively slowly, ~100Hz, and the radiation reflected by the sample is sent through a spectrometer for wavelength analysis, detected by a wideband detector and the output fed into two lock-in amplifiers tuned to each frequency. The outputs of the lock-ins are fed into a ratiometer to obtain $\Delta R/R$ where ΔR signal at the audio frequency and R is the 100 Hz signal. ΔR will only be finite near critical points.

Photoluminescence[16] is rapidly being accepted as one of the most useful characterization techniques, especially for MBE films. The advantage of this technique is that in addition to luminescence at the

fundamental bandgap, there may also be radiative transitions which either begin or end on impurity states. Such transitions can be used to identify impurities and their crystallographic environment. Further, by careful calibration it is possible to determine the 'quality' of the film from the width of the photoluminescnece. The scattering mechanisms which contribute to the mobility are the same as those causing line broadening. In principle therefore, reasonable estimates can be made of the mobility from the photoluminescent data.

It is more difficult to perform photoluminescence on narrower bandgap materials since they have emission spectra which may extend beyond the range of the most sensitive of detectors, the photomultiplier tube. InGaAsP films grown at Georgia Tech have bandgaps near 1.2 and 1.6 μm and, therefore it is necessary to use Ge bolometers and PbS detectors. The photoluminescent data shown in this report was obtained by Steve Bishop and colleagues at NRL.

2.3.3. Hall Measurements

For thin lamellar samples the standard method for determining the electrical characteristics of the samples is to use the van der Pauw[17] variation of the Hall effect. Since this is a widely used technique it will not be discussed here in any detail. The only point worth mentioning is the need for correction of errors introduced by the finite size of the contact pads. The sample is a 3.5 mm square with 0.5 mm diameter contacts placed in each corner. Therefore, the total contact dimension relative to the sample size is significant and cannot be ignored. The correction analysis suggested by van der Pauw has been applied to the results obtained here.

2.3.4 Reflection Electron Diffraction

Reflection electron diffraction is a relatively simple technique

for investigating surface smoothness and confirming epitaxial growth. The penetration depth of the electron beam is low due to the high inelastic scattering cross-sections for the electrons. This means that only the first few atomic layers are probed by RED. Therefore, the diffraction pattern represents order within the film and not the substrate. A detailed analysis is beyond the scope of this report. It suffices to say that epitaxial growth together with a smooth surface is confirmed by a distinctive streaking in the diffraction patterns. Broadening and spotting are evidence of poorer quality films.

3.0 MBE GROWTH OF InGaAsP

3.1 Introduction

There have been two distinct phases in the growth of InGaAsP during the period covered by this report. Firstly, there was an effort to improve the general quality of the films in terms of lattice-matching and mobility and, at the same time, to determine the reproducibility of the MBE system on a run-to-run basis. Secondly, there was a phase directed towards establishing the growth conditions required for an InGaAsP film with a bandgap near 1.55 μm. This wavelength was specifically chosen since it is near the region of minimum attenuation of silica-based optical fibers and hence may be expected to be of great use in long distance communication systems, including undersea communications and hydrophonic detection of ships. The development of an InGaAsP laser at a wavelength of 1.55 μm would also require confining layers of n- and p-type InP. Therefore, with an overall objective of growing a structure suitable for processing into a double heterostructure InGaAsP/InP diode laser (for more details, see section 3.2) the following tasks were identified: Growth of InGaAsP films of good quality at 1.55 μm, growth of suitable doped n- and p-type InP, and also examination of problems associated with ohmic contacts to p-type InP. This section is concerned solely with the growth and analysis of InGaAsP films.

3.2 Double Heterostructure Diode Lasers

A simple design structure of a double heterostructure diode laser is shown in figure 6. Both the active and confinement layers are fabricated from direct bandgap semiconductor materials, Indirect gap materials such as silicon require the involvement of a lattice

InGaAsP DIODE LASERS

Double-heterostructure

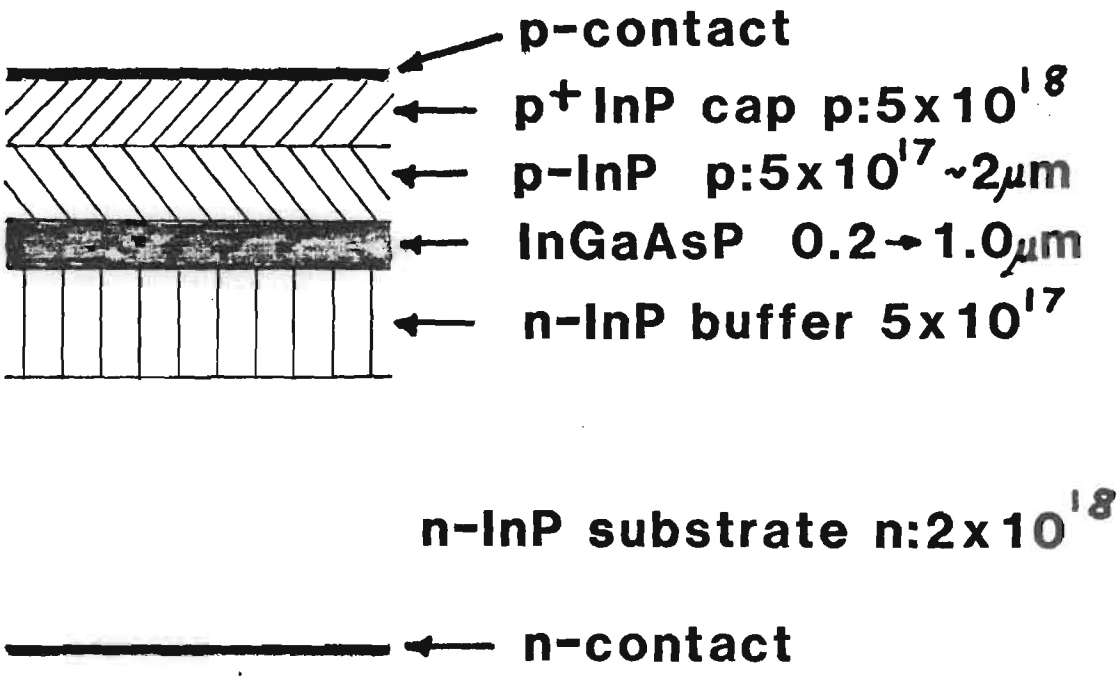

Figure 6

vibration during the recombination process which lowers the transition probability signficantly. This would give rise to the necessity of very high currents to compensate for the low transition probability. The surrounding layers serve to confine both the injection electrons and holes as well as the generated photons. The carrier confinement is achieved by sandwiching the active medium between higher energy bandgap materials. The potential barrier established at each junction, either p or n type relative to the active medium and taking into account the bias direction, serves to confine the carriers. The photons are confined by having lower refractive index materials surrounding the active layer. The refractive index difference maintains a high reflectivity at the interfaces, thereby confining the photons. The relationship between bandgap energy and refractive index for semiconductors is forruitious in that higher bandgap energy is always associated withlow refractive indices, as given by the empirical relationship

$$E_g = \frac{108}{n^4}$$

when InGaAsP is used as the active layer medium then InP is a suitable confinement material. See figure 6 for a typical double-heterostructure diode laser structure. However, since the bandgap of the quaternary can be adjusted, the efficiency of confinement (and hence of lasing) will vary. The leakage current, due to tunnelling electrons and holes will increase as the lasing wavelength decreases. The situation of present interest, i.e. of long wavelength lasing should be an efficient combination of active and confining materials.

Suitable doping levels for the n- and p-type InP confining layers are given in figure 6. Part of the program is concerned with determining growth conditions and suitable dopants for these layers.

3.3 MBE Growth of Reproducible InGaAsP

A number of InGaAsP films have been grown on Fe-doped semi-insulating InP substrates using growth conditions similar to a sample grown at Georgia Tech on a previous program.[10] Although that program was successful in that reasonably good quality film of InGaAsP were grown (in fact the films were the best grown using MBE at that particular time) there were problems in that the films did not seem to be easily reproduced. This led to a reevaluation concerning the control and consistency of the growth procedures as well as material analysis. It was proposed to grow some films under virtually identical conditions and to make a very careful analysis of the bandgaps using electroreflectance. With the addition of Hall data, this experiment would be sufficient to determine the consistency of the growth runs.

A major contribution to the possible variation of the composition of the runs came, not from a inherent irreproducibility of the growth procedure but from the use of Auger spectroscopy to determine composition parameters. It is unfortunate in retrospect that Auger spectroscopy was used earlier as the primary composition measurement technique since even under optimum condition Auger is unlikely to give the composition to better than 20%.

The deposition parameters and electrical properties of the films together with that of D0206-II which was grown under the previous program are given in table 1. Electro-reflectance was used to measure E_1 and $E_1 + \Delta_1$ of three samples, including D0206-II, and are shown in figure 7 where it is clear that they have almost identical values. If the composition parameters for D0206-II as deduced from Auger measurements are used to calculate the fundamental bandgap, a value of

Layer	Thickness μm	Mobility $cm^2V^{-1}s^{-1}$	Concentration cm^{-3}	E_1 eV	$E_1 + \Delta_1$ eV
D0206-II	0.8	2126	1.6×10^{17}	2.613	2.883
D0922-II	1.25	4000	1.9×10^{17}	2.615	2.885
D0925	0.39			2.611	2.876
D1026	0.52	3635	2.4×10^{17}	-	-

Table 1

Deposition parameters and properties of four similar MBE grown $In_{1-x}Ga_xAs_yP_{1-y}$ on InP. X and y are nominally 0.25 and 0.72 ($\pm$ 0.02) for all layers.

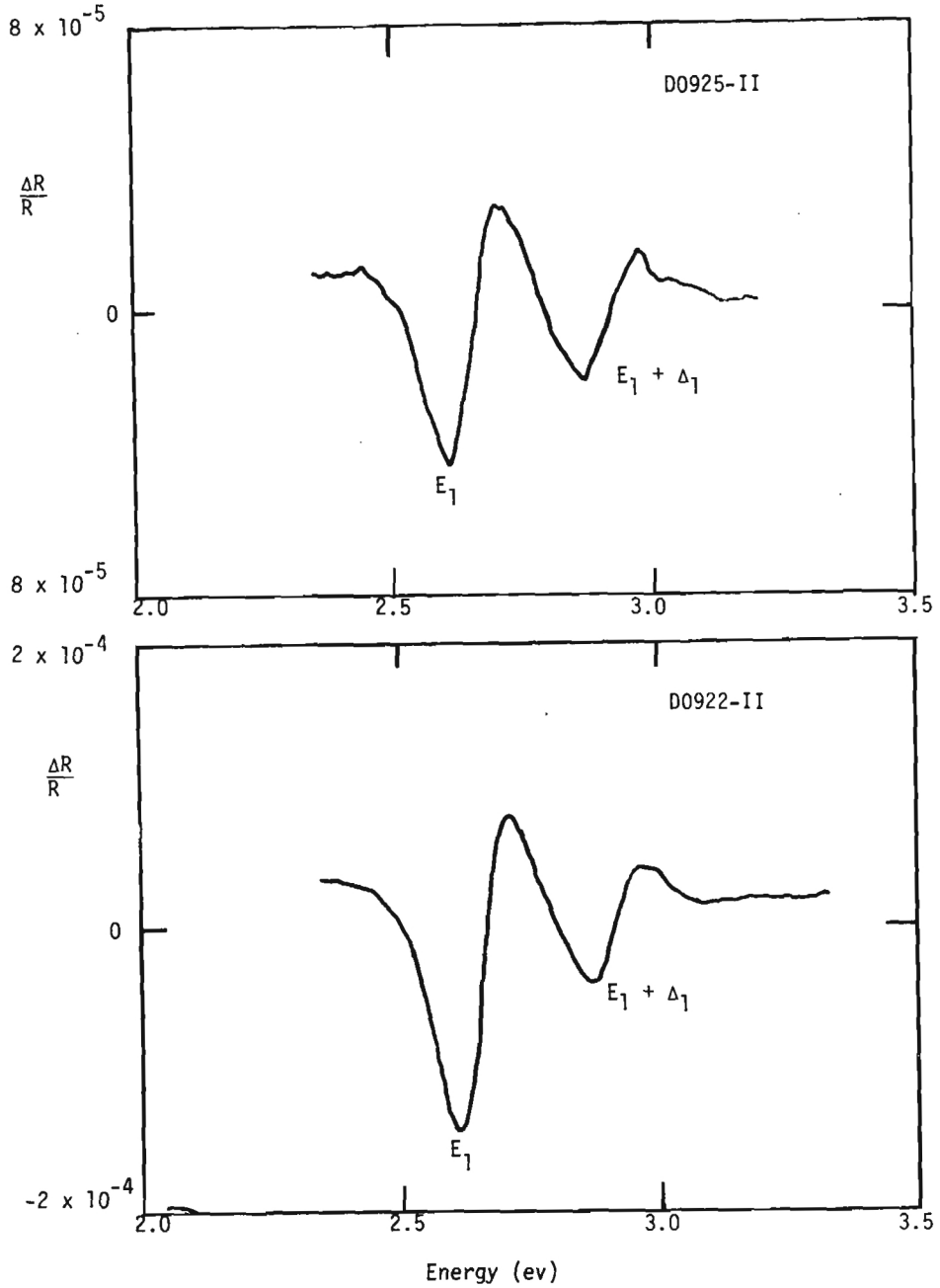

Figure 7a Electroreflectance spectra of two $In_{1-x}Ga_xAs_yP_{1-y}$ MBE layers on InP substrates.

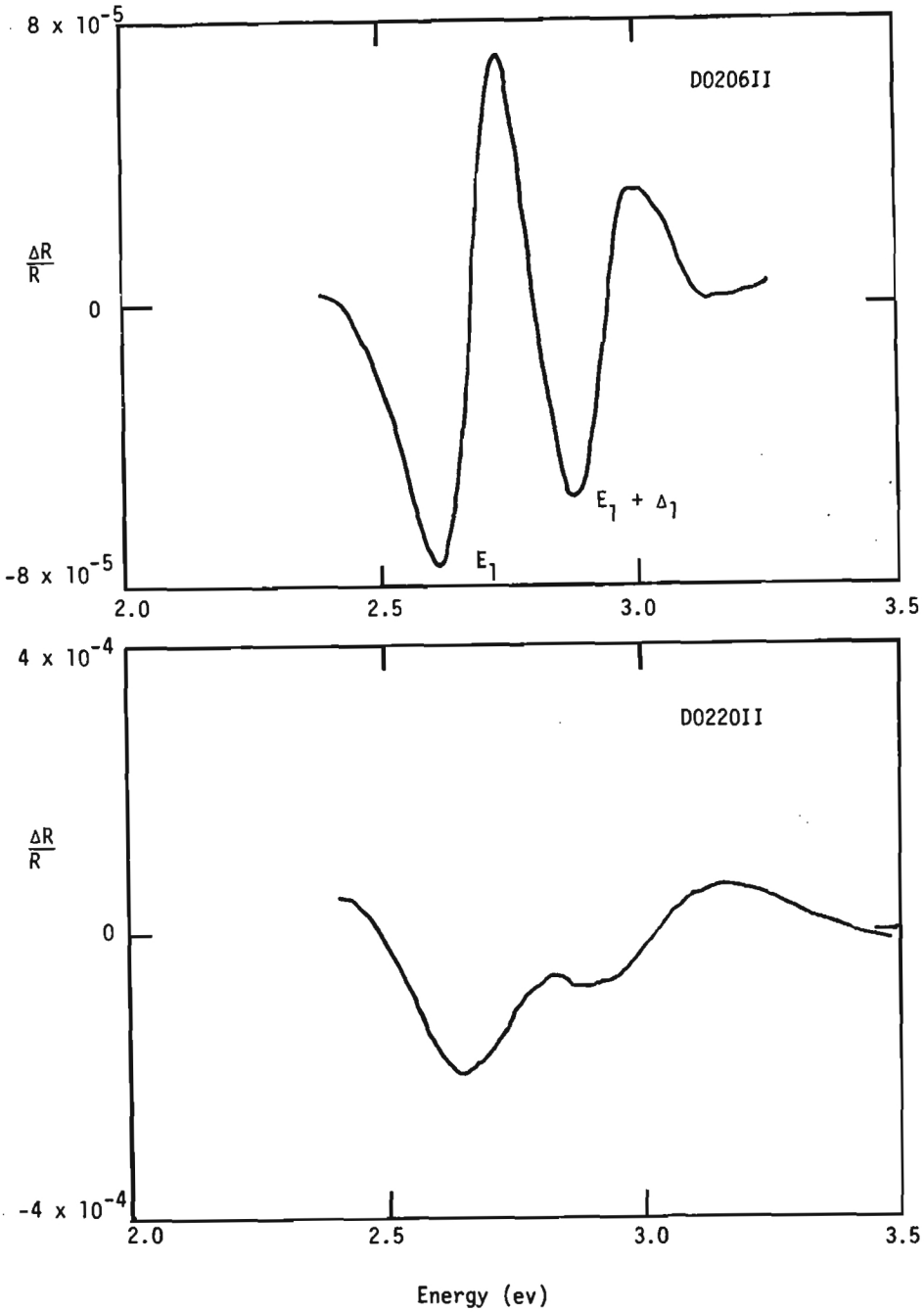

Figure 7b Electroreflectance spectra of two $In_{1-x}Ga_xAs_yP_{1-y}$ MBE layers on InP Substrates.

E_o = 0.68eV is obtained.

Pollack[18] and co-workers have made a detailed study of the electroreflectance spectra of LPE grown InGaAsP as a function of y, assuming lattice matched conditions. Transition such as E_o, $E_o + \Delta_o$, E_1, and $E_1 + \Delta_1$ have all been determined for lattice matched material. These are shown in figure 8. Although the samples shown in figure 7 are not perfectly lattice-matched, it is not expected that a mismatch of 0.5% will have much effect on the transition energies. Therefore it can be deduced from the values of E_1 and $E_1 + \Delta_1$ for the Georgia Tech samples that the fundamental energy, E_o, is 0.82 eV. This is to be compared to the value of 0.68 eV deduced from Auger measurements of the composition. The electroreflectance data has therefore confirmed the reproducibility of the growths and at the same time shown that previous composition determinations based on Auger spectroscopy to be in error.

From table 1 it can readily be seen that the mobilities of the films have also increased. Since the growth conditions were nominally the same, it is not clear why the later films should be of higher quality. However, there may be some variation due to differences in the purity and treatment of the oven loads and in the cleanliness of the substrate prior to growth. Visually the later samples looked more mirror-like; however, D0206-II gave good electro-reflectance data which suggests that its mobility may have been higher than that suggested by the original Hall measurement. Poor luminescence was observed from these early samples, as will be discussed, luminescence improved considerably with later samples.

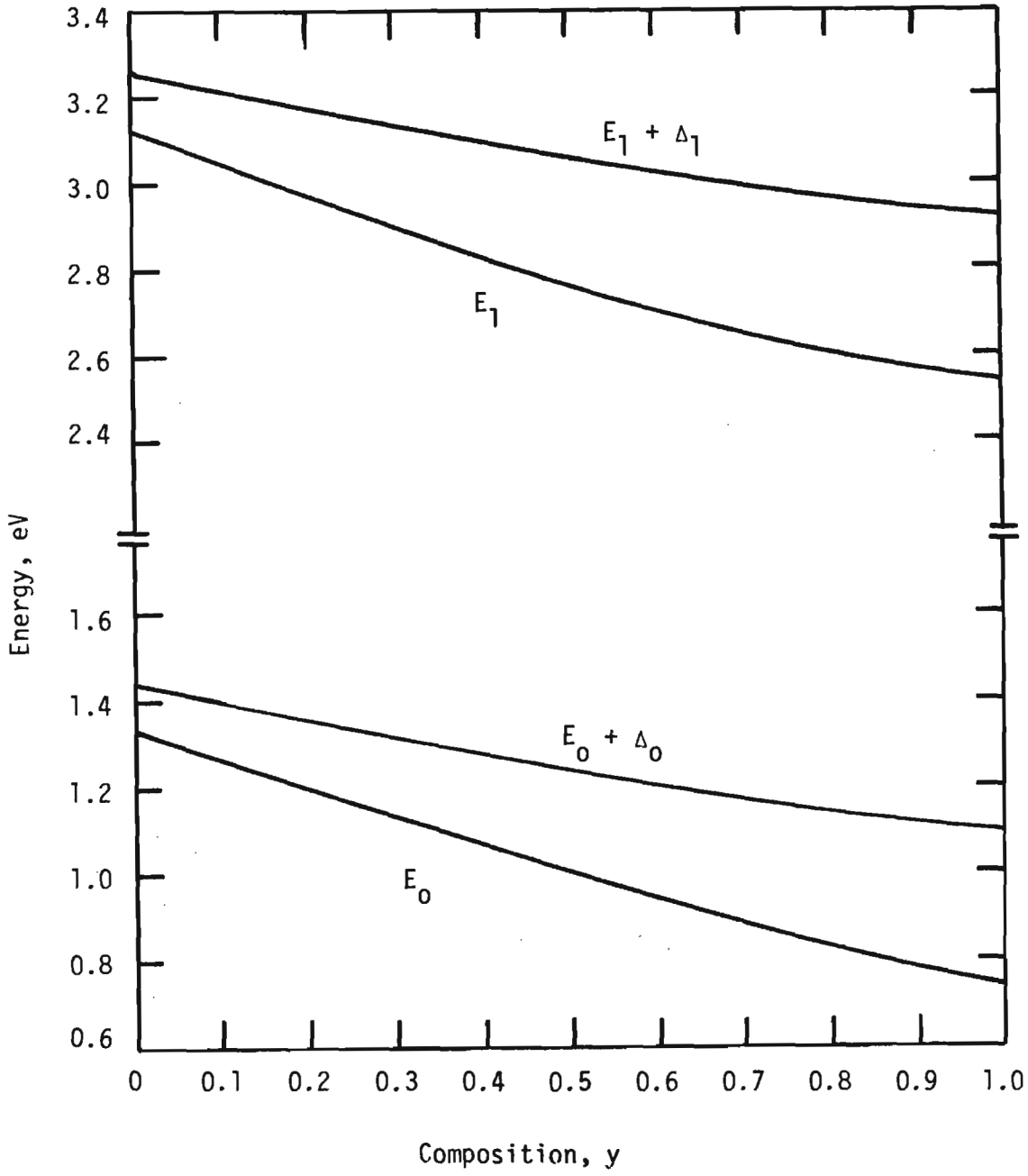

Composition dependence of electroreflectance peaks, after Laufer et.al.

Figure 8

It is not possible to determine uniquely the composition of the InGaAsP from knowledge only of the bandgap. The degree of lattice-matching must be known. As discussed in more detail previously, the lattice constant is measured using x-ray rocking curves. Such a curve is shown in figure 9 for sample D1026-II together with a curve obtained from the InP substrate alone showing the clearly resolved $CuK\alpha_1$ and $CuK\alpha_2$ lines. The diffraction from the InGaAsP film appears as a broad sideband on the diffraction peaks from the underlying InP substrate. The breadth of the diffraction peak is due to both vertical and horizontal spatial inhomogeneity; although, since the maximum vertical (depth) homogeneity is limited due to the small film thickness, the main contribution to the broadening is horizontal broadening. The x-ray beam was a slit approximately 100 μm wide with a height larger than the samples. The peak due to the InGaAsP MBE film corresponds to a lattice constant of 5.897Å. Since the lattice constant can be expressed in terms of x and y, this relationship can be solved simultaneously with that from the bandgap energy to obtain a unique set of x and y values. For this case $y = 0.70 \pm 0.01$ and $x = 0.26 \pm 0.01$. These values lie within 25% of the Auger-deduced figures of $y = 0.60$ and $x = 0.32$.

Reflection electron diffraction (RED) has been used to study the surface morphology. The diffraction pattern for D0922-II is shown in figure 10. The distinctive streaking confirms that growth was epitaxial with smooth surfaces.

Further evidence as to the surface quality of the layers is furnished by the 500X magnification optical micrograph of layer D1026-II shown in figure 11. All films had a mirror-like appearance. It is clear from figure 11 that the surface is smooth and free from cross-hatching. The phenomenon of cross-hatching is usually associated with

Figure 9

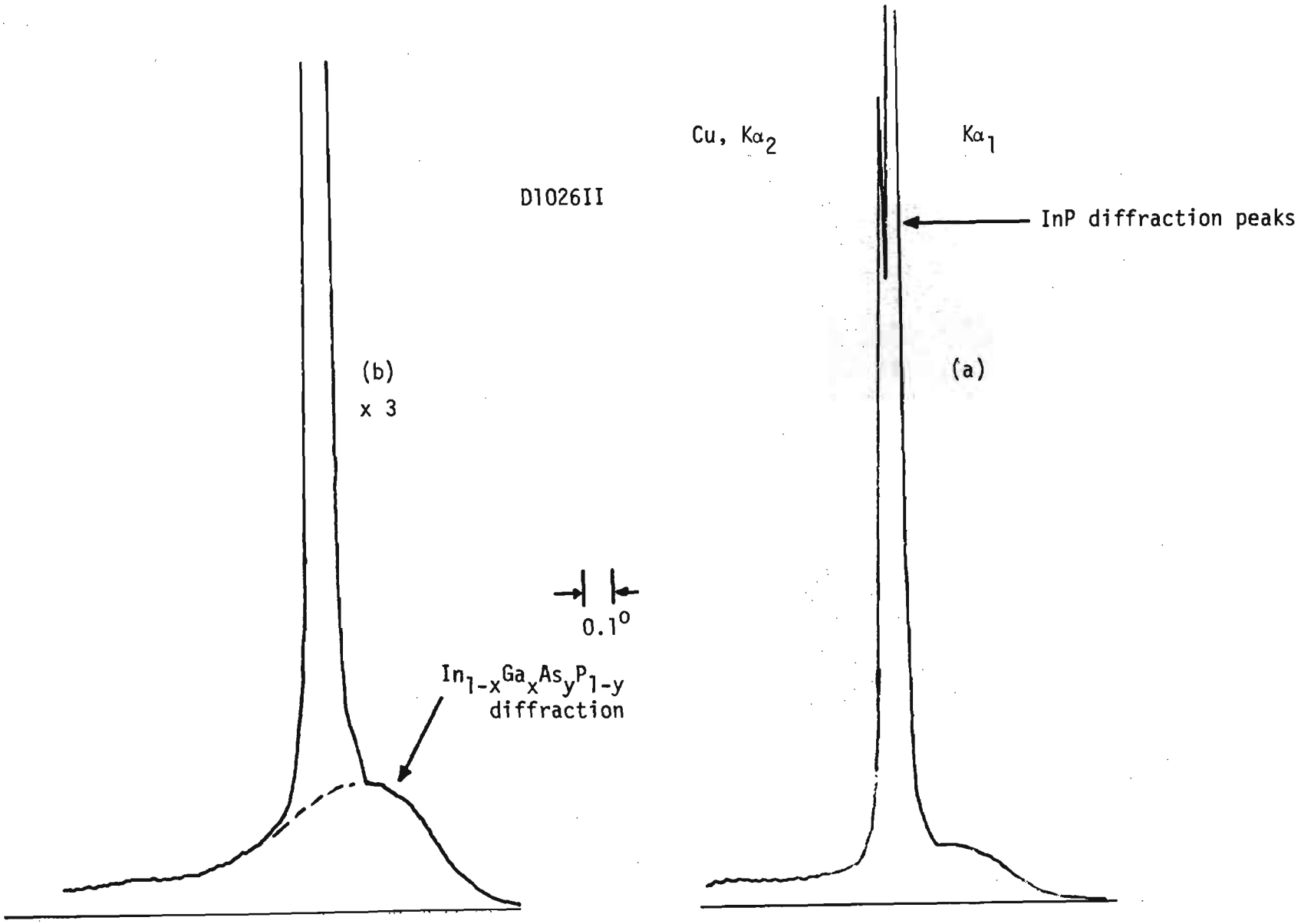

X-ray rocking curve for MBE $In_{1-x}Ga_xAs_yP_{1-y}$ layer on InP substrates. {400} Cu Kα reflection.

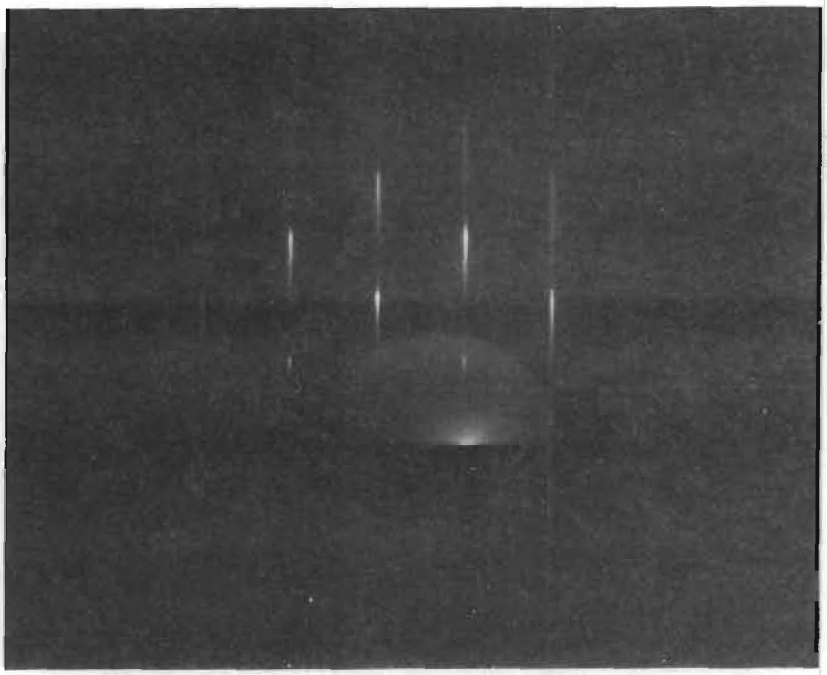

Reflection Electron Diffraction of MBE $In_{1-x}Ga_xAs_yP_{1-y}$ on InP substrate, layer D0922II.

Figure 10

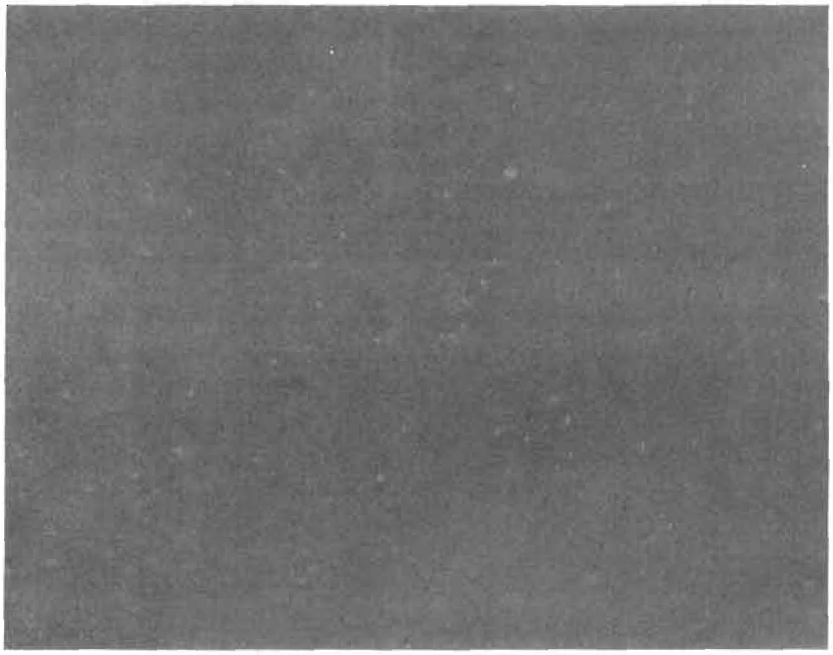

Optical Micrograph, magnification X500, of MBE $In_{1-x}Ga_xAs_yP_{1-y}$ on InP, layer D1026II.

Figure 11

gross lattice mismatch. The correlation between lattice match and appearance of cross-hatching has been studied in some detail by Oe[19] et al who found that, for LPE-grown InGaAsP layers on InP, cross-hatching only occurred for lattice mismatch greater than 0.005. Since figure 11 shows no evidence of cross-hatching this would seem to imply that the upper limit for lattice mismatch of the samples grown here is 0.005. This value is consistent with that deduced from x-ray diffraction.

Mobility measurements have been made as a function of temperature using the van der Pauw configuration of the Hall technique. Contacts were formed by evaporating Au:Ge (88:12) pads and then alloying for 20s at 450^{o} in 10% H_2:90% N_2 gas flow. Results for two samples are shown in figure 12. The temperature dependence does not extend to sufficiently low temperatures to allow a detailed quantitative analysis to be made, however, the relatively flat response shows the significance of alloy scattering in this temperature range.

3.4 Growth of MBE InGaAsP with Bandgaps near 1.55 microns

3.4.1 Introduction

The films which were discussed in the previous section had a bandgap energy of 0.82 eV, and whilst this is close to the optimum value of 0.8 eV for long distance fiber communications, it is desirable to decrease the bandgap energy and to increase the mobility which will give rise to more efficient lasing action. This was demonstrated by the width of the photoluminescence spectra discussed previously. This section is concerned therefore with an attempt to adjust the bandgap energy closer to 0.8 eV and at the same time to improve lattice matching and mobility.

The previous samples of MBE grown $In_{1-x}Ga_xAs_yP_{1-y}$ had x and y

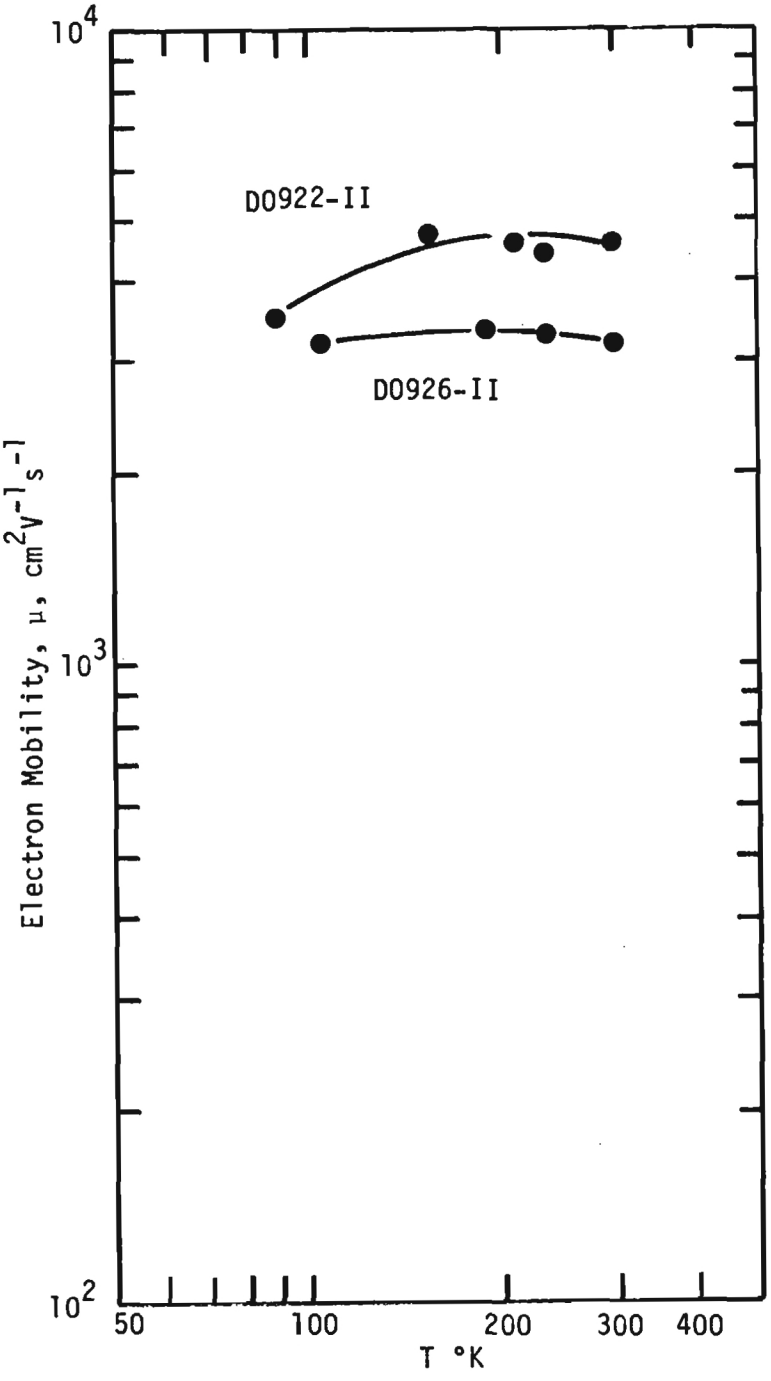

Temperature dependence of Hall mobility for two similar $In_{1-x}Ga_xAs_yP_{1-y}$ layers on InP.

Figure 12

values of 0.26 and 0.7 respectively, the y/x ratio is somewhat higher than that for perfect lattice match (ideally y/x = 2.1). The relative amounts of arsenic and phosphorous are more difficult to control than those of the group III atoms due to the complex dependencies of the sticking coefficients on substrate temperature and group III flux rates and the high vapor pressures of these elements. The intial decision was therefore to change the x and 1-x compositions by varying the temperature of the gallium oven. At the same time in order to improve the mobility it was also decided to raise the substrate temperature by $30^{o}C$ to $510^{o}C$ rather than the $480^{o}C$ which has been used to grow all the previous samples. No detailed studies have been made of the effect of substrate temperature on the quality of MBE growth of InGaAsP. Since the exact contribution of the GaAs oven to the overall Ga flux was unknown and since the flux from the Ga oven seemed to be rather low, the first growth of the new series used no Ga oven in order to establish a baseline. The data for the samples are given in table 2 and it is clear from the mobility measurement that the results are quite encouraging. A preliminary absorption measurment indicated that the bandgap was at the correct value and consequently the following runs used similar growth conditions except for the substrate temperature which was varied in order to observe any dependence of growth on substrate temperature.

There is a major problem with the use of InP as the P_2 source due to the rapid depletion of the phosphorous. This necessitates frequent opening of the growth chamber which means that the internal conditions of the system may be different from run to run. Further, it has been deduced, by observing the partial pressure of the InP oven before and after growth, that the flux decreases significantly during the hour or

so normally used for growth. This factor is empirically compensated for by increasing the oven temperature during growth; however this is not a satisfactory solution and future growths will need to solve this problems either by using a red phosphorous source and/or a continuous flux monitor.

The samples have been analyzed using infrared absorption, x-ray rocking curves, optical microscopy, photoluminescence, reflection electron diffraction and Hall measurements.

3.4.2 Layer Characterization

The lattice match has been determined by x-ray rocking curves, which have been discussed in detail in a previous section. X-ray rocking curves for sample E0326-II are shown in figure 13. This includes diffraction from the back surface of the InP substrate as well as from the MBE film. Aligning the InP peaks removes the need for absolute calibration and it is clear that, to within the resolution of the x-ray equipment, the film is well lattice matched with only a slight assymmetrical broadening observed. This represents a significant improvement over previous samples. For lattice matched films the y/x ratio is approximately 2.1; this condition yields both y and x from bandgap energy measurements. Bandgaps have been measured using both infrared absorption and photoluminescence.

A single-beam infrared spectrometer has been constructed at Georgia Tech using a Jarrel-Ash 0.5 meter monochromator and with a Golay cell as the detector. Infrared transmission spectra have been obtained and are shown in figure 14. These spectra have been obtained by ratioing the transmission of the InP substrate plus InGaAsP film against the transmission of an InP substrate. Since the substrates were not all of

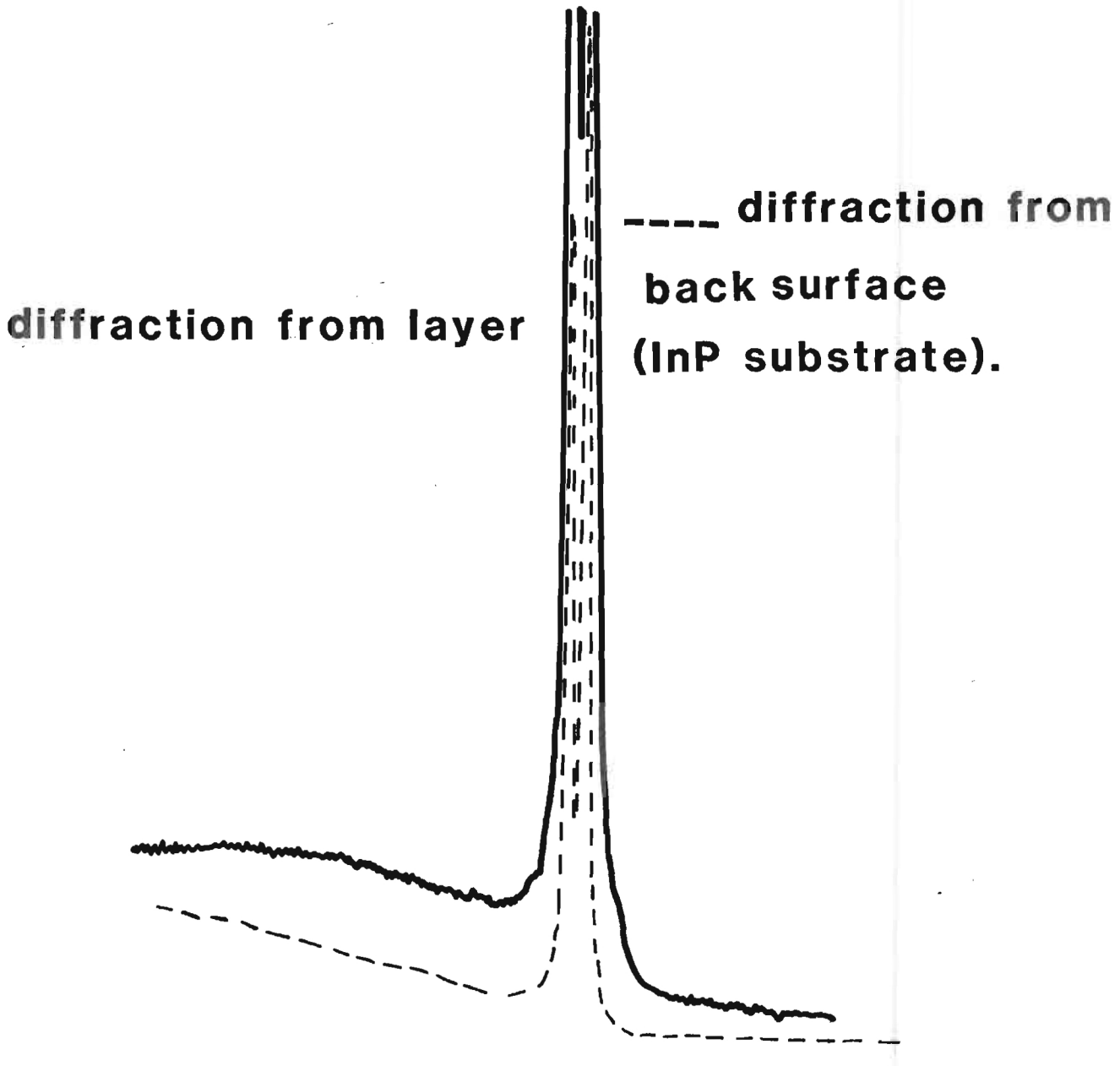

X-ray rocking curves for InGaAsP MBE layer E0326-II

Figure 13

Infrared transmission of MBE InGaAsP layers on InP substrates.

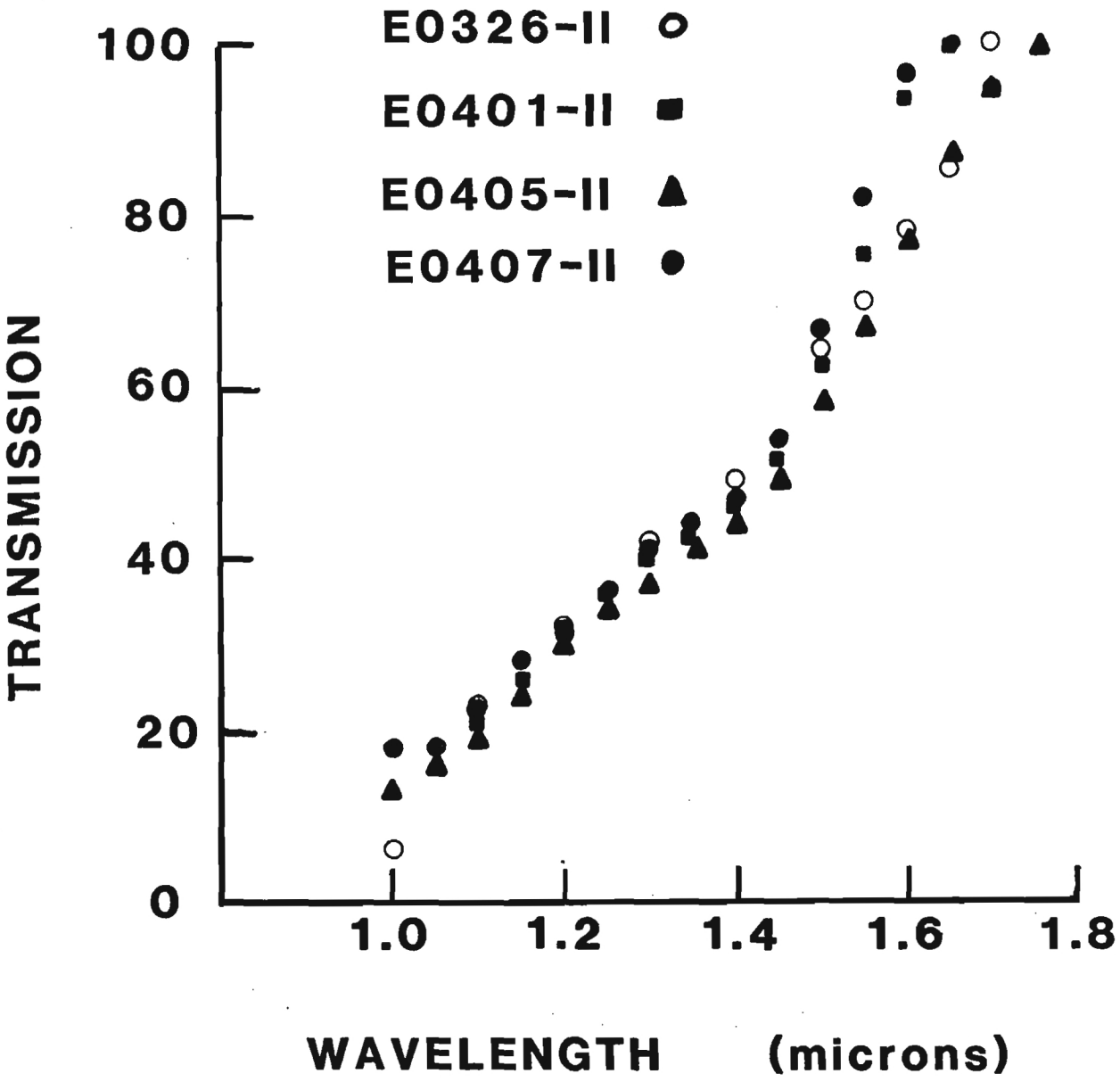

Figure 14

exactly the same thickness, the spectra were also normalized relative to the maximum transmission of the film. The spectra are very similar with the only significant difference existing in the steepness of the slope near 1.6 μm. E0326-II and E0405-II have a less steep shape than E0401-II and E0407-II. In principle this could be expected to correlate with mobility values, in that the better quality material ought to have a steeper edge. However, other factors such as compositional homogeneity may also play a role. E0326-II and E0405-II have the highest and lowest mobility, respectively, and it is clear that other contributions are influencing the band edge shape. The apparent tailing of the edge to shorter wavelengths is consistent with absorption coefficients of 10^4 cm^{-1} and with thin films. In order to determine the bandgap energy, the transmission spectrum has been plotted as an absorption coefficient vs. energy curve, shown in figure 15. It is not straightforward to determine precisely what is defined as the bandgap from such spectra. In order to make a meaningful determination, this spectrum was compared to that of GaAs which has a well-known and accepted bandgap energy. From this comparison the bandgap energy for this ample has been determined to be 0.80 $\pm$ 0.02 eV, which corresponds to a wavelength of 1.55 µm $\pm$ 0.04 µm; this is exactly the required wavelength. The y and x values corresponding to this wavelength are 0.86 and 0.41 respectively. This corresponds to increases in both x and y relative to prior values. The increase in y may in part be attributable to the higher substrate temperature causing the phosphorous to have its sticking coefficient reduced relative to the arsenic. The major cause however is that the GaAs oven temperature was at a somewhat higher temperature than normal. The temperature of the GaAs oven was 850^{o}C compared to the 737^{o}C used

Absorption coefficient vs. energy for MBE InGaAsP layer E0326-II.

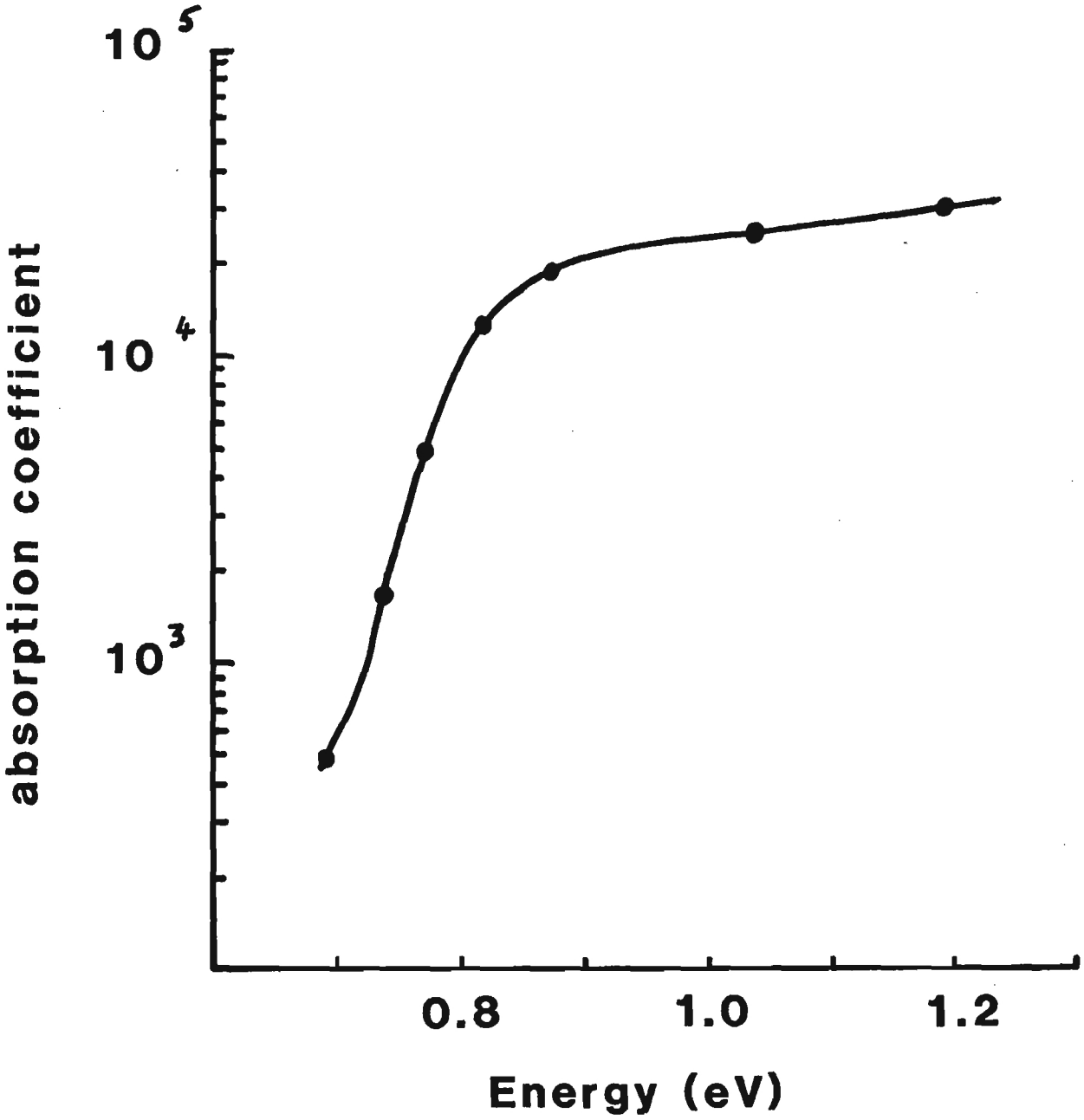

Figure 15

previously. This would explain both x and y increasing.

An optical technique which is becoming increasingly popular in the analysis of epitaxial films is that of photoluminescence. This method consists of photoexciting carriers, usually across the bandgap, from valence band to conduction band but also from and into impurity levels, and then observing the reradiated recombination processes. The characterization of materials has been discussed in detail by Bishop[16] and will not be repeated here. It suffices to say that from the recombination spectra information about impurity complexes can be obtained in addition to the fundamental bandgap energies, excition transitions and phonon-assisted processes. The results given here were obtained by Steve Bishop and colleagues at NRL. The photoluminescence associated with the fundamental bandgap transitions for three samples are shown in figure 16. These spectra were obtained at $4^{o}K$ using a krypton laser for excitation and were analyzed using a 3/4 m monochromater together with a cooled Ge bolometer. The samples were also studied using a PbS detector which extends the wavelength range to 4 μm. No data was obtained beyond those wavelengths shown in figure 16. The photoluminescence peaks are at the following wavelengths: sample E0326-II at 1.626 μm, sample E0401-II at 1.493 μm and sample E0405-II at 1.552 μm. The halfwidths are as indicated in figure 16, typically about 40 meV without allowing for any instrumental broadening. The peak positions represent the spread inherent in the growth control since the growth conditions were nominally the same except for substrate temperature. The precision of photoluminescence compared to absorption spectra is clearly indicated. These spectra are the first meaningful luminescence data obtained from molecular beam epitaxial InGaAsP and as

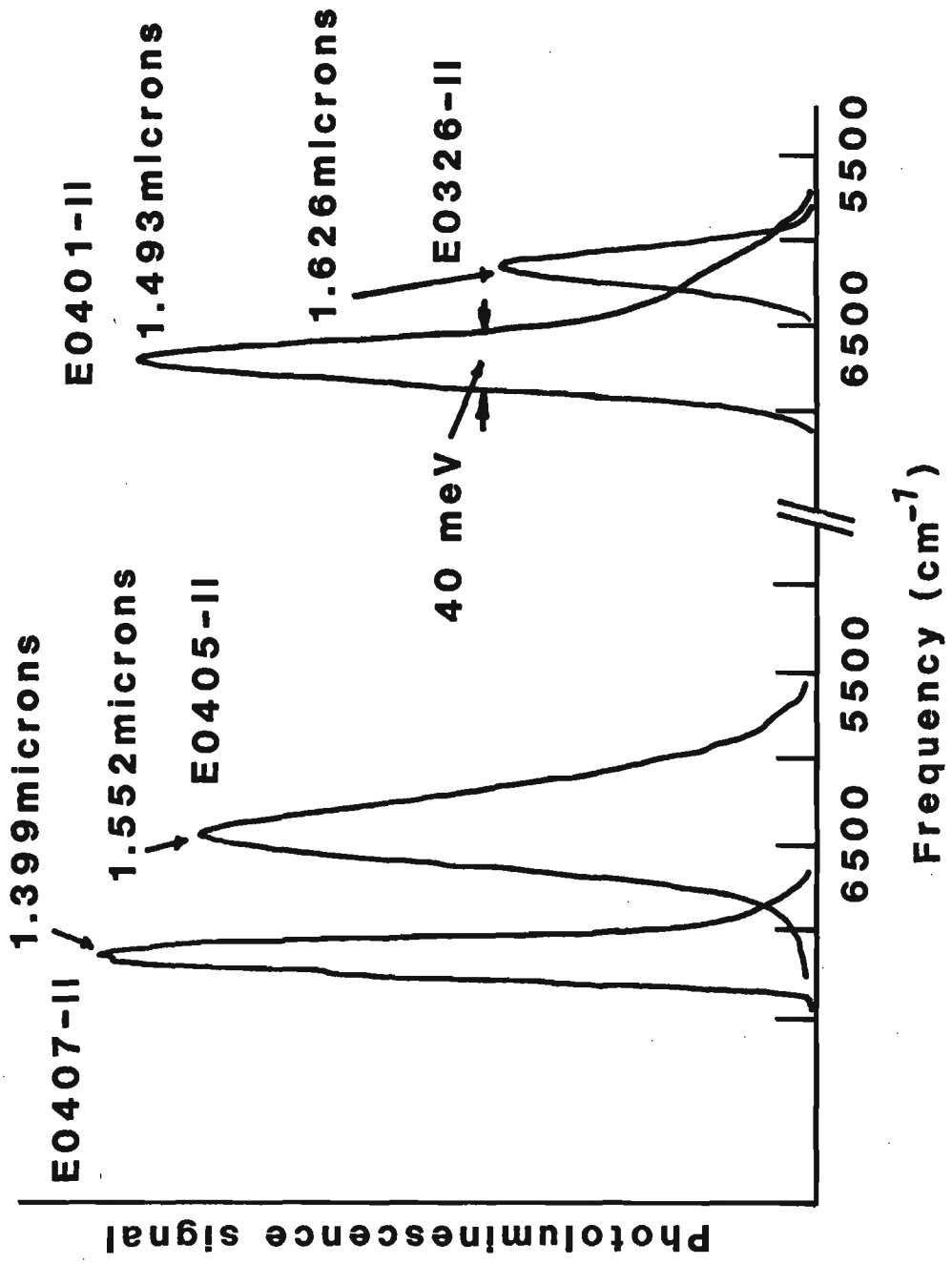
E0407-II
1.399microns
E0405-II
1.552microns
E0401-II
1.493microns
E0326-II
1.626microns
40 meV
6500
5500
5500
6500
Frequency (cm-1)
Photoluminescence signal

Figure 16

such represent a significant improvement in the material quality.

The halfwidths of the peaks can be used as a further comparative parameter with respect to material 'quality'. The halfwidths shown in figure 16 are comparable to those found for unintentionally doped n-type InGaAsP grown using vapor phase epitaxy.[20] Although in principle, the carrier concentration can be deduced from the photoluminescence halfwidth, no effort was made to do this since a wider range of samples would be required for calibration.

The MBE InGaAsP films have been characterized for their electrical properties at room temperature using van der Pauw-Hall measurements. Contact pads were formed on the unintentionally doped n-type material by evaporating sequentially Au:Ge/Ni/Au. The Au:Ge ratio was 88:12. The contact pads were alloyed for 20s at 450^{o} in 10%:90%H_2:N_2 flowing gas. The results are given in table 2.

The mobility value of 4600 $cm^2V^{-1}s^{-1}$ measured for sample E0326-II is the highest yet reported for an MBE InGaAsP film. The mobility values of all the MBE films compare very favorably with those of LPE and VPE samples of the same electron concentration and composition. The carrier concentrations of this series of growths is lower than those of previous MBE growths, mainly due to better lattice-matching and hence fewer defects, Carrier concentrations still remain somewhat higher than those of LPE and VPE material. The lowest reported value for VPE material is 0.3×10^{16} cm^{-3} and that for LPE is $1.3 \times 10^{16} cm^{-3}$. These data should be compared with $3 \times 10^{16} cm^{-3}$, the lowest value for the present MBE material.

Also shown in table 2 are the substrate temperatures. Although there are insufficient data to enable an unambiguous conclusion to be

ROOM TEMPERATURE HALL DATA

SAMPLE	MOBILITY	CONCENTRATION	THICKNESS	SUBSTRATE TEMP.
E0326-II	4630 $cm^2V^{-1}s^{-1}$	$4.8 \times 10^{16} cm^{-3}$	0.65μm	510 C
E0401-II	4200 $cm^2V^{-1}s^{-1}$	$1.25 \times 10^{17} cm^{-3}$	0.64μm	510
E0405-II	3160 $cm^2V^{-1}s^{-1}$	$1.5 \times 10^{17} cm^{-3}$	0.66μm	500
E0407-II	3900 $cm^2V^{-1}s^{-1}$	$3 \times 10^{16} cm^{-3}$	0.66μm	520

Bandgap for all samples about 0.8 eV, lattice matching implies x = 0.41, y = 0.86, wavelength = 1.55 microns

Table 2

drawn, it appears that the highest mobilities occur at a substrate temperature of 510°C. Furthermore, the carrier concentration seems to be reduced as the substrate temperature is increased. Additional experiments are required to confirm these observations.

In order to study the effect of substrate temperature further, optical micrographs have been taken of the MBE films and of those parts of the substrates which were covered by a tantalum foot during growth and hence did not have film growth. These optical micrographs are shown in figure 17. The film grown at the lowest substrate temperature shows the least density of defects. All other films show regularly spaced and oriented defects whose size and density increase with substrate temperature.

A step profiler scan of the epilayer is shown in figure 18 which reveals that these defects consist of projections above the surface of up to a maximum height of 2000Å. The defects have a square cross-section with a tapered profile, being widest at the base. They all have the same orientation. An optical micrograph of the area under the foot of sample E0326-II reveals similar looking defects to those on the film. Interestingly enough, however, the defects under the foot are not projections but pits, with depths up to 400Å. This is demonstrated in the step profile shown in figure 19. There does not appear to be any correlation between low defect density and high mobility.

The origin of the defects under the foot is probably due to thermal effects on the InP substrate. The higher substrate temperature giving rise to increased thermal etch pits due to selective phosphorous evaporation. Although the defects on the MBE film have the same orientation, as one may expect, since the crystal orientation predisposes certain directions, there is no obvious correlation. It may

be that selective substrate defects give rise to perferred growth conditions. However further studies are clearly indicated.

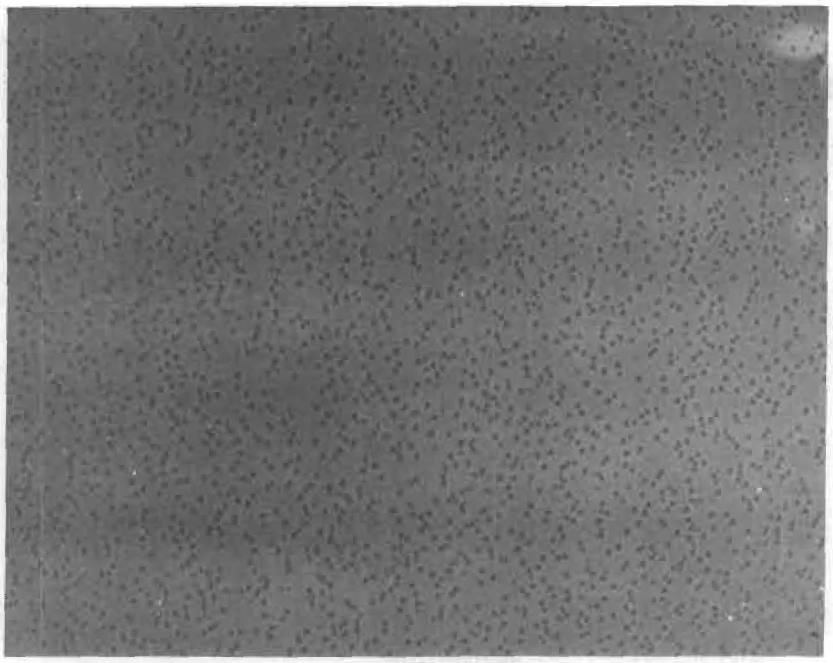

UNDER FOOT

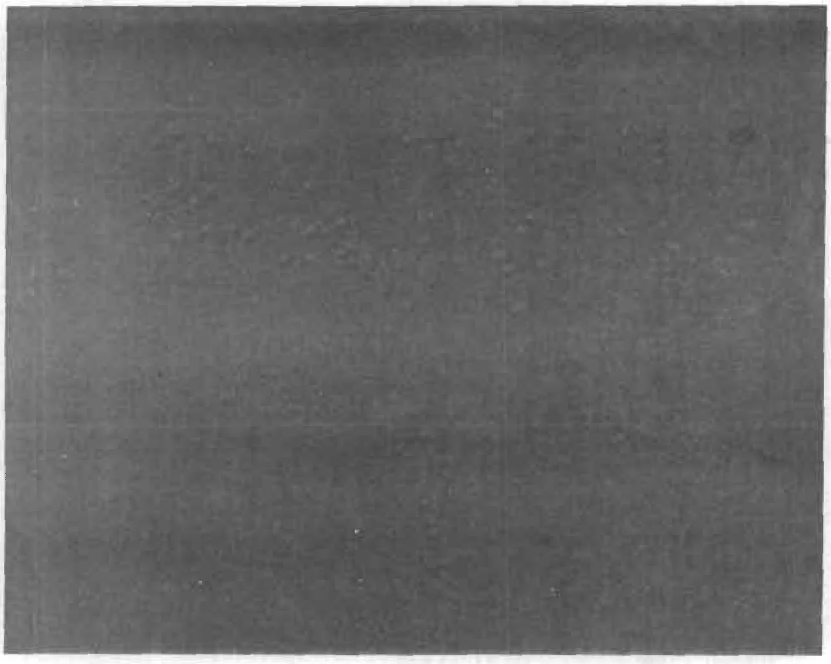

MBE LAYER

InGaAsP LAYER E0326 MAGN. 200X

T(sub):510 C

Figure 17a

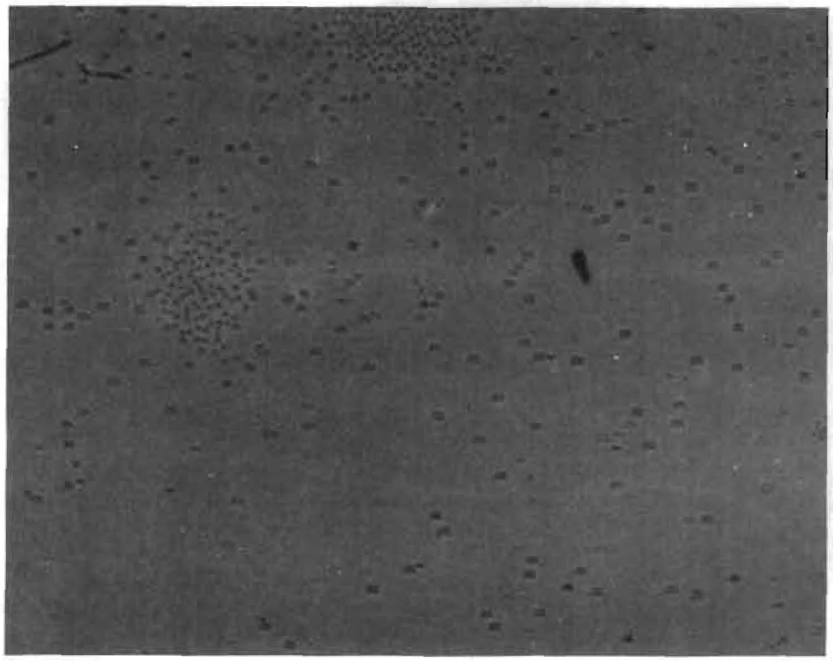

UNDER FOOT

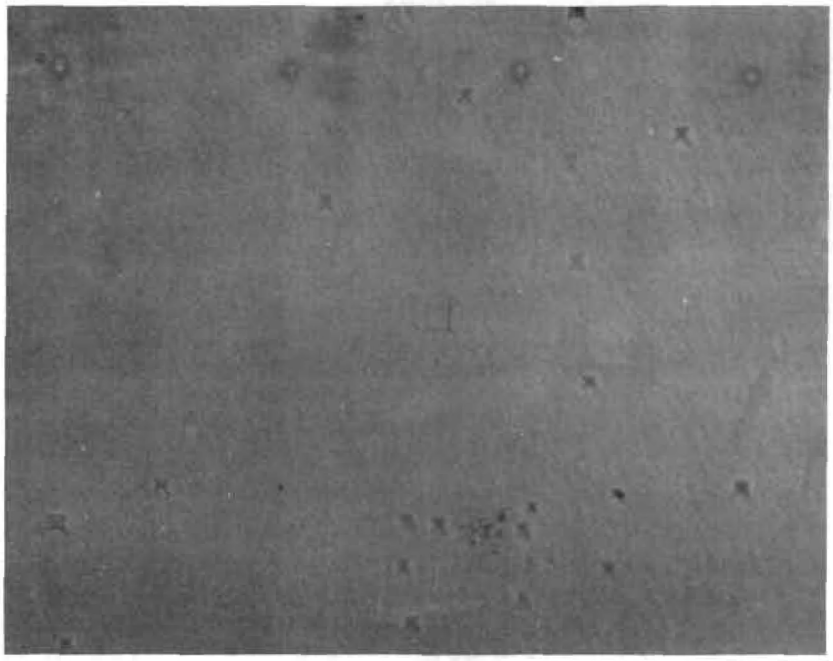

MBE LAYER

InGaAsP MBE LAYER E0401 MAGN. 200X

T(sub):510 C

Figure 17b

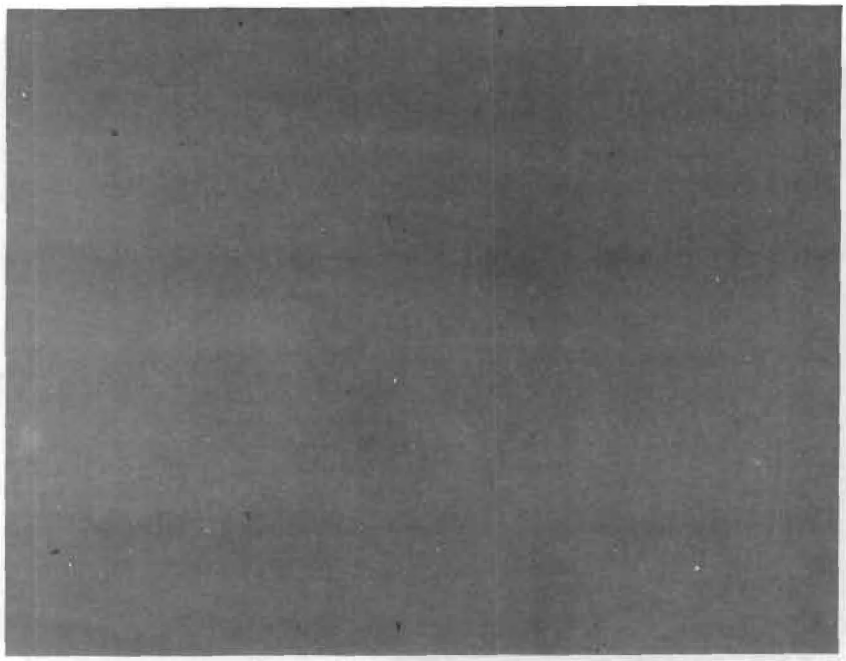

MBE LAYER

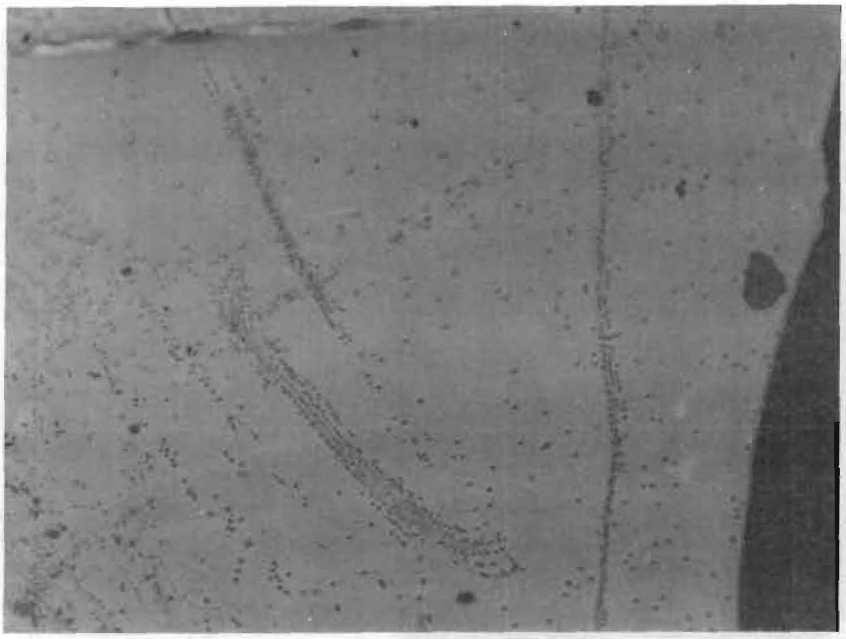

UNDER FOOT

InGaAsP MBE LAYER E0405 MAGN. 200X

T(sub):500 C

Figure 17c

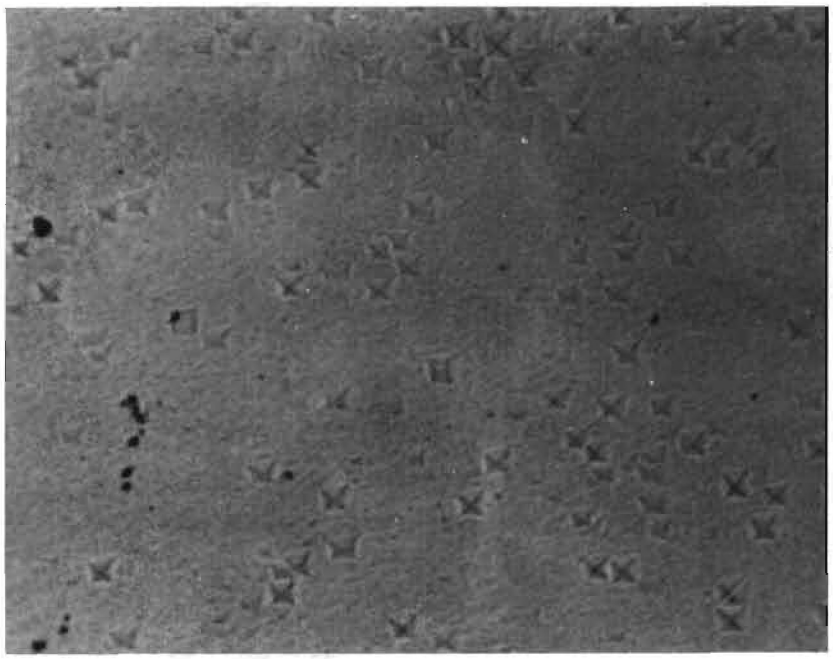

InGaAsP MBE LAYER E0407 MAGN. 200X

T(sub):520 C

Figure 17d

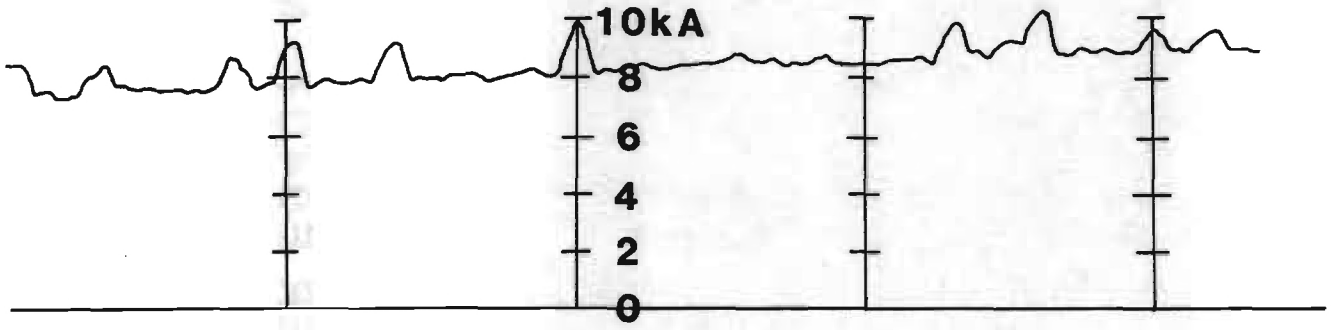

Figure 18

Tencor scan across MBE InGaAsP film.

Scan shows projections up to 2000A in height.

Projections have square horizontal cross-section and triangular vertical cross-section.

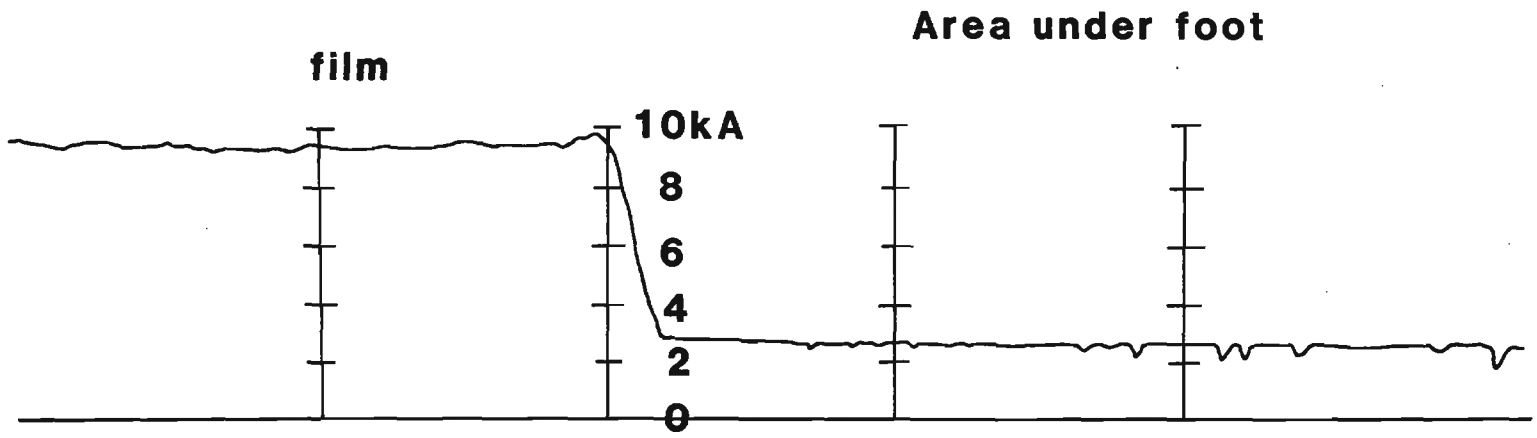

Tencor scan from film to foot of MBE InGaAsP on InP substrate

Foot scan shows presence of pits up to 400A deep.
Pits have square horizontal cross-section and
triangular vertical cross-section.

Figure 19

4.0 MBE GROWTH OF INTENTIONALLY-DOPED n^- and p-TYPE InP

As mentioned earlier, in order to fabricate double-heterostructure diode lasers, it is necessary to incorporate n- and p-type InP into the structure. These layers serve to confine both electrons and photons to the active lasing area. This section is concerned with the growth of n- and p-type InP using MBE. Since one of the major problems was expected to be the fabrication of ohmic contacts to InP, this section will also include studies on possible contacting methods.

4.1 Growth of n-type InP by MBE

Although InP is potentially a very important material for the fabrication of high-frequency microwave devices, relatively little work has been reported on the growth of InP by MBE. Growth has previously been achieved using In and either InP or red phosphorous as the phosphorous source. Substrate temperatures which range between 350^{o}C and 510^{o}C have been reported. The lowest carrier concentration which has been achieved at the time of writing is approximately 2×10^{16} cm^{-3} and the highest mobility reported is 3800 cm^{2}V^{-1}s^{-1}, these being the room temperature values, which were achieved with a substrate temperature of 530^{o}C. This material was grown at Georgia Tech.[15] As the substrate temperature is increased, the ratio of phosphorous to indium flux has to be increased in order to compensate for increased loss of phosphorous from the surface. The congruent evaporation temperature for InP is 365^{o}C. For substrate temperatures above 410^{o}C Norris and Stanley[13] have reported the existence of defects which consisted of whiskers anchored to In droplets. Such defects were not observed in the present work; only the regularly oriented defects previously mentioned have been seen and these were observed for T_s

500°C.

The question of surface cleaning has received some attention. Norris and Stanley[13] have used argon ion sputtering followed by annealing to remove the oxygen and carbon layers. Sputter cleaning was used in preference to thermal cleaning since it was supposed that the temperatures needed to remove oxygen and carbon would be too high relative to the congruent evaporation temperature, resulting in significant phosphorous depletion. However, as shown in the present work, thermal cleaning at temperatures up to 560°C can be used as long as an adequate arsenic-phosphorous passivation flux is present.

The conditions used to grow the unintentionally doped n-type InP layers are given in table 3, along with the results of electrical measurements. Indium and indium phosphide were used as the In and P_2 sources. These, together with a substrate temperature of 510°C, gave a growth rate of 0.4 μm/hr. The oven temperature of the InP source was set at that used for the growth of InGaAsP. This facilitates the change from growth of InP to that of InGaAsP.

The electrical data show mobilities typically of 2000 $cm^2V^{-1}s^{-1}$ and carrier concentrations of 1 2 x $10^{17}cm^{-3}$. The mobility values are lower than that of 3800 $cm^2V^{-1}s^{-1}$ previously achieved and the concentration values higher. These later values are most likely to be due to increased contamination of the MBE system during the overall accumulative growth periods. This system has been routinely used to grow films using In, Ga, GaAs, InP, Be, Mn, and Sn; and with the frequent opening to opening to replenish the InP, a steady increase in background level is to be expected. Furthermore, evidence for the existence of a low level vacuum leak became apparent, which could also

ROOM TEMPERATURE HALL DATA

SAMPLE	MOBILITY $cm^2V^{-1}s^{-1}$	CONCENTRATION cm^{-3}	THICKNESS μm	SUBSTRATE TEMP. °C
E0528-II	1600	1.3×10^{17}	0.7	510
E0610-II	1100	4×10^{17}	0.25	510
E0611-II	2300	2.5×10^{17}	0.56	510
E0624-II	2500	2.3×10^{17}	0.36	510
*E0625-II	1900	2×10^{18}	0.4	520

*Sn-doped

Table 3

have contributed to the measured values.

The n^+ confining layer of InP in a InGaAsP/InP diode laser needs to have a concentration of $2 \times 10^{18} cm^{-3}$. Having established the background growth conditions, a Sn oven was introduced into the system and was used to increase the electron concentration. The Hall data are given in Table 3 and is the first reported value for Sn-doping of InP. The Sn oven temperature was $640^{o}C$ and produced exactly the required doping level with a room temperature mobility of 1900 $cm^2V^{-1}s^{-1}$. This was a particularly encouraging result and showed that Sn is a good candidate for n-type doping of InP by MBE growth.

4.2 Search for a suitable ohmic contact to p-type InP

Before looking at suitable dopants for p-type InP, some means of making the ohmic contacts needed for Hall measurements on p-type material has to be available. Various contacting schemes for fabricating ohmic contacts on p-type InP have been proposed and used for ohmic contacts, with varying degrees of success. The systems which have been used include Au-Zn,[21] Au-Mg,[22] Au-Cd,[21] In-Zn,[21] and In-Cd.[21] The success of these systems has not been completely satisfactory. Au-Zn[23] fabricated using a plating process, seemed to produce the most promising results. Plating was found to be necessary since the high vapor pressure of Zn makes it difficult to control the thickness of the zinc layer by evaporation. Au-Be,[24, 25] sequentially evaporated (Be first), has also been shown to give good ohmic contacts to p-type InP. However, due to the toxicity of Be, it was decided to investigate first whether or not some less undesirable process could be found. Accordingly, some studies were made of ohmic contacts to p-type InP using Au:Mn alloys.

4.2.1 Contacts to p-Type InP using Au-Mn Alloys

The metals were evaporated using separate boats for the Mn and Au.

The intial tests were performed on p-type InP substrate material using a 95% Au: 5% Mn alloy with the Mn being evaporated first. The total weight of Au + Mn was 50 mg. The substrates were either Zn or Zn^+ doped InP. Values for the carrier concentrations of the substrates are not available but are probably in the region 1 - 2 x $10^{18} cm^{-3}$. Following the deposition, the contacts are alloyed in forming gas at 450°C for various lengths of time.

The contacts were made by evaporating through a Hall sample mask. The behavior of the contacts were determined from I-V curves.

The bulk samples were prepared by either cleaning in organic solvents or by cleaning and then etching. The etch was a standard InP etch. Generally there was little difference in the ohmic properties of cleaned and cleaned/etched samples. The minimum alloying time at 450°C was three minutes. Alloying times shorter than three minutes exhibited poorer I-V curves. Presumably this is due to the diffusion time of the Mn into the InP. A series of I-V curves for the 95:5 Au:Mn alloy after various alloying times is shown in figure 20. The contacts are clearly symmetric but non-linear. The final curve after annealing for six minutes at 450°C did become linear with a contact-contact resistance of 30 . Although not perfect, this was sufficiently encouraging to repeat the procedure on an MBE p-type InP film.

Figure 21 shows the I-V curves obtained using a Au(90):Mn(7) contact alloy on p-type InP MBE sample D0920-II after annealing for 4 mins at 450°C in hydrogen. This shows a contact-contact resistance of 7.5Ω. The contacts were not consistent however. Figure 21 also shows two I-V curves for this system which represent the characteristics of various pairs of the four contacts. The key signifies which of the four

after 1 minute anneal.

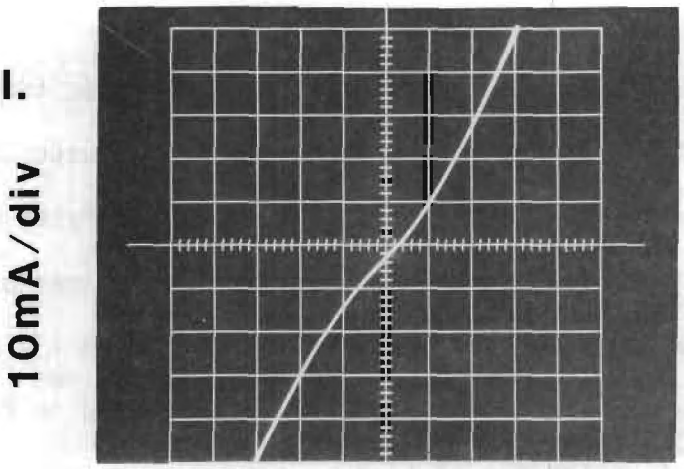

after 2 minute anneal.

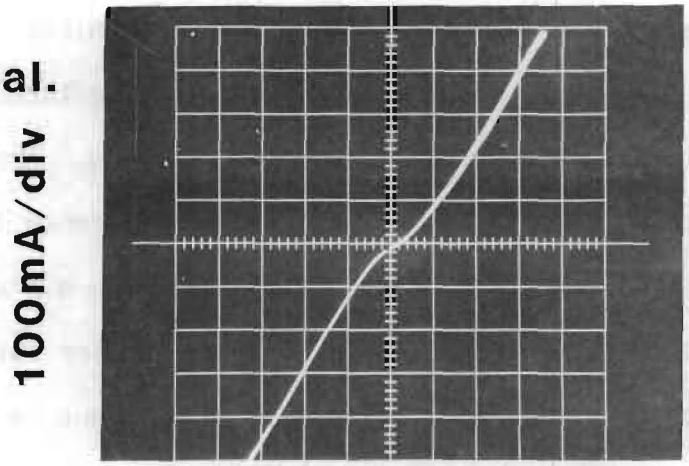

after 4 minute anneal.

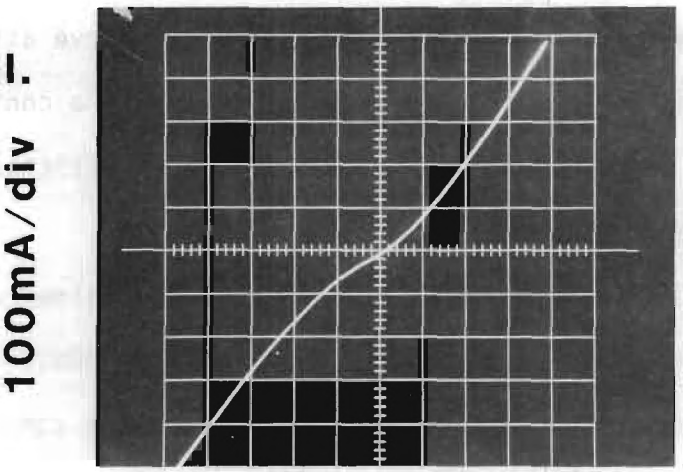

Figure 20

I-V curves for Au:Mn contacts on p-type InP.

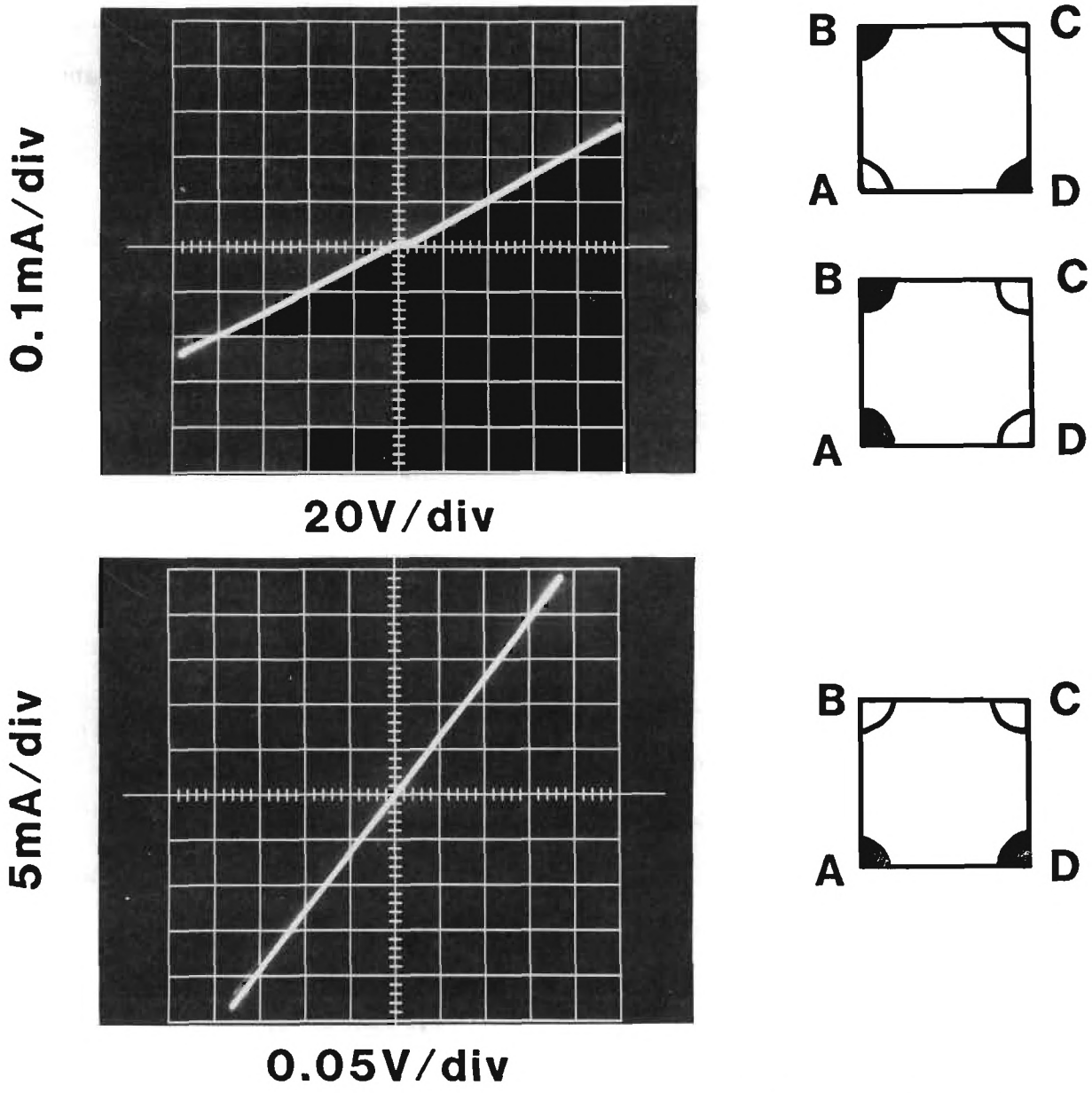

I-V curves for Au:Mn(90:7) contacts on p-type InP(Mn doped) D0929-II

contacts annealed in hydrogen at 450 C for 4 mins.

Figure 21

contacts are being studies. Good linearity and ohmic behavior, at least under conditions pertaining to the Hall measuring conditions of 1 mA and 1V, are achieved, but only for one pair of contacts.

Following a discussion with Brad Boos of NRL, contacts were fabricated from similar alloy ratios but with simultaneous evaporation from the same boat. Contrary to results reported with Au:Zn alloys, no improvement was observed with the Au:Mn system. However, it was not possible to pursue this technique further due to the small amount of p-type InP material available at that time. It is possible that further studies may have shown some improvement.

The fabrication of ohmic contacts on p-type InP using a Au and Zn periodic plating procedure together with photolithographical defintion of the contact area was recently published.[26] This procedure has produced the lowest resistance contacts and is ideally suited for fabricating contacts on a complete diode laser structure since the photolithographic process can be used to define the contact geometry and hence the lasing area.

Summary

A procedure for fabricating ohmic contacts on p-type InP has been devised using Au-Mn alloys. Some success was achieved and ohmic behavior was exhibited for some contacts, however, the the contacts were not consistent and in this respect the procedure is not a significant improvement over other reported techniques. Hoever, if an evaporation procedure is required for contacts, the Au:Mn system is comparable to Au-Zn and less harmful to vacuum systems. Further studies will undoubtedly improve the inconsistencies found in the contact quality.

4.3 Investigation of Be as a possible p-type dopant for InP

There has, at the time of writing, been no report of successful p-type doping of MBE InP. Elements which have been used for InP p-type dopants with other epitaxial techniques include zinc,[26] beryllium,[27] cadmium,[28, 29] magnesium[38] and manganese.[30] Cadmium and zinc have low sticking coefficients and therefore do not lend themselves readily to MBE growth. Additionally, there are problems due to vacuum system contamination. Be, Mg, and Mn are more logical choices. Some success has been reported using Mn to dope p-type InGaAsP grown by MBE at Georgia Tech.[10] Be has also been used successfully as a p-type dopant for MBE GaAs[31] and has been found to be well-behaved and reproducible. McFee[14] et al report only limited success with either Be or Mn as p-type dopants.

In view of the utilization of Be as the p-type dopant for GaAs at Georgia Tech it was decided to see how Be performed as a possible candidate for p-type doping of InP. The electrical data for sample E0728-II is given in Table 4. Only one growth was possible using Be due to time and financial constraints.The sample in Table 4 was grown under exactly the same condition as the unintentionally-doped InP except for the addition of the Be oven. Thermal cleaning was performed at 560^{o}C with phosphorous passivation from the InP oven. The growth duration was one hour and yielded a layer 0.4 μm thick. The Hall data showed a room temperature mobility of 2500 $cm^2V^{-1}s^{-1}$ and a carrier concentration of 2 x $10^{16}cm^{-3}$. The material was n-type. Since the expected background carrier concentration was $10^{17}cm^{-3}$, it is clear that significant compensation took place. As mentioned previously no further studies have been possible, but the initial results are very promising and it would seem that Be is a likely candidate for a p-type dopant for MBE

Sample	Thickness μm	Mobility $cm^2V^{-1}s^{-1}$	Concentration cm^{-3}	Substrate Temp. °C
E0728-II	0.4	2500	$n = 2 \times 10^{16}$	520

Deposition parameters and electrical properties of Be-doped InP. Background dopant level, $n \sim 10^{17} cm^{-3}$.

Table 4

InP. Additional material must be grown at various Be doping levels to evaluate completely the usefullness of Be as a p-type dopant.

5. SELECTIVE EPITAXIAL GROWTH OF GaAs ON PREPARED SUBSTRATES FOR FET FABRICATION

5.1 Introduction

Selective molecular beam epitaxy is a planar process which lends itself readily to the production of various high speed logic devices such as FET structures. Recently,[32] the simultaneous deposition of single crystal and polycrystalline GaAs has been used to fabricate a number of devices. This section reports efforts on similar growth procedures using patterned samples provided by NRL. In addition to MBE growth in windows opened by selective etching of grown oxide layers on GaAs, MBE layers were also deposited on samples which had regions defined by ion implantation.

5.2 Substrate Preparation

The procedure normally used to prepare substrates suitable for MBE growth could not be used for these specially prepared substrates since the etches would remove the SiO_2 patterned region. For the ion implanted samples, the implanted depth was only about 3000Å which would be removed by the regular etch. The oxide patterned substrates also could not be etched extensively since significant undercutting of the GaAs would occur which would severely degrade any device potential. It was decided to aim for a removal of about 300Å of GaAs.

The etching rates of the Bromine-Methanol 1% etch was measured and found to be about 2.5 μm/min. Figure 22 shows the results of the present study together with previously reported data for GaAs[33] and InP[34]. The strength was reduced by a factor of 10 which gave an etching rate of 3000Å/min. Finally, an etch of 0.01% Bromine-Methanol for 30s seemed to give the required removal. The Tencor Thickness Monitor used

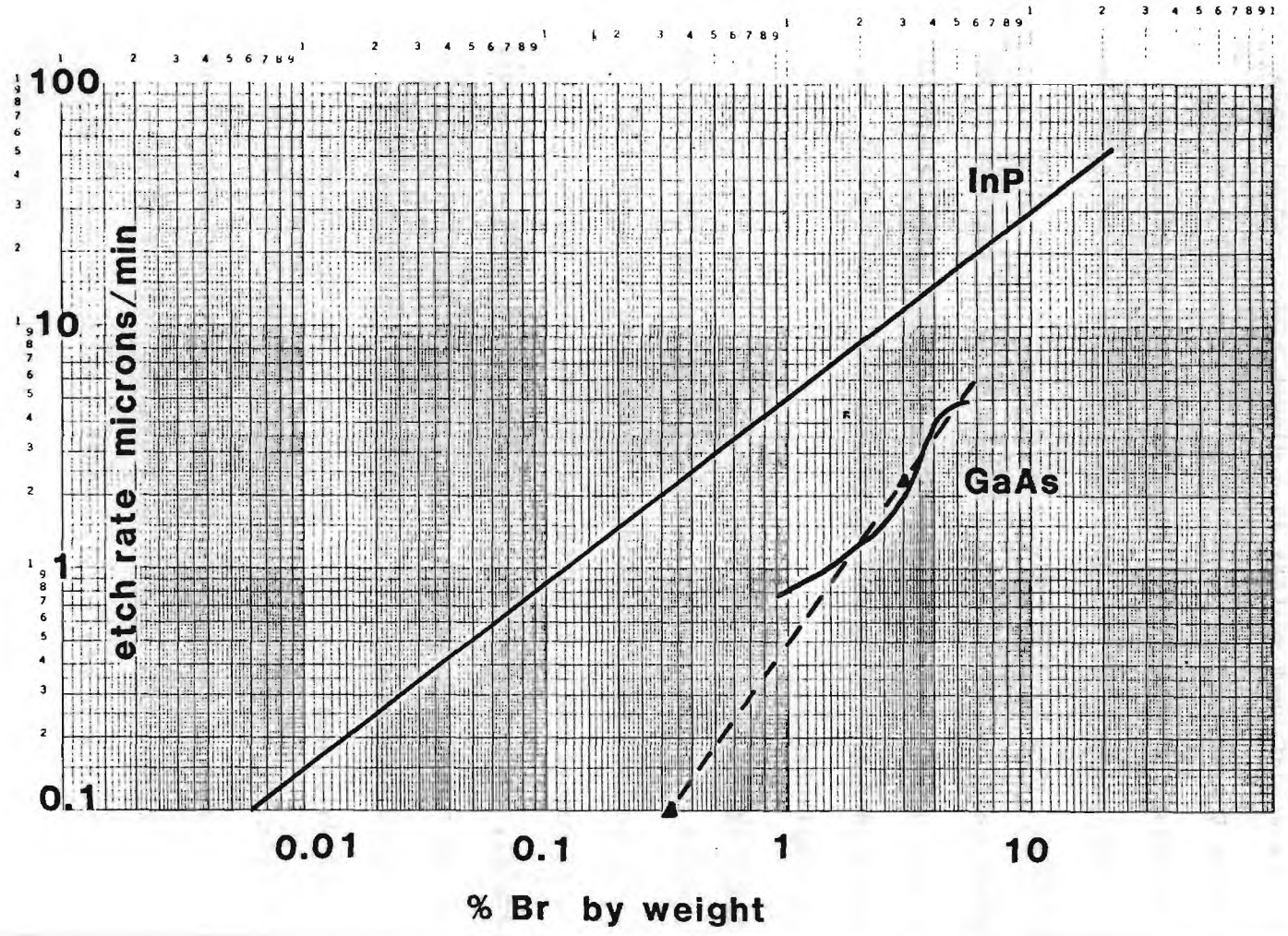

Figure 22

Etching rate of Bromine-Menthanol etches for (100) InP and GaAs versus etchant composition. --- represents present results, solid lines are from ref. 6 for GaAs and 7 for InP.

to measure the depth of the etched step was at its highest sensitivity, and the generated curve contained appreciable fluctuations. The 5:1:1/H_2SO_4:H_2O_2:H_2O etching step in the normal preparation procedure was avoided completely. The preparation procedure included the standard organic solvent stages followed by the Br:Meth etch and then washing in deionized water.

Problems in getting the substrate to adhere to the sample holder were immediately encountered. It proved extremely difficult to get the molten indium to adhere to the substrate rear surface. A number of the initial samples which were supplied by NRL were during this period due to excess indium getting on the front surface while mounting the substrate. The problem was initially attributed to the relatively unetched rear surface. To overcome this, the front surface of the sample was mounted on a glass slide using black wax and the rear surface etched using the H_2SO_4:H_2O_2:H_2O etch followed by a 1% Br:Meth etch. Although this improved the tinning level of the substrate considerably, difficulties still occur and this presently represents the major problem area. No difficulty has been encountered with any other substrate, so the problem is clearly associated with the prepared sample in some as yet unknown way. There is also the possibility that the substrates may not have been sufficiently flat.

5.3 Growth Conditions

The important parameters for an FET structure are layer thickness and carrier concentration. These were required to be 3000A and 1×10^{17} cm^{-3} respectively. The growth rate for the MBE system, using Ga and As as sources, was 1 μm/hr. Si was used as a n-type dopant. The dopant level as a function of Si oven temperature had been determined from

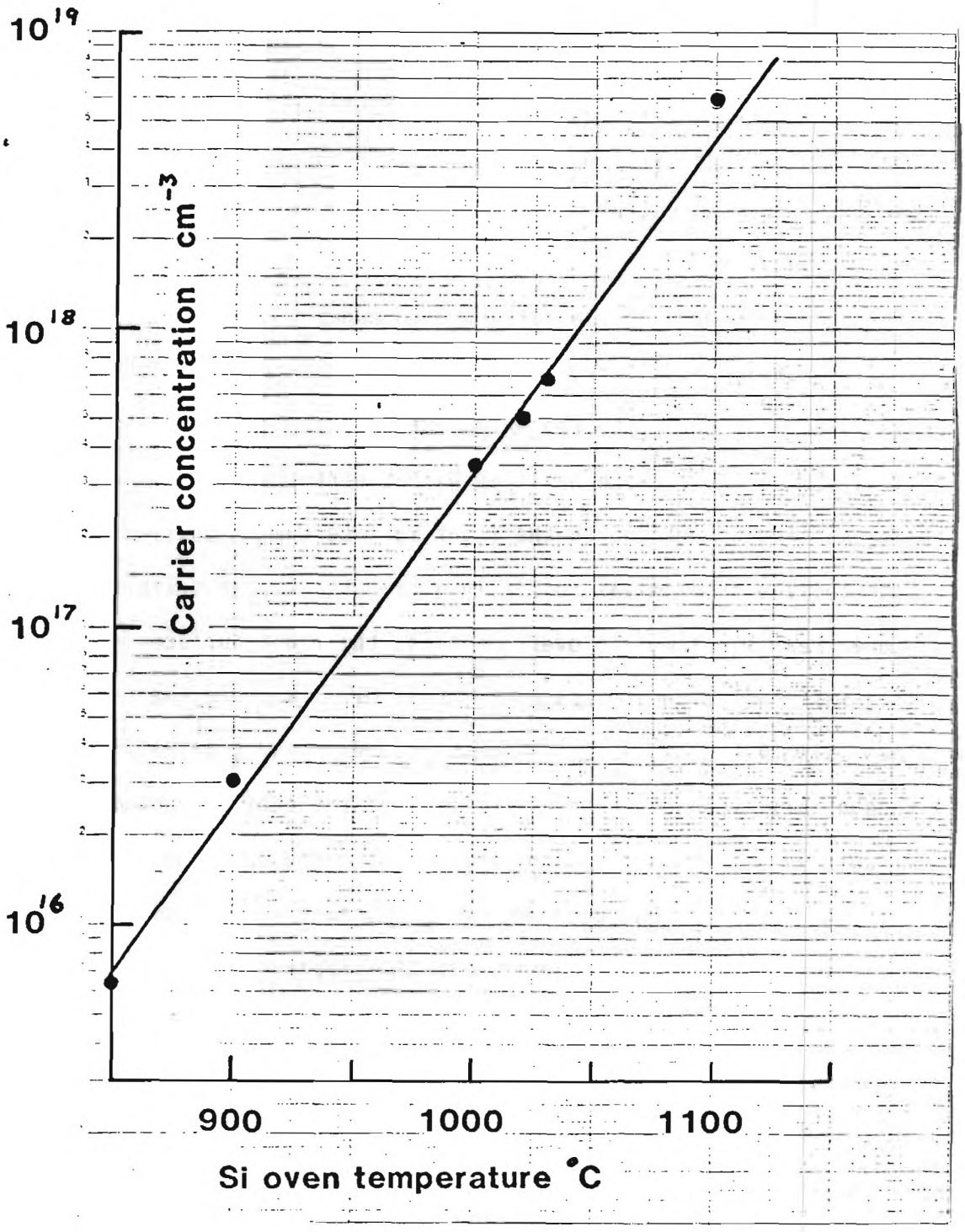

Carrier concentration versus Si oven temperature for MBE grown GaAs. Thickness of samples ~ 1 μm.

Figure 23

calibration runs on 1 μm thick samples and is shown in figure 23. In order to measure the thickness and carrier concentration of the layer, an extra piece of semi-insulating Cr-doped GaAs substrate material was inserted adjacent to the patterned sample, and the thickness and Hall measurements were made on that piece.

It was found that the thickness followed the previous calibration runs exactly, but the carrier concentration was always less than that expected from the calibration runs. The reasons for this are not certain at the moment, but the differences in the layer thicknesses may be a factor. It is probable that the effect of carrier depletion near the substrate/film interface has signficiant effect on the average carrier concentration for the thin film whilst being relatively unimportant for the thicker films.

Typical MBE growth conditions were: substrate temperature 580^{o}C, Ga pressure 4 x 10^{-7} torr and As pressure 1.6 x 10^{-6} torr. The Si oven temperature expected for a concentration of 10^{17} cm^{-3} is 990^{o}C, however, temperatures between 950 and 1000^{o}C were used. Growth rates are typically 1 μm/hr; for the 3000Å thick layers grown, this required 19 minutes growth time. The substrate is heated under an incident arsenic flux at all times.

Presently the layer is grown without a buffer layer; however, future runs may incorporate an undoped 0.5 μm or thicker buffer layer.

5.4 Results on MBE Grown GaAs Layers

5.4.1 Electrical Measurements

In order to make Hall-van der Pauw measurements as well as thickness measurements, a piece of Cr-doped GaAs was placed next to the sample on the substrate holder and the measurements were made on that

piece. This indirect characterization may lead to some discrepancy between the actual characteristics of the sample and the data reported here. Any difference is most probably due to difficulties of bonding the sample onto the substrate holder as discussed earlier, since the plain substrate probably had better thermal contact than the patterned piece. This may give rise to a different effective substrate temperature, and hence growth rate, or to a temperature variation across the sample therby leading to inhomogeneity. Additionally, the surface may not be completely free of contaminants. If fact, some of the earlier results showed the presence of whiskers which typifies surface contamination. Later samples were essentially devoid of whiskering except on the polysrystalline areas. Presumably this is due to the lack of cleaning and etching of the oxide layer.

Room temperature Hall data for four runs are shown in Table 5 toegther with the film thickness d and temperature of the Si doping oven. The samples corresponding to these runs have been delivered to NRL and are awaiting processing. The Hall data have been corrected for the error introduced by using relatively large contacting pads.[17] For these samples, no further correction for assymmetry was necessary, except for sample V14/4. The defined Hall Resistances for this sample varied by more than a factor of 60 for the two orthogonal directions. To interpret these data in order to obtain meaningful measurements is not straightforward. The usual correction factor, van der Pauw f factor, relates to a difference in the Hall resistances which is due to a geometrical assymmetry which is not applicable in the present case. Probably the simplest way to analyze the data is just to use the lowest Hall resistance and attribute the difference as due to contact problems.

Sample	Run No.	Mobility ($cm^2V^{-1}s^{-1}$)	Carrier Concentration (cm^{-3})	d(μm)	Growth Time	(T_{Si})
VI4/1	E0304-III	4100	3.5×10^{16}	.36	18 min	950°C
VI4/4	E0317-III	3300	3×10^{16}	.30	17 min	970°C
VI4/6	E0330-III	3600	3.5×10^{16}	.33	18 min	990°C
VI4/7	E0401-III	3500	1.6×10^{17}	.38	19 min	1000°C

Table 5

If this is done a mobility for VI4/4 greater than 5000 $cm^2V^{-1}s^{-1}$ is obtained. The number given in the table is the average of the two Hall resistances without consideration of the differences and should be taken as being somewhat pessimistic.

The data obtained for VI4/7 is very similar to data obtained elsewhere for a similar system but with an undoped GaAs buffer layer.[32] It is clear from the Hall data that the MBE layers are of good quality. The ability to control the thickness can be deduced from Table 5. The variation in deposition time was between all samples was less than two minutes which lead to a spread of 800Å in layer thickness. This suggests that the layer can be controlled to about 100Å. The dopant level is the most difficult parameter to control and, as seen from Table 5, Si oven temperatures from 950 to 990°C did not appear to change the concentration significantly. However, sample VI4/7 has approximately the correct value of concentration.

5.4.2 Surface Characteristics

All of the GaAs monitor samples appeared highly reflecting. The main samples however had a variety of defects which presumably therefore are due to a specific sample-related cause and not due to growth conditions.

Initially, the degree of the cleaning etch was reduced relative to the more usual procedure and this results in extensive whiskering over large parts of the surface. The presence of these whiskers is directly related to the presence of contaminants or other defects on the surface. Growth on plain substrates requires significant etching to achieve a surface sufficiently clean for epi growth. The normal preparation typically removes 10 to 20 μm, which cannot be used in the present case which is limited to 200A. It is important therefore that since the

substrates cannot be etched after the patterned regions are fabricated, they must be etched in 5:1:1/$H_2H_2SO_2$:H_2O_2:H_2O prior to this process. The very light 0.01% Br:Methanol etch used on the prepared wafer, which removes about 300A in 30s, may be insufficient to produce a good surface for growth.

A selection of optical micrographs is shown in figure 24. Nominally, the clean/etch process was identical in all cases. A further variable may be due to indium spillover sometimes incurred when bonding the sample to the holder. These microgrpahs generally are of areas not obviously contaminated with spillover of In or scratches inadvertently made when wetting the sample.

Figure 24a shows a 200X micrograph of E0304-III, VI4/1. The crystalline areas is essentially free of whiskers and other defects; significant whiskering appears just outside this window. This high whisker density does not extend into the polycrystalline region and therefore suggests a localization of defects.

Figure 24b shows sample E0317-III VI4/4 at a magnification of 125x. The localization of whiskers in this case is very muchg reduced. Very little whiskering is evident in either the winsow or oxide regions. Visually this appeared to be one of the better samples; unfortunately, the Hall data for this sample were the most unreliable.

The micrographs shown in figures 24c and 24d of samples E0330-III, VI4/6 and E0401-III, VI4/7 are somewhat similar. There is a uniform density whisker defect within the oxide regions and little indication of clustering around the edges of the window. The window region is relatively free of defects.

All the above figures represent the best part of each sample but are nevertheless an indication of the quality of layers achievable using

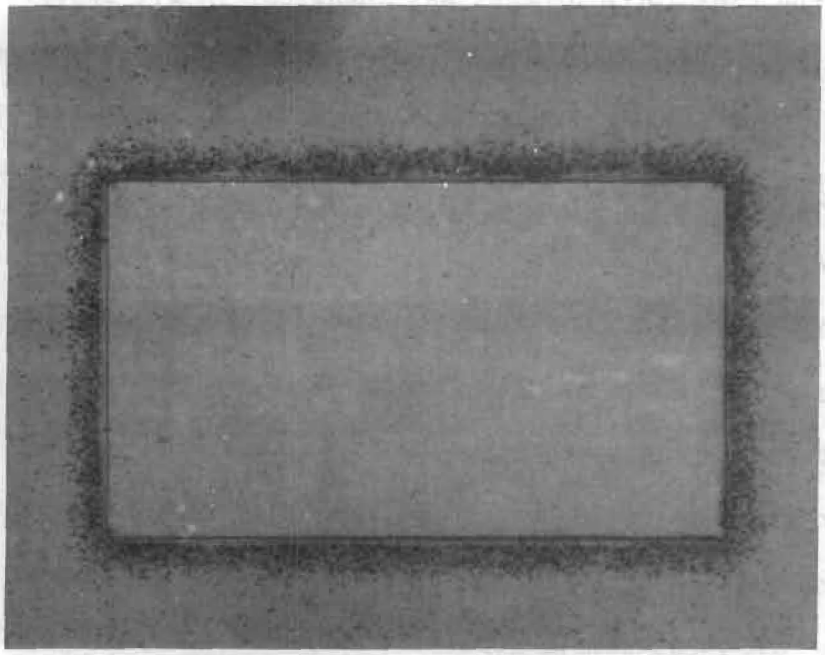

Optical micrograph of one window and surrounding oxide layer for sample VI4/1, Run E0304-III. Substrate temperature 560°C.

Figure 24a

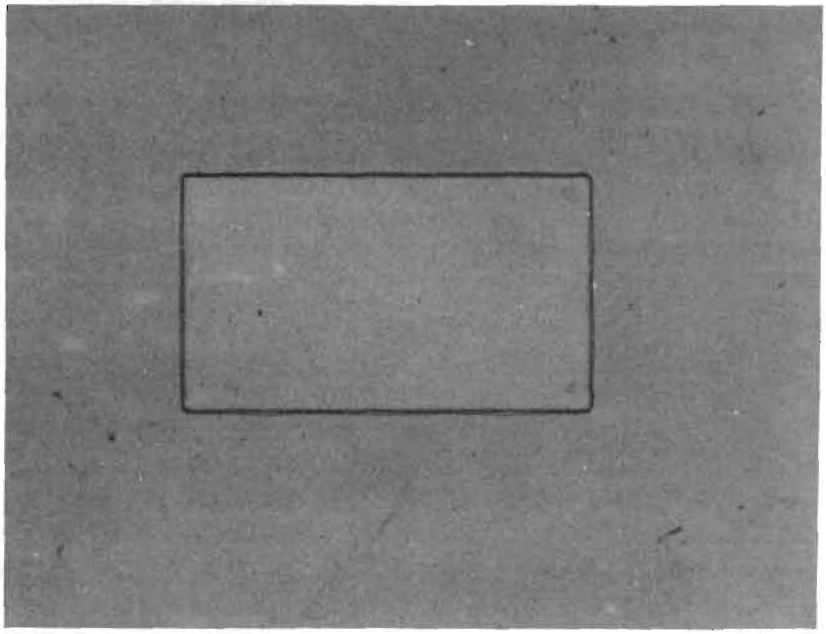

Optical micrograph of one window and surrounding oxide layer for sample VI4/4, Run E0317-III. Substrate temperature 560°C.

Figure 24b

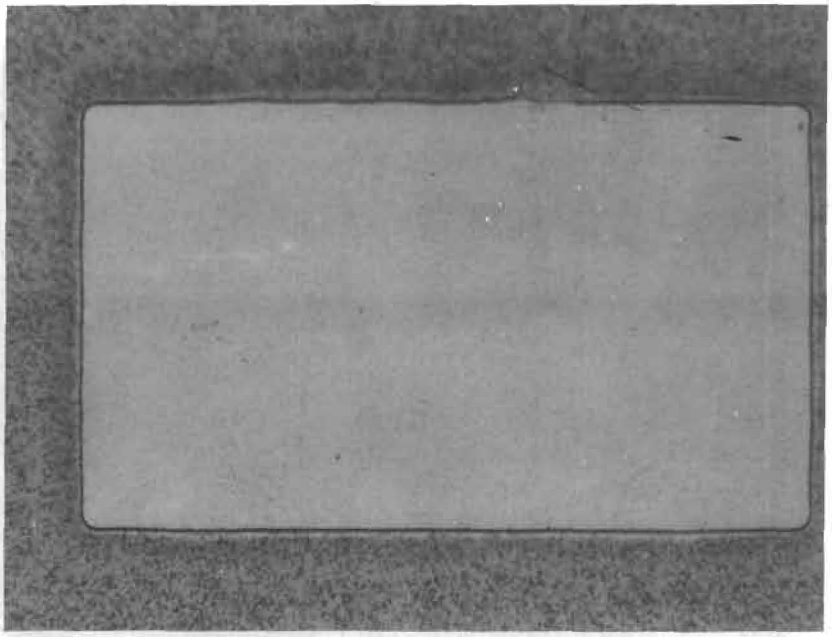

Optical micrograph of one window and surrounding oxide layer for sample VI4/6, Run E0330-III. Substrate temperature 560°C.

Figure 24c

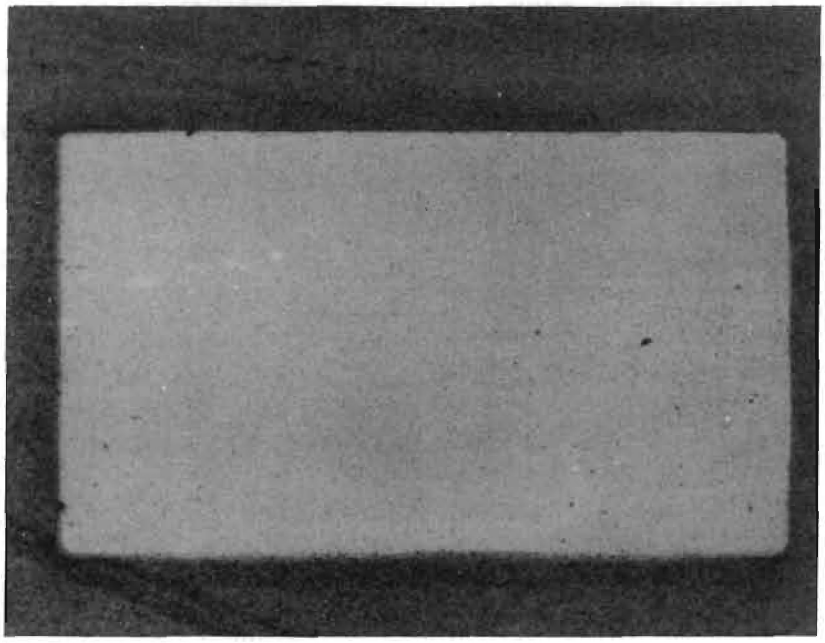

Optical micrograph of one window and surrounding oxide layer for sample VI4/7, Run E0401-III. Substrate temperature 560°C.

Figure 24d

selective molecular beam epitaxy.

5.4.3 Growth on Ion Implanted GaAs

In addition to MBE growth on the patterned oxide layered substrates, some growths were also made on ion implanted GaAs. The objective was to determine if selective implantation could be used to generate regions of damage which would then give rise to high resistivity regions of GaAs when a layer is grown using MBE. Non implanted area would have good crystalline growth. In this way a pattern of high resistivity GaAs with windows of high mobility GaAs suitable for FET fabrication could be achieved. Unfortunately, the high temperature of the GaAs substrate durng growth essentially anneals out the implanted damage and all the films grown on these implanted areas showed good crystallinity.

5.5 Summary

The results discussed in the previous section are the outcome of a number of test runs to establish operating conditions. These have now been established as far as the growth of a suitable layer is concerned. However, two problems which may be interrelated, still remain. These are:

1) Presence of whiskers due to inadequate surface etching - this may be solved by either etching the substrate before pattern definition and/or by light etching immediately prior to growth using a H_2SO_4 based etch rather than the 0.01% Br:CH_3OH presently used.

2) Etching of the wafer prior to pattern definition in a 5:1:1/H_2SO_4:H_2O etch may also help overcome the problems in tinning and bonding the sample to the substrate holder.

It should be pointed out that the eight sections cut from wafer

VI/4, four were degraded by overflow and scratches which occurred duirng the bonding stage.

6. CONCLUSIONS AND RECOMMENDATIONS

This program has investigated and characterized the basic material properties and device fabrication procedures required to construct a double heterostructure diode laser using molecular beam epitaxially grown InGaAsP and InP. Significant progress was made in establishing growth conditions for high-mobility InGaAsP with bandgaps near 1.55 μm as well as in identifying suitable n- and p-type dopants for the InP confining layers. The results clearly demonstrate the effectiveness of MBE for growing high quality InGaAsP suitable for laser material.

The principal achievements of this study are:

1) Reproducible MBE growth of InGaAsP was demonstrated
2) High mobility InGaAsP lattice matched to InP with bandgap energies corresponding to wavelengths near 1.55 μm has been grown for the first time.
3) Room temperature mobilities in excess of 4500 $cm^2V^{-1}s^{-1}$ have been achieved which are superior to liquid phase epitaxy material.
4) Good photoluminescence efficiencies in InGaAsP have been achieved at 4^oK. These are the first reported photoluminescence data for MBE InGaAsP.
5) Ionization gauge continuous flux monitoring has been demonstrated which will improve future growth control.
6) Be and Sn have been established as p- and n-type dopants respectively for InP.
7) Au-Mn has been shown to be a possible ohmic contact to p-type InP.

Unfortunately severe system malfunction towards the end of the

program prevented the growth of a complete laser structure.

Despite the progress made in this study, the complexity of MBE growth of INGaAsP ensures that further studies will still be required before a complete understanding is possible.

Areas identified during this program as needing further study include:

1. Investigation of red phosphorous with a cracking oven as a P_2 source.
2. Study of layer quality as a function of substrate temperature and growth rates.
3. Investigation as to whether high diffusion rates at high substrates temperature will reduce device performance when multilayer structures such as diode lasers are grown.
4. Verification of dopant properties of Be in InP.
5. Completion of studies on improved ohmic contacts to p-type InP.

Future Applications for MBE InGaAsP

The next phase in the investigation of molecular beam epitaxy of the quaternary system is to develop and grow a series of laser diodes with emission wavelengths between 1.1 μm and 1.6 μm. The control needed for such bandgap adjustments will necessitate tighter control of flux rates than is presently available. This may require the incorporation of individual flux monitors similar to that successfully demonstrated in this program.

The important application of the quaternary system to optical fiber communication systems needs to be reinforced and consolidated by the development of photodetectors and finally the monolithic integration of detectors, electronic components (e.g. MESFETs) and sources. Molecular

beam epitaxy, with its slow growth rates and flexibility including in situ masking, is ideally suited for this. The area of integrated opto-electronic circuits, although still in its relative infancy, is expanding rapidly and it is clear that InGaAsP will have an important role to play. Diode lasers with emission wavelengths between 1.3 and 16 m have attracted a considerable amount of attention. However the area of longwavelength InGaAsP photodiodes has only recently been studied extensively. Further effort, especially towards avalanche photodiode structures, with the objective of increasing efficiency, are clearly called for, in addition to integration techniques.

The present study has indicated that good quality InGaAsP can be grown using molecular beam epitaxy and has opened the way towards individual device fabrication and finally monolithic integrated opto-electronic circuits. The successful and efficient implementation of these ideas is only likely to be realized because of the tremendous growth control possessed by molecular beam epitaxy. Of the other epitaxial techniques, only metal organic-chemical vapor deposition has this advantage. The next few years is going to be an exciting time as the next generation of opto-electronic devices come to maturity.

7. REFERENCES

1. D. Botez, "InGaAsP/InP Double Heterostructure Lasers: Simple Expressions for Wave Confinement, Beamwidth, and Threshold Current over Wide Ranges in Wavelength, (1.1 - 1.65 μm), IEEE J. Quantum Electron 17, pp. 178-186, (1981).

2. R. E. Nahory, M. A. Pollack, W. D. Johnston, Jr., and R. L. Barnes, "Band Gap versus composition and demonstration of Vegard's Law for $In_{1-x}Ga_xAs_yP_{1-y}$ Lattice-matched to InP," Appl. Phys. Lett. 33, pp. 659-661 (1978).

3. R. L. Moon, G. A. Antypas, and L. W. James, "Bandgap and Lattice Constant of GaInAsP as a function of Alloy Composition," J. Electron, Mater., 3, pp. 635-644, (1974).

4. S. R. Forrest, "Performance of $In_xGa_{1-x}As_yP_{1-y}$ Photodiodes with Dark Current Limited by Diffusion, Generation Recombination, and Tunnelling," J. Quantum Electron 17, pp. 217-226, (1981).

5. S. Arai and Y. Suematsu, "1.11 - 1.67 m GaInAsP/InP Injection Lasers Prepared by Liquid Phase Epitaxy," IEEE J. Quantum Electron 16, pp. 197-205, (1980).

6. G. H. Olsen, C. J. Neuse, and M. Ettenberg, "Low-threshold 1.25 m vapor grown InGaAsP cw lasers," Appl. Phys. Lett. 34, pp. 262-264, (1979).

7. M. A. Littlejohn, J. R. Hauser and T. H. Glisson, "Velocity-field characteristics of $Ga_{1-x}In_xP_{1-y}As_y$ quaternary alloys," Appl. Phys. Lett. 30, pp. 242-244, (1977).

8. J. Andrews, S. Bandy, S. Chiao, and J. Crowley, "Advanced III-V Compound Microwave Device Investigation," AFAL Report TR-79-1174 (1979).

9. Y. Takeda, M. A. Littlejohn, and J. R. Hauser, "Electron Hall mobility in $Ga_xIn_{1-x}As_yP_{1-y}$ calculated with two-longitudinal optical phonon model," Appl. Phys. Lett. 39, pp. 620-621 (1981).

10. G. D. Holah, E. L. Meeks, F. L. Eisele, and D. W. Covington, "Growth and Characterization of $In_{1-x}Ga_xAs_yP_{1-y}$ and GaAs using Molecular Beam Epitaxy," Final Report, Contract No. N00173-79-C-0033, Naval Research Laboratory, 1982.

11. A. T. Cho, "Recent Developments in Molecular Beam Epitaxy (MBE)," J. Vac. Sci. Technol. 16, pp. 275-284, (1979).

12. C. T. Foxon, B. A. Joyce, and M. T. Norris, "Composition Effects in the Growth of $Ga(In)As_yP_{1-y}$ by MBE," J. Cryst. Growth, 49, pp. 132-140, (1980).

13. M. T. Norris and C. R. Stanley, "Substrate Temperature Limits for epitaxy of InP by MBE, Appl. Phys. Lett. 35, pp. 617-620, (1979).

14. J. H. McFee, B. I. Miller, and K. J. Bachmann, "Molecular Beam Epitaxial Growth of InP," J. Electrochem. Soc. 124, pp. 259-272, (1979).

15. E. L. Meeks and F. L. Eisele, "Growth of InP by Molecular Beam Epitaxy," U.S. Army Research Office DAAG-29-80-K-K-0100 (1982).

16. S. Bishop, "Characterization of Semiconductors by Photoluminescence," SPIE, Vol. 276, 1981

17. L. J. van der Pauw, "A Method of Measuring Specific Resistivity and Hall Effect of Disc of Arbitrary Shape," Phillips Res. Repts., 13, pp. 1-9, (1958).

18. P. M. Laufer, F. H. Pollack, R. E. Nahory and M. A. Pollack, "Electroreflectance Investigation of $In_{1-x}Ga_xAs_yP_{1-y}$ Lattice-matched to InP," Solid State Commun. 36, pp. 419-422, (1980).

19. K. Oe, Y. Shimoda, and K. Sugiyama, "Lattice deformation and misfit dislocation in GaInAsP/InP double-heterostructure layers," Appl. Phys. Lett. 33, pp. 962-964, (1978).

20. G. H. Olsen and T. J. Zamerowski, "Vapor-Phase Growth of (In,Ga)(As,P) Quaternary Alloys." IEEE J. Quantum Electron. 17, pp. 128-138, (1981).

21. F. A. Thiel, D. D. Bacon, E. Buehler, and K. J. Bachmann, "Contacts to p-type InP," J. Electrochem, Soc. 124, pp. 317-318, (1977).

22. L. P. Erickson, A. Waseem, and G. Y. Robinson, "Characterization of Ohmic Contacts to InP," Thin Solid Films 64, pp. 421-426, (1979).

23. K. Tabatabaie-Alavi, A.N.M.M. Choudhury, N. J. Slater, and C. G. Fonstad, "Very low resistance ohmic contacts on p-type InP by direct plating," Appl. Phys. Lett. 40, pp. 398-400, (1982).

24. G. Y. Robinson, "A Study of Metal-Semiconductor Contacts in InP," RADC Report No. TR-81-169, (1981).

25. H. Temkin, R. McCoy, V. G. Keramidas and W. A. Bonner, "Ohmic contacts on p-type InP using Au-Be metallization," Appl. Phys. Lett. 36, pp. 444-446, (1980).

26. G. H. Olsen and T. J. Zamerowski, "Vapor-Phase Growth of (In,Ga)(As,P) Quatnerary Alloys," IEEE J. Quantum Electron 17 pp. 128-144, (1981).

27. E. B. Abrams, S. Sumski, W. A. Bonner, and J. J. Coleman, "Be-doping of liquid-phase-epitaxial InP," J. Appl. Phys. 50, pp. 4469-4475, (1979).

28. E. Kuphal, "Preparation and Characterization of LPE InP," RADC TM-80-07, pp. 443-454 (1980).

29. M. G. Astles, F. G. H. Smith, and E. W. Williams, "Indium Phosphide, II Liquid Epitaxial Growth," J. Electrochem. Soc. 120, pp. 1750-1754, (1973).

30. E. L. Meeks and F. L. Eisele, "Growth of InP by Molecular Beam Epitaxy," Final Report, Contract No. DAAG-29-80-K-0100, U.S. Army Research Office, (1982).

31. M. Ilegems, "Beryllium Doping and Diffusion in Molecular Beam Epitaxy of GaAs and $Al_xGa_{1-x}As$," J. Appl. Phys. 48, 1278-1283, (1977).

32. H. M. Levy, G. M. Metze, D. W. Woodard, W. O. Camp, R. C. Tiberio, C.E.C. Wood, and L. F. Eastman, "GaAs Integrated Circuits by Selective Epitaxy and Electron Beam Lithography," Solid State Technology 24, pp. 127-130, (1980).

33. Y. Tarui, Y. Komiya, and Y. Harada, "Preferential Etching and Etched Profile of GaAs," J. Electrochem. Soc. 118, pp. 118-122, (1971).

34. S. Adachi, H. Kawaguchi, and G. Iware, "InGaAsP/InP Planar Stripe Lasers with Chemically Etched Mirrors," J. Electrochem. Soc. 129, pp. 883-886, (1982).